GROWTH OF CADMIUM SULPHIDE FILMS FOR ACOUSTOELECTRIC DEVICES

by

Douglas D.M. Allan, B.Sc.

Thesis Presented for the Degree of
Doctor of Philosophy of the University
of Edinburgh in the Faculty of Science.

April, 1972.

UNIV. EDINBURGH EX BIBL

ABSTRACT :

Films of cadmium sulphide prepared by conventional methods such as sublimation, sputtering and co-evaporation, normally consist of material which because of its polycrystalline nature yields devices which compare unfavourably with their bulk single crystal counterparts. Single crystal films are of particular interest in the rapidly expanding field of microwave acoustic engineering where surface wave devices are rapidly maturing to practical component status.

The design of a film deposition system incorporating several special features is discussed in the light of conventional film and bulk growth systems. Development of this system has permitted the conditions for single crystal epitaxial growth of cadmium sulphide on sapphire to be determined. A critical dependence of epitaxy on substrate condition has been observed and optimum substrate preparation is described. The method of growth is not peculiar to cadmium sulphide, but may be applied to other compounds.

High field instabilities have been observed in a polycrystalline sample although their nature was not compatible with acoustoelectric oscillations.

C O N T E N T S

Page

ABSTRACT.

CHAPTER 1. ACOUSTOELECTRIC DEVICES.

1.1 Introduction. 1.

1.2 The Acoustoelectric Effect. 1.

1.3 The Acoustoelectric Effect in Bulk Piezoelectric Crystals. 3.

1.4 High Field Domains. 5.

1.5 Experimental Configurations. 8.

1.6 Thin Film Acoustoelectric Devices. 8.

1.7 Microwave Acoustic Engineering. 12.

1.8 Thermal Limitations. 18.

1.9 Comparison of Thin Film and Bulk Device Operation. 19.

1.10 Choice of Material. 21.

CHAPTER 2. CONVENTIONAL PRODUCTION OF CADMIUM SULPHIDE FILMS.

2.1 Cadmium Sulphide. 23.

2.2 Vaporization of Cadmium Sulphide. 27.

2.3 Condensation of Cadmium Sulphide. 30.

2.4 Cadmium Sulphide Film Deposition Systems. 32.

2.5 Influence of the Substrate. 37.

2.6 Recrystallisation of Cadmium Sulphide Films. 49.

CHAPTER 3. ADVANCES IN CADMIUM SULPHIDE FILM PRODUCTION TECHNIQUES.

3.1 Improvements in Film Deposition Techniques. 51.

3.2 Vapour Growth of Bulk Cadmium Sulphide Crystals. 59.

Chapter 3 - continued. Page

3.3 Design Criteria - System 1. 66.

3.4 Deposition Procedure - System 1. 74.

3.5 Results - System 1. 81.

CHAPTER 4. THE DESIGN AND OPERATION OF A DEPOSITION SYSTEM TO PRODUCE SINGLE CRYSTAL FILMS.

4.1 Design Criteria - System 2. 88.

4.2 Deposition on Silicon Substrates. 95.

4.3 Deposition on Sapphire Substrates. 99.

4.4 The Effect of System Parameters on Epitaxy. 104.

4.5 Conditions for Epitaxial Growth. 112.

CHAPTER 5. PREPARATION OF SUBSTRATES.

5.1 Chemical Substrate Etching. 128.

5.2 Orientation Determination by Optical Examination. 131.

5.3 Orientation Determination by X-ray examination. 133.

5.4 Angles Between Planes - Sapphire. 137.

5.5 Angles Between Planes - Cadmium Sulphide. 141.

5.6 Specimen Orientations by The Back Reflection Laue Technique. 141.

CHAPTER 6. ELECTRICAL MEASUREMENTS ON CADMIUM SULPHIDE FILMS.

6.1 The Metal Semiconductor Contact. 151.

6.2 Techniques of Ohmic Contact. Fabrication. 154.

6.3 Examination of Contacts. 155.

6.4 Electrical Characteristics of Cadmium Sulphide Films. 160.

6.5 Comment. 167.

Page.

ACKNOWLEDGEMENTS. 173.

APPENDIX 1. SOLID STATE CONTROL UNIT. 174.

APPENDIX 2. HIGH VOLTAGE PULSE GENERATOR. 178.

REFERENCES. 180.

CHAPTER 1.

ACOUSTOELECTRIC DEVICES

1.1 INTRODUCTION :

It has been demonstrated theoretically[1,2] that surface wave acoustic devices comprising a thin acoustoelectrically active layer in contact with an acoustoelectrically inactive substrate, may possess an intrinsic gain rate which is comparable with that of the more conventional bulk wave devices. In practice, however, this has not proved to be the case, one major obstacle being the lack of success in synthesising a thin acoustoelectrically active film which retains essential properties the magnitude of which can be compared with those of the bulk material. The primary interest of this work is in the design, fabrication and development of a system of film growth which attempts to retain the properties of the parent acoustoelectrically active material in a thin film.

1.2 THE ACOUSTOELECTRIC EFFECT :

Following observation of field dependent attenuation in certain classes of materials came predictions of negative attenuation in piezoelectric and non-piezoelectric semi-conductors by Hutson et al [3] and Weinreich, [3] respectively. The basis of this phenomenon, the acoustoelectric effect, is that when an acoustic wave propagates through a material which contains conduction electrons, its energy and momentum are attenuated by the atoms which form the crystal lattice.

This momentum attenuation constitutes a force which, although it cannot transport valence electrons can cause a translation of conduction electrons in the direction of this force. If a closed circuit exists in this direction then a direct acoustoelectric current is produced. If, however, the electrical circuit is open, a space charge is created by the drifting electrons and the electric field thus induced opposes the effect of the acoustoelectric force on the electrons.

By imparting to the conduction electrons by secondary means a net drift velocity which exceeds the velocity of acoustic waves in the active material it is possible to reverse the direction of momentum transfer and thus initiate a transfer of energy from the drifting electron stream to the acoustic flux. This is the principle of acoustoelectric amplification.

The cause of momentum attenuation is strain potential in semiconductors and polarization in piezoelectric materials. A collision process is not directly involved and it is interesting to note that the drifting electron stream need only be in close proximity to the acoustic wave for interaction to occur [4]. Only piezoelectric materials need be considered for practical acoustoelectric devices, since non-piezoelectric materials depend on a combination of high magnetic field and liquid helium temperature for their efficiency [5].

White's [6] classic paper presents a linear

treatment of amplification in piezoelectric semiconductors and predicts that the amplification depends on $\frac{p^2}{4\epsilon c}$ where p is a piezoelectric constant, ϵ is the dielectric permittivity and c is an elastic constant. Amplification reaches a maximum when the electron drift velocity, v, attains approximately 1.6 times the acoustic wave velocity, v_s.

The theory of large signal acoustoelectric amplification is not well understood, due mainly to the large number of non-linear interacting parameters involved. Acoustoelectric coupling is numerically large compared with the more familiar coupling which occurs in travelling wave tubes and, in addition, the acoustic wave serves as a means of preserving phase information during the amplification process [7].

1.3 THE ACOUSTOELECTRIC EFFECT IN BULK PIEZOELECTRIC CRYSTALS

Early attempts to achieve acoustoelectric amplification in practical terms, Fig. 1.5.1, by launching an acoustic signal into a piezoelectric semiconductor at the crystal cathode and recovering it at the crystal anode, revealed that net gain could be achieved at frequencies of the order of tens of MHz [8]. In addition, a growing acoustic flux could be observed at the anode transducer. This observation of non-injected hypersonic wave amplification was mooted as a possible explanation [9] for the onset of current saturation which occurred shortly after

the application of a sufficiently high voltage pulse to semiconducting cadmium sulphide and cadmium selenide crystals. During the transition from ohmic to saturated behaviour, current oscillations were observed and later Kroger [10] et al observed current oscillations of period dependent on crystal length, electron density and temperature, as well as applied drift voltage. These oscillations were continuous and independent of the rise time of the applied voltage, in contrast to earlier observations of oscillations which were sensitive to the applied voltage rise-time.

In most cases, the active materials employed were cadmium sulphide or cadmium selenide, both difficult materials to prepare in single crystal form. Their inhomogeneous character must have coloured to some extent the observed anomalies, and in practice reproducible results were seldom achieved. Extension of the frequency range of MHz to GHz highlighted the complexity and expense of launching and receiving acoustic waves. To quote a typical example [11], for a 1-GHz acoustic wave is to propagate through a crystal from transducer to transducer, the opposite faces of the crystal for launching and reception must be flat to within half a wavelength of sodium light and parallel to 10" seconds of arc. For frequencies in excess of 200 MHz transducer techniques were extended to include crystalline quartz buffers with ends inserted into tuned R.F.

cavities. Such techniques are patently imcompatible with mass production.

1.4 HIGH FIELD DOMAINS :

Current oscillations in bulk semiconductors due to travelling high field domains have been reported by several authors and three basic types of domain, each characterised by its rate of progress through the sample, must be distinguished. One type has been observed in gold doped germanium by Ridley & Pratt [12] and in copper doped germanium by Zhdanova [13] et al. Its velocity is approximately 10^{-2} metre /sec and its appearance is due to carrier trapping at ionized impurity sites. Another type has been observed in gallium arsenide by Gunn [14,15]. Its velocity is in excess of 10^{5} metre /sec and it owes its existence to transfer of electrons within the conduction band from the central valley to a satellite valley where their effective mass is higher. A third type has been observed by Haydl and Quate [16], Yamashita et al [17] and numerous others to propagate through a sample of cadmium sulphide at, or near, the velocity of sound in that sample.

The latter type of domain is a region of high acoustic activity and high electric field, and is superimposed on an acoustic flux build-up which is reflected in an increasing electric field distribution from cathode to anode.

Domain formation in cadmium sulphide involves the amplification of acoustic energy to a high level

Repetitive domain transits were initially considered to occur through reflection of acoustic flux from anode to cathode in a situation where the resulting loop gain exceeded unity [18]. Although this mechanism accounts for the appearance of damped or continuous oscillations, depending on the loop gain, it fails to explain the onset of domain formation with the first acoustic transit time observed by Haydl et al [19]. It has been suggested [20] that domain incubation is due to the acoustic shock wave impressed on the sample by sudden application of the necessarily pulsed drift field to bulk samples, domain formation being absent with drift field pulses of long rise time. It appears, however, that provided the sample gain is sufficient, thermal acoustic flux at the cathode may provide the initial signal for amplification [21]. A more reasonable conclusion would appear to be that domain formation is merely stimulated by rapid drift field application. In conjunction with the value of acoustic gain predominating within the crystal this hypothesis explains the observed results of domain formation dependence on drift field application rate, the assumption being that acoustic gain although insufficient to amplify thermal acoustic flux to the required level, is capable of producing the required level when presented with a more substantial acoustic input signal.

In accordance with the basic theory of acousto-electric amplification presented in paragraph 1.2 and with the theories of Haydl et al [19] it is postulated

that the acoustoelectric field opposing the drift field may, under conditions of high acoustic flux,increase mor rapidly than the applied drift field thus producing a sample current which is a decreasing function of applied field. After domain formation occurs most of the applied electric field is absorbed in the domain and the level of acoustic flux elsewhere in the crystal is small until the domain reaches the anode when the crystal again reverts to an amplifying condition and the cycle repeats.

Details of the high field domain are significantly different in semiconducting and photoconducting cadmium sulphide. Domain width is of the order of 100 microns in semiconducting material [22] but may be of the order of millimetres wide in photoconducting material [23].

The Domain Originated Functional Integrated Circuit [24], which offers the possibility of complex waveform synthesis is a single device which includes a domain path, shaped physically to the required waveform profile is an example. Of the three types of domain the third type is most suited to device applications because its velocity provides signals at a rate which is compatible with associated electronic devices. In addition to the facility of addressing the domain by optical means the number of signal levels exhibited by the device may be varied by controlling the point at which the domain forms, either optically by illuminating the undesired features, or electrically by reducing the drift voltage.

1.5 EXPERIMENTAL ACOUSTOELECTRIC AMPLIFIER CONFIGURATIONS :

Practical configurations which exploit the acoustoelectric effect, excepting domain operated or passive devices, comprise basically a piezoelectric crystal fitted with transducers at each end and which either transports, Fig.1.5.1, or is in close proximity to a drifting electron stream of supersonic velocity, Figs. 1.5.2 and 1.5.3 [5,25].

These configurations impose certain individual requirements on the piezoelectric material employed, the device shown in Fig. 1.5.1 demands an active material which is at once piezoelectric and electrically conductive, while the devices of Figs. 1.5.2 and 1.5.3 impose only a piezoelectric demand on the active material. In practice the device of Fig. 1.5.2 compares unfavourably with the rest, because of difficulty in concentrating the free electron beam close to the active material. This imposes severe restrictions at high frequencies. It offers, however, the advantage that the beam current is low in comparison with the drift current required in Figs. 1.5.1 and 1.5.3,thus easing heat sinking requirements.

1.6 BASIC THIN FILM AMPLIFYING DEVICES :

Attractive alternatives to the bulk wave devices of Figs. 1.5.1, 1.5.2 and 1.5.3, are surface wave devices shown in Figs. 1.61, 1.6.2 and 1.6.3. Surface waves have all the desirable properties of bulk waves and in addition they are accessible.

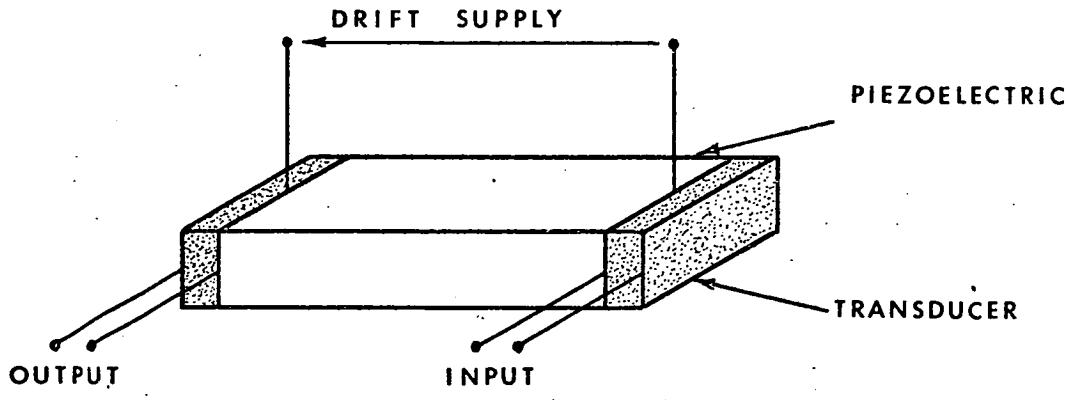


FIG 1.5.1.

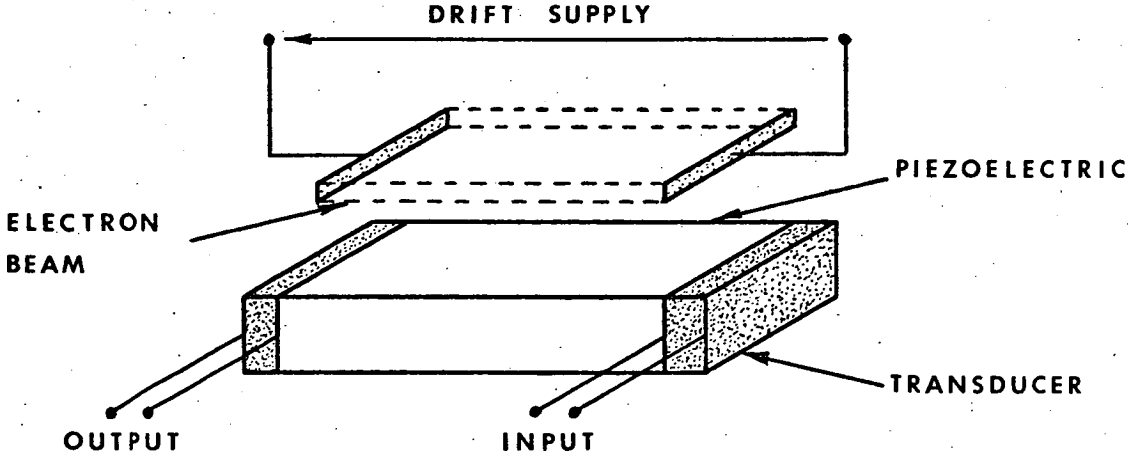


FIG 1.5.2.

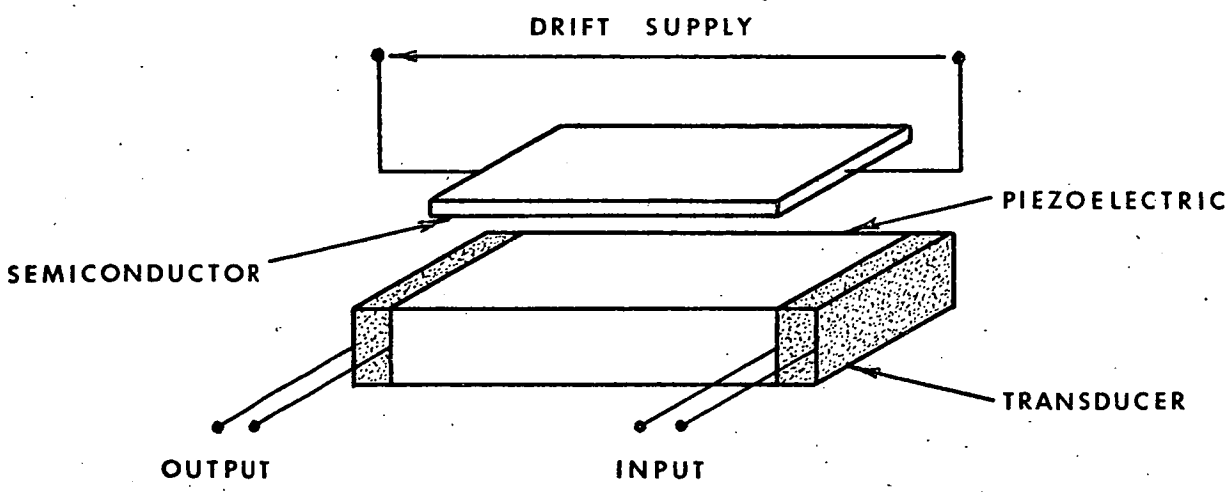


FIG 1.5.3.

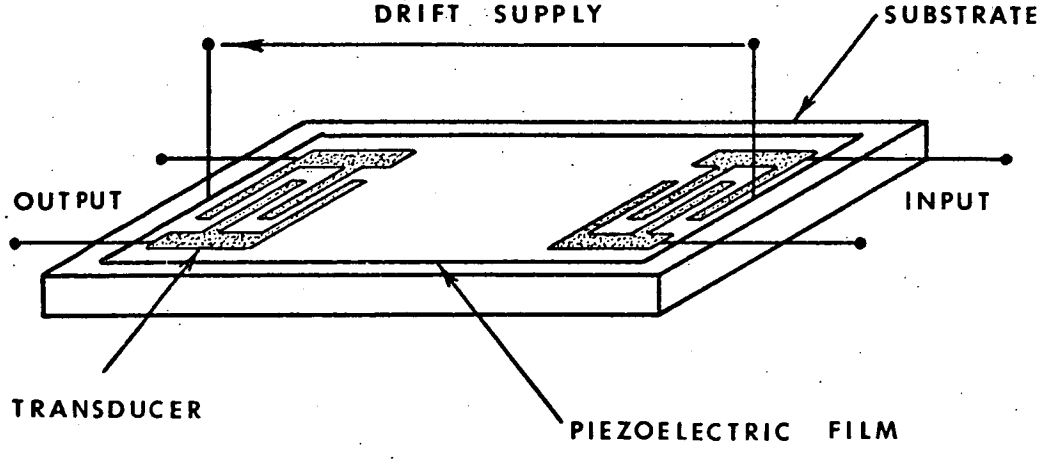


FIG 1.6.1.

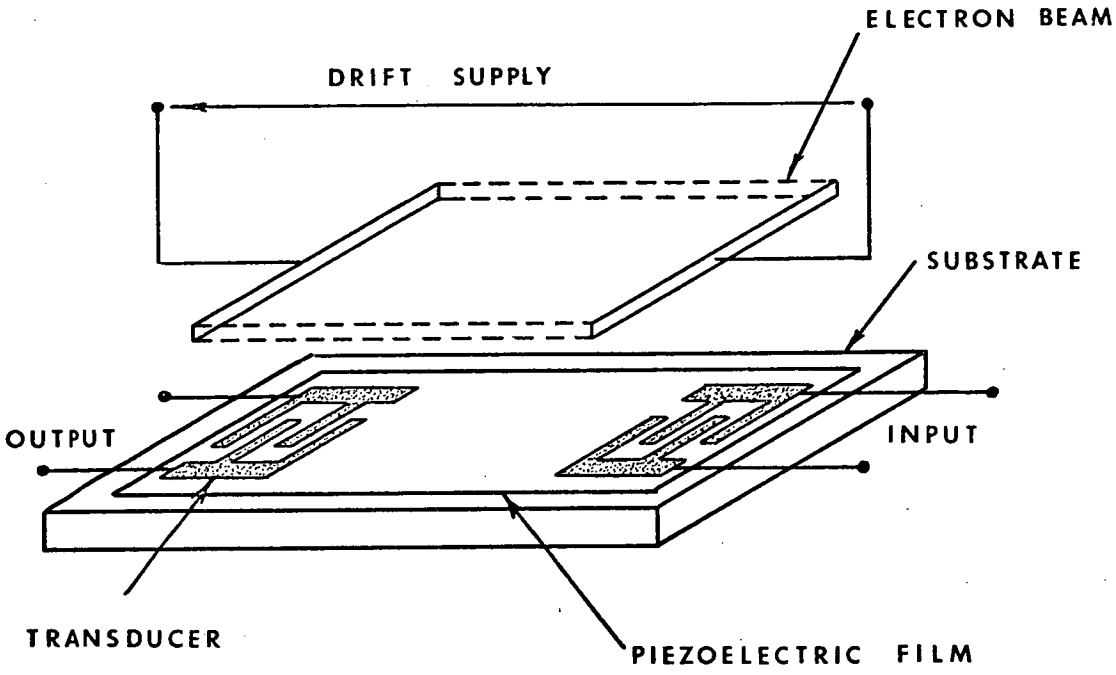


FIG 1.6.2.

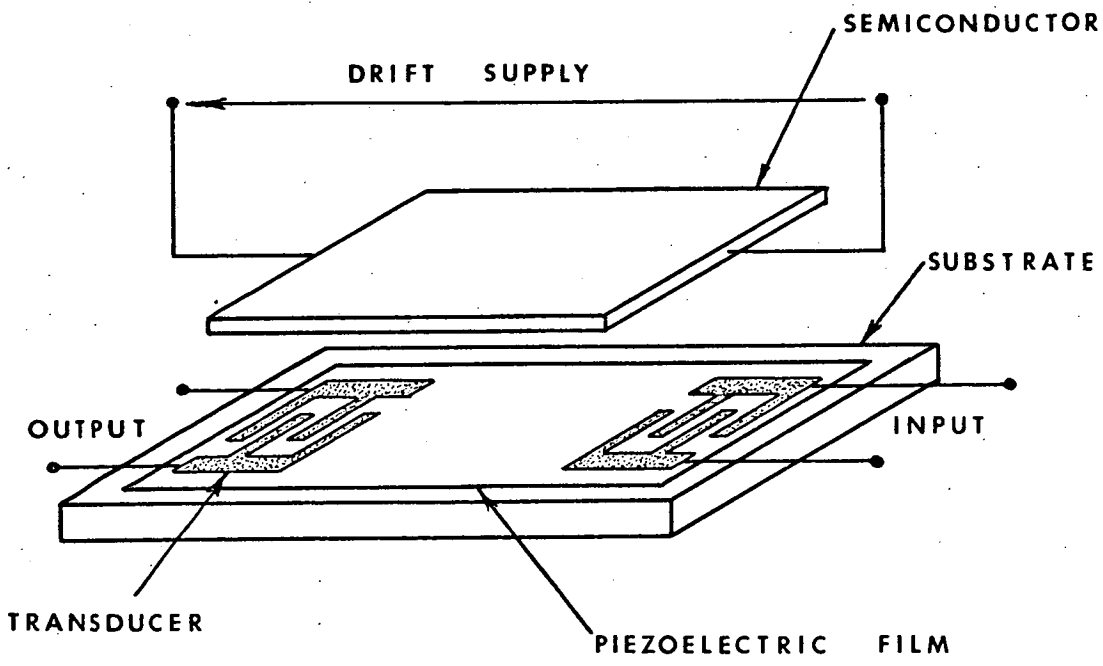


FIG 1.6.3.

Interdigital surface wave transducers are simple, two dimensional and compatible with mass production techniques. Further, their efficiency exceeds that of bulk wave transducers, and various combinations of bandwidth and frequency are available by simply altering the number and spacing of the transducer electrodes.

The device of Fig.1.6.3 has particular advantages from an amplification viewpoint since not only are the piezoelectric and semiconducting properties of the device optimised independently by virtue of the separate and electrical paths, but by the addition of further transducers on the longitudinal axis of the device, a combination of amplification and/or variable delay may be realised. Moreover, at high frequencies the transducer dimensions are very small and the planar device becomes compatible with modern integrated electronic technology.

1.7 MICROWAVE ACOUSTIC ENGINEERING :

The basis of the acoustoelectric effect has been stated and illustrated in a series of amplifier configurations. In this restricted field, preferential selection of materials to perform specific functions has already become apparent and the upsurge of microwave acoustic engineering within the last decade has stimulated interest in a still wider range of piezoelectric materials to perform more diverse functions.

Acoustic waves are typically five orders of magnitude slower than electromagnetic waves thus components whose size is of the order of a wavelength could theoretically be realized in dimensions five orders of magnitude smaller than their electromagnetic counterparts. Most typical microwave components fall in this category. For example, microwave acoustic delay lines are rapidly maturing to practical component status, utilising both bulk and surface waves. Using a zinc oxide thin film transducer bonded to a delay medium and electromagnetic matching network a delay of 4 microseconds and insertion loss of 20 dB at a centre frequency of 1.65 GHz with a 3 dB bandwidth of 3o% is available in a bulk wave configuration of less than 16×10^{-6} metre ^{3} in volume [26]. An electromagnetic delay line of high quality coaxial cable requires 1220 metres of cable introducing an insertion loss of 200 dB to perform the same function. It is obvious that acoustic wave delay lines provide functions not previously available at microwave frequencies [27].

Delay devices may be classified as fixed delay devices, and signal processing devices which provide more complex functions. It is chiefly this latter class of devices which illustrates the increased flexibility available with surface waves although thin piezoelctric films find major applications in both sectors.

Bulk microwave acoustic delay lines follow closely the form shown in Fig.1.5.1 except that no drift voltage supply is connected. Conventionally, a microwave signal is coupled via a matching network to the input transducer which in turn transmits the signal into the acoustic delay medium. Recovery of the acoustic signal is performed by the output transducer which yields an electromagnetic signal delayed by the propagation time through the acoustic medium. Delays of the order of 100 microseconds per metre of delay material are common. The propagation of acoustic bulk waves is non-dispersive in the cases of longitudinal and shear mode plane waves[28,29] and provided that the transducer cross-sectional dimensions are large compared with an acoustic wavelength the acoustic waves generated are considered to possess beam like characteristics [30]. Delay materials are preferably single crystal to minimise attenuation and scattering, commonly employed crystals include sapphire, quartz, lithium niobate, yttrium aluminium garnet (YAG) and yttrium iron garnet (YIG) providing wave velocities of 3.32×10^3 metre / second to 3.76×10^6 metre /second. The difficulties experienced in fabricating efficient transducers for use at GHz frequencies have already been described although advances in piezoelectric thin film transducers are rapidly improving this situation. Zinc Oxide appears to have ousted cadmium sulphide as a

transducer material in this application since the effective electromechanical coupling constant for cadmium sulphide of 0.14 compares unfavourably with the value of 0.22 for zinc oxide. Longitudinal wave transducers vibrate in the thickness mode, accurate control of transducer film thickness being essential since acoustic wave generation occurs at each transducer face requiring the face spacing to be $\frac{\lambda}{2}$ at the centre frequency of interest to ensure constructive acoustic interference. Impedance matching networks are necessary in broadband devices to tune out the effects of transducer capacitance.

Associated with acoustic delay is the appearance of spurious signals resulting from multiple travel of the desired signal within the device. Triple transit signals are most troublesome and triple transit suppression (TTS) is limited to approximately 20dB by the inability to terminate thin film transducers without excessive signal loss.

Similar basic general considerations apply to surface wave delay devices but their added accessability renders them suitable for broader application. Rayleigh waves [31] have been known to seismologists for many years and propagate along the free surface of solids. They involve eliptically polarized particle displacements and decay in amplitude exponentially from the surface. In isotropic

materials the Rayleigh wave velocity is typically 5-10% below that of the bulk wave since volume elements of the material transmit disturbances with different velocities depending on their position relative to the surface. Consider after Adler et al [32] a volume element in the bulk of the material which transmits a disturbance with velocity $(\frac{c}{\rho})^{\frac{1}{2}}$ where c is an elastic constant and ρ is the mass density of the material. Surface elements transmit disturbances with velocity $(\frac{c'}{\rho})^{\frac{1}{2}}$ since surface elastic constants are lower in value than bulk constants due to the absence of a proportion of the natural restraining forces provided by the crystal lattice and thus if a surface mode exists its velocity will be lower than the bulk value by a factor $(\frac{c'}{c})^{\frac{1}{2}}$. Such waves are evanescent in the transverse direction as in the electromagnetic case, and also non-dispersive like bulk waves. In contrast to the bulk wave case the facility for fabrication of dispersive surface wave delay lines is readily available simply by placing thin layers of different materials on the substrate surface. Dispersion is determined by the layer thickness and the velocity difference between the layer and substrate media [26]. The addition of such a layer also provides a facility for guiding [33,35] and focussing [34] acoustic waves in an acoustic analogue of the dielectric microwave guide. It is this system which may require single crystal material to control losses at higher frequencies [36].

One of the most important contributions to surface wave device efficiency was the introduction of the interdigital surface wave transducer by White [37]. Adjacent fingers are located $\frac{\lambda}{2}$ apart and conversion losses of as little as 4dB are available, [38], 3dB of this is due to the bi-directivity of the device and bandwidth may be of the order of 30%. The ease of forming non-reflecting terminations improves triple transit suppression compared with bulk devices and non-dispersive or dispersive delay is available simply by dimensioning the piezoelectric overlay. Optical photolithographic methods permit transducer fabrication to within a one micron resolution limit corresponding to approximately 800MHz. In order to extend the frequency range electron beam fabrication techniques have been employed [39].

The amplification configuration mentioned in paragraph 1.6 may be used to improve triple transit suppression in delay lines but attention has tended to focus more on signal processing devices such as pulse compression filters and analogue matched filters. Acoustic convolution has also been realised [40] in photoconducting cadmium sulphide in a device which accepts input signals through interdigital transducers located at either end of the specimen and permits nonlinear mixing of these signals to occur at an illuminated region in the centre of the specimen where the output signal is

obtained. For high frequency applications, single crystal material would be desirable.

1.8 THERMAL LIMITATIONS :

A fundamental requirement of active acousto-electric devices, is an electron stream of supersonic velocity. This implies in all cases, a measure of heat generation, which is unavoidable and dictates the physical size of the device, its duty cycle, and its efficiency in terms of power consumption.

Any reduction in power consumption is thus desirable, this is achieved in Figs. 1.5.2 and 1.6.2 by the use of a free electron beam which unfortunately restricts high frequency response, or in Figs. 1.5.3 and 1.6.3, by optimising semiconducting properties of the electron drift system. The same technique is to some extent applicable to the device of Fig.1.5.1, but a balance must be set between the possibly conflicting material properties affecting electrical and acoustic conduction, and piezoelectric coefficients. The configuration of Fig.1.5.1 cannot however be dismissed, in spite of its obvious inherent inferiority to the others in optimisation of vital parameters since it is the basis of high field domain operated devices.

The bulk acoustoelectric domain device of this type is limited by thermal considerations to a typical maximum of ten domain transits per second[41], which corresponds to 200 levels/second. This compares

unfavourably with the possible 10^7 levels/second associated with hypothetical continuous operation. The proposed thin film surface wave analogue, Fig.1.6.3, of the device shown in Fig. 1.5.1,presents an attractive alternative by attacking the thermal problem with its reduced cross-sectional area exposed to the electron stream, combined with some measure of electrical optimisation in the active material.

1.9 COMPARISON OF THIN FILM AND BULK AMPLIFIER DEVICE OPERATION :

A short numerical comparison of the devices in Figs. 1.5.1 and 1.6.1,will demonstrate the feasibility of continuous operation in the latter. In order to impart the necessary drift velocity for acousto-electric amplification to the electron stream, an electric field E is required where :

$$E = \frac{v}{\mu} \qquad (.1.9.1)$$

The values of v and μ in high quality bulk single crystal cadmium sulphide are respectively 2×10^3 metre/sec and 200×10^{-4} metre^2/volt sec. Thus the required electric field is of the order of 10^5 volts/metre. For a typical cross-sectional area,A, normal to the electron stream of 0.25×10^{-4} metre, length, ℓ , 10^{-2} metre and resistivity, ρ , of 1×10^{-2} ohm metre, the electrical resistance presented to the external circuit is given by :

$$R = \frac{\rho \ell}{A} \qquad (1.9.2)$$

In this case R is 4 ohms and this corresponds to a power dissipation of 2.5×10^5 watts, for continuous

operation. Heat-sinking in this case is impractical, hence the restriction to operation by a pulsed drift supply of low duty cycle. The corresponding figure for cadmium sulphide of 10 ohm metre , which is typical of illuminated photo-conducting cadmium sulphide, is 2.5×10^{2} watts.

The device proposed in Fig. 1.6.1 with a cross-sectional area normal to the electron stream of 10^{-8} metre ^{2} (1 micron thick film, 10^{-2} metre wide) length 10^{-2} metre , with resistivities 10^{-2} ohm metre and 10 ohm metre would have power dissipations of 10^{2} and 10^{-1} watts respectively in continuous operation. This situation is much more attractive thermally, especially if deposition of the piezo-electric semiconducting film is arranged on a thermally conductive substrate, sapphire for example, which is in turn coupled to a thermal sink.

Deposition of the film on an insulating substrate imposes thermal limitations on the device since the process of thermal conduction in insulators relies on phonons rather than on electrons as is the case in metals [42]. The thermal conductivity of sapphire, although regarded as high for an insulator, compares unfavourably with that for metals. Typical figures for thermal conductivities in units of watt /metre ^{o}K at room temperature are as follows [43, 44] :

Copper	3.85×10^{-2}
Aluminium	2.38×10^{-2}
Sapphire	0.21×10^{-2}
Cadmium Sulphide	0.20×10^{-2}

Within the temperature range of interest the substrate thermal transfer characteristic for the specimens described in the fourth chapter is approximately 0.3 ^{o}K/watt. The temperature dependence of this conductivity, within the range of interest, may be expected to be approximately inversely proportional to absolute temperature.

1.10 CHOICE OF MATERIAL :

The calculations of 1.9 assumed for the thin film, a constancy with the bulk case of materials properties which enhance or interfere with the desired interaction. Of particular thermal importance is electron mobility, a feature of current cadmium sulphide films which compares most unfavourably with the high quality single crystal bulk material, being of the order of 10^{-3} metre ^{2}/volt sec. This cancels to a great extent the possible advantage over a bulk crystal in heat generation.

Of acoustic importance, is the polycrystalline nature of cadmium sulphide films and its effect on acoustic attenuation. This, in conjunction with the inability to preserve phase information reliably due to acoustic scattering at grain boundaries, results in degradation of the acoustoelectric amplification factor.

While acknowledging the superiority of the devices of Figs. 1.5.3 and 1.6.3, as acoustoelectric

amplifiers in view of their facility for independent parameter optimisation, it was decided to concentrate on development of a cadmium sulphide film suited to the requirements of Fig.1.6.3, bearing in mind its broader application in domain operated devices and in the passive devices described in paragraph 1.7.

CHAPTER 2.

CONVENTIONAL PRODUCTION OF CADMIUM SULPHIDE FILMS

2.1 CADMIUM SULPHIDE :

The multiplicity of potentially useful properties which characterise cadmium sulphide have prompted investigations into its synthesis over a period of many years. Its photoconducting, semiconducting and piezoelectric properties are of particular interest and their prominence is associated with varying degrees of crystal perfection and deviation from stoichiometry. For this reason, a measure of control over the composition, purity and homogeneity of the material is desirable. Recently fresh interest has been aroused by its potential for solar cell fabrication, yielding units featuring an attractively high radiation damage resistance compared to silicon cells[45]. Cadmium sulphide belongs to the IIB-VIB group of compounds. In common with related compounds such as cadmium selenide and cadmium telluride it is dimorphic, the wurtzite and sphalerite structures differing only in the stacking sequence of the elemental sublattices. It occurs naturally as greenockite in its wurtzite structure which consists of two interpenetrating hexagonal close-packed lattices, one containing the anions and the other the cations, Fig. 2.1.1. The cubic modification is less common, Fig. 2.1.2.

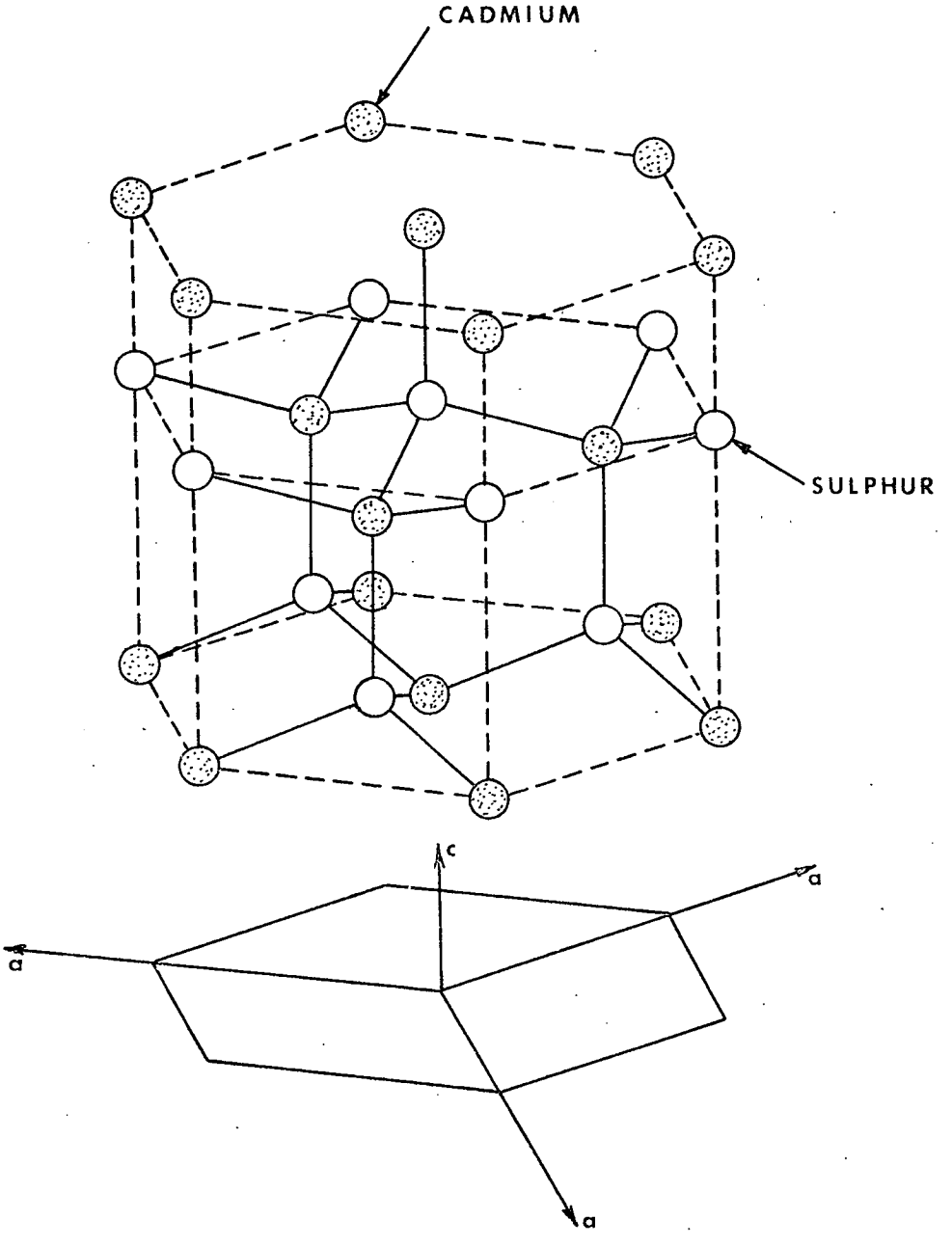


FIG 2.1.1

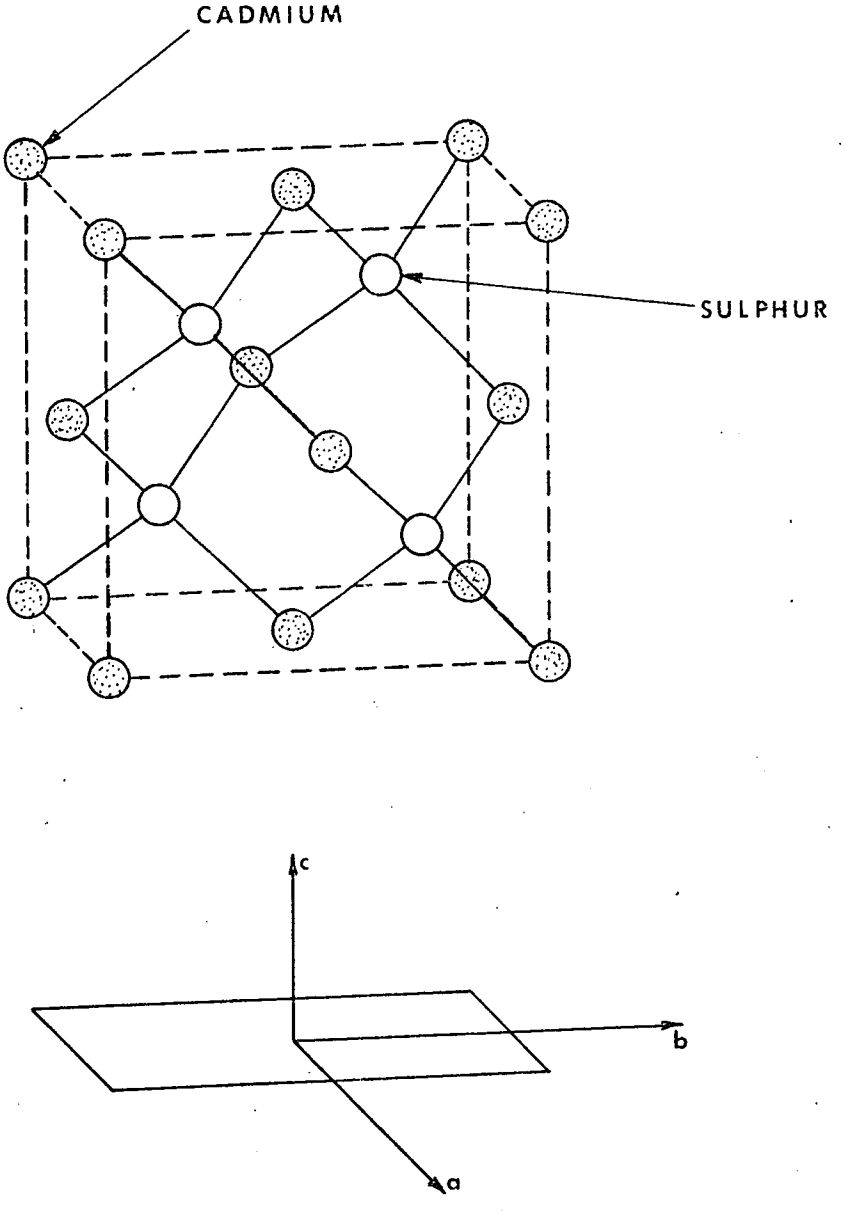


FIG 2.1.2.

Pure or "compensated" crystals exhibit resistivities, after a period in the dark, of approximately 10^{10} ohm metre and thus resemble semi-insulators rather than semiconductors. The forbidden energy gap is 2.45 eV. At room temperature, cadmium sulphide is effectively an n-type material, a quality attributed to vacant anion sites which trap electrons with such a small binding energy that they are released into the conduction band at room temperature. Cadmium doped material may have a resistivity of about 10^{-3} ohm metre. It is pertinent to note that this apparent electrical flexibility is exceptionally sensitive to the conditions of synthesis to an extent which frequently obstructs the attainment of reproducible characteristics.

The unaccommodating nature of the material is again manifest in its mechanical chracteristics of softness and an unfortunate tendency to cleave along its basal plane. In consequence, it is difficult to achieve a flat and polished surface, the outcomes being mutually exclusive and although 1.5μ thick platelets have been produced by polishing [46] it is unlikely that this process could compete with vapour phase growth as a mass-production process for thin layers.

The growth of germanium, and later silicon crystals and thin films, has reached a degree of perfection unequalled by binary systems, which are

fundamentally less tractable than elemental systems. The elements cadmium and sulphur exhibit the relatively low melting points of 321°C and 119°C, respectively, at a pressure of one atmosphere [47]. In contrast, to approach the stoichiometric melting point of the binary compound requires a temperature of 1475°C with an associated pressure of 3.8 atmospheres [1]. This precludes economic growth from the melt, a common technique in elemental growth. This technique has, however, been successfully applied to cadmium sulphide by Medcalf et al [48] and Belyaev et al [49]; to cadmium selenide by Wardzumski [50] and Heinz [51]; and to cadmium telluride, the lowest melting II - VI compound by Lorenz [52] and Yamada [53].

2.2 VAPORIZATION OF CADMIUM SULPHIDE :

In common with most other II-VI compounds, cadmium sulphide undergoes dissociative sublimation on heating in vacuum. Dissociation pressures for cadmium sulphide have been investigated by Goldfinger and Jeunhomme [54], Spandau and Klanberg [55], and Hsiao and Schechten [56].

Vaporisation is generally assumed to proceed according to the reaction :

$$2\ CdS \rightleftarrows 2\ Cd + S_2 \qquad (2.2.1).$$

and the equilibrium constant for this reaction K_p is plotted in Fig. 2.2.1. The presence of cadmium sulphide molecules or associates in the vapour phase is advocated by Bulakh [57], Caveney [58], Samuelson [59], and Reynolds et al [60].

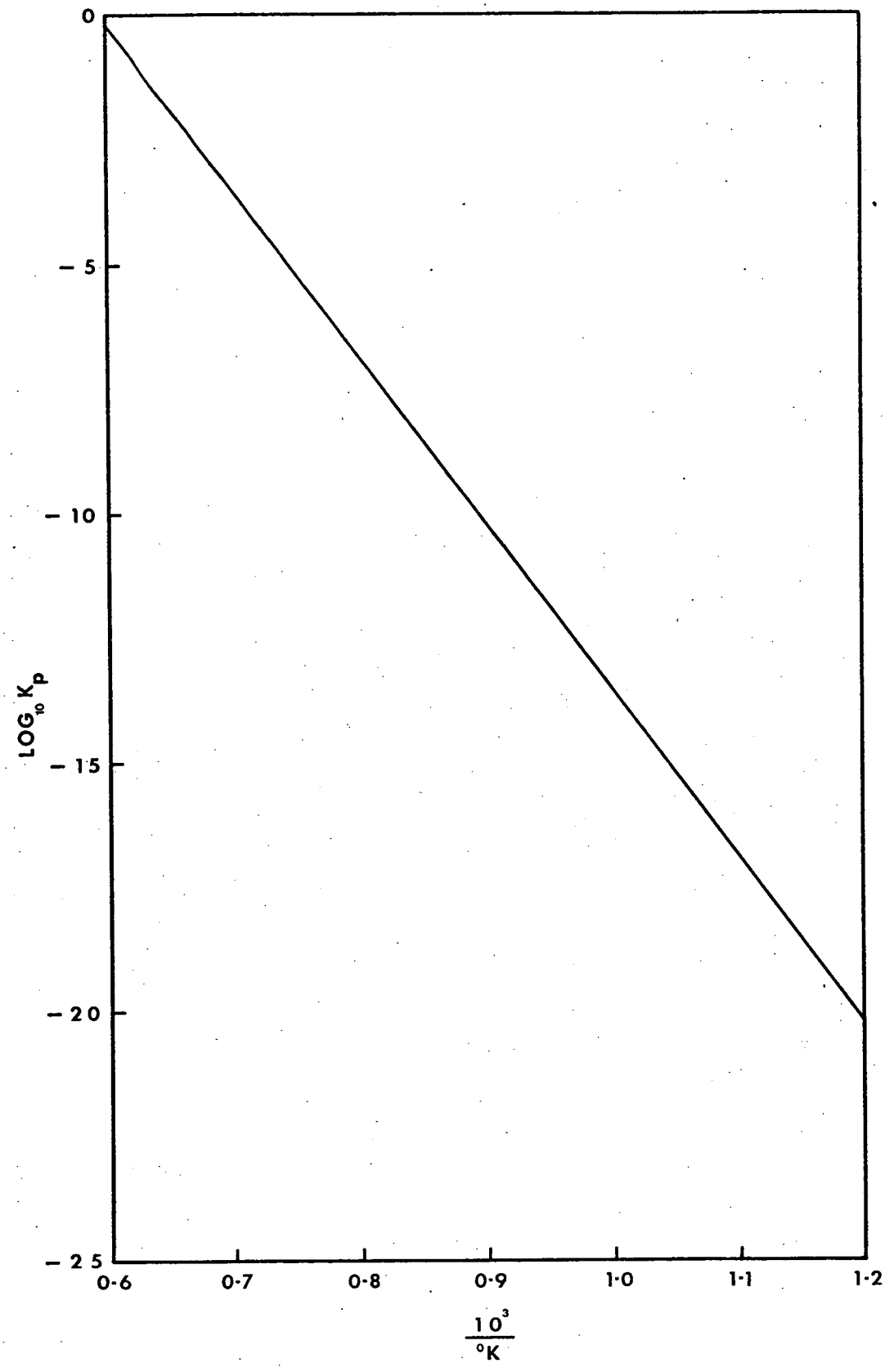


FIG 2.2.1.

However, this view is not shared by other workers [54,61,62,63

The rate of sublimation is sensitive to the source composition [64,65,66] and to the recipient atmosphere [67], both variables being experimentally accessible.

Although the exact mechanism of vaporization is not fully understood, the operation of a step process is accepted in principle, the rate determining step being a surface reaction [68] which is followed by relatively rapid desorbtion from the source. The significance of charge transfer which must necessarily occur prior to the release of neutral species from the partially ionic crystal is underlined by response of the sublimation rate to illumination of the source by photons with energies which exceed the forbidden band gap energy of cadmium sulphide [69].

Inhibition of charge transfer occurs as a result of small surface concentrations of excess cadmium or sulphur which may be supplied temporarily by impingement of that species on the surface, or more permanently by diffusion to the surface of internally trapped excess species. In practice, the former phenomenon is more pronounced in an atmosphereof excess sulphur [70,71]. In a sealed system, the latter process [72] initiated by non-stoichiometery of the charge may dominate the growth mechanism, whereas a vacuum pumped sublimation system offers less scope for the continued operation or either.

Congruent vaporization of cadmium sulphide is assumed by Jeunhomme[73], but Reisman et al [74], on the basis of the existence of an appreciable range of solid solubility of cadmium in cadmium selenide predict incongruent vaporization of this related compound. Nelson[75], at an early stage pointed out the influence of charge purity on the reproducibility of evaporated layers of cadmium sulphide and postulated this, possibly in some measure correctly, to account for the large discrepancies in current values of resistivity and photosensitivity [76]. Spitting and outgassing of the source in vacuum evaporation equipment is not uncommonand films thus produced often exhibit clouding attributed to the formation of oxides, or peeling due to volatile hygroscopic chloride formation between film and substrate [76]. Foreign impurity atoms may also augment native non-stoichiometries in their effect on the rate limiting charge transfer process which precedes sublimation [74]. To minimise the number of variables controlling the vaporization process it is thus desirable to operate a high purity source of large volume to surface ratio and of stoichiometric composition, in an atmosphere which does not contain a large excess of either constituent element. These criteria have been adopted as design requirements.

2.3 CONDENSATION OF CADMIUM SULPHIDE :

The phenomenon of heterogeneous condensation comprises discrete stages of adsorption, surface

diffusion and nucleation [77], these processes respond to numerous factors which include substrate temperature, deposition rate and substrate material. Particles approaching the substrate experience the effects of a combination of attractive and repulsive forces which, in the case of a crystalline substrate, exhibit periodicity in the substrate plane. Collisions with the substrate are in most cases inelastic and the visiting particle may either be re-emitted or adsorbed depending on the interfacial and re-evaporation energies. Nucleation on the substrate subsequent to surface diffusion is favoured by the formation of clusters of particles and since the probability of this process occurring is related to the rate of particle incidence, the condition for progressive condensation at a particular substrate temperature involves exceeding a critical incident flux, N_c, which exactly balances the re-emission capability, N_e of the substrate at that temperature. It is reasonable to assume variations in N_c for different species and substrates.

A more intricate situation arises from the presence of two different vapour species which react chemically to form a compound characterised by an adsorbtion energy not peculiar to either component. This situation is typified by II-VI compounds which retain their solid status at temperatures in excess of the vaporization point of either constituent.

This corresponds to an increase in adsorbtion energy provided the reaction occurs between adsorbed surface species, other things being equal [78].

Some indication of N_e for cadmium and for sulphur may be inferred from Fig. 2.3.1 which demonstrates the considerable imbalance in vapour pressures at any particular temperature. The inference of this situation is that for comparable rates of component incidence, condensation of the following materials is likely in order of increasing substrate temperature :

a) Cadmium, Sulphur, Cadmium Sulphide $T < T_a$

b) Cadmium, Cadmium Sulphide $T < T_b$

c) Cadmium Sulphide $T > T_b$

This is an oversimplification since the effects of interfacial and chemical energies also operate and it would be naïve to predict crossover temperatures for given rates of incidence. At T_a, sulphur ceases to condense as sulphur without the assistance of chemical reaction with cadmium to stabilize the process. At T_b, cadmium similarly ceases to condense as cadmium. Formation of cadmium sulphide will be inhibited at $T << T_a$ by limited surface diffusion of component species.

2.4 CADMIUM SULPHIDE FILM DEPOSITION SYSTEMS :

Early interest in cadmium sulphide evaporated films centred primarily on their photoconductive properties [80,82,83]. Most of these depositions were on amorphous substrates and the sensitivity

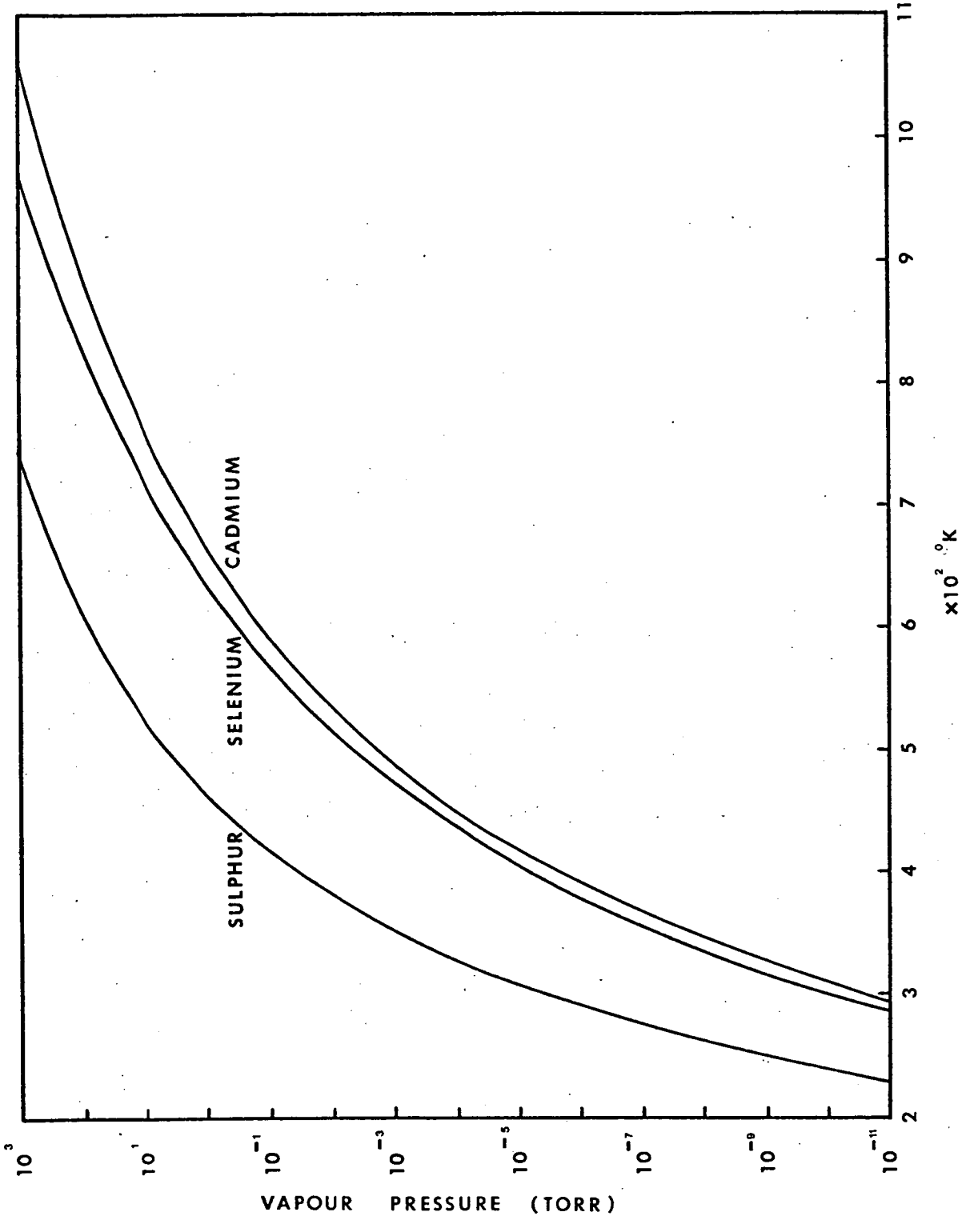

CADMIUM
SELENIUM
SULPHUR
VAPOUR PRESSURE (TORR)
10^{3} 10^{1} 10^{-1} 10^{-3} 10^{-5} 10^{-7} 10^{-9} 10^{-11}
2 3 4 5 6 7 8 9 10 11
$\times 10^{2}$ °K

FIG 2.3.1.

of the films to substrate temperature [84], residual vacuum [79] and purity of the starting material [75] was immediately apparent, some form of post-evaporation heat treatment being conventionally employed to increase the dark resistivity and photosensitivity. With the advent of the thin film transistor and acoustoelectric transducer, interest was further stimulated [85,86,87] to include crystalline substrates [88,89] which could encourage a more ordered film structure. The simple basic deposition configuration predominated and the films, as deposited, remained non-stoichiometric and could vary in colour from almost black [90,91] through orange to yellow as the substrate temperature was increased.

To overcome this inherent lack of stoichiometry, Miller et al [92] employed separate sources of cadmium and sulphur in an attempt to enhance the sticking. probability of sulphur through an increase in its relative vapour pressure. The principle of co-evaporation is shown in Fig. 2.4.1. Subsequently films were produced by Pizzarello [93] using cadmium sulphide and sulphur sources, de Klerk and Kelly [94] who employed both cadmium sulphide/sulphur and cadmium/sulphur sources, and Foster [95] using cadmium sulphide/sulphur sources. The latter investigations were prompted by piezoelectric transducer considerations which require a resistivity of approximately 10^2 ohm metre , obtained by post evaporation heat treatment

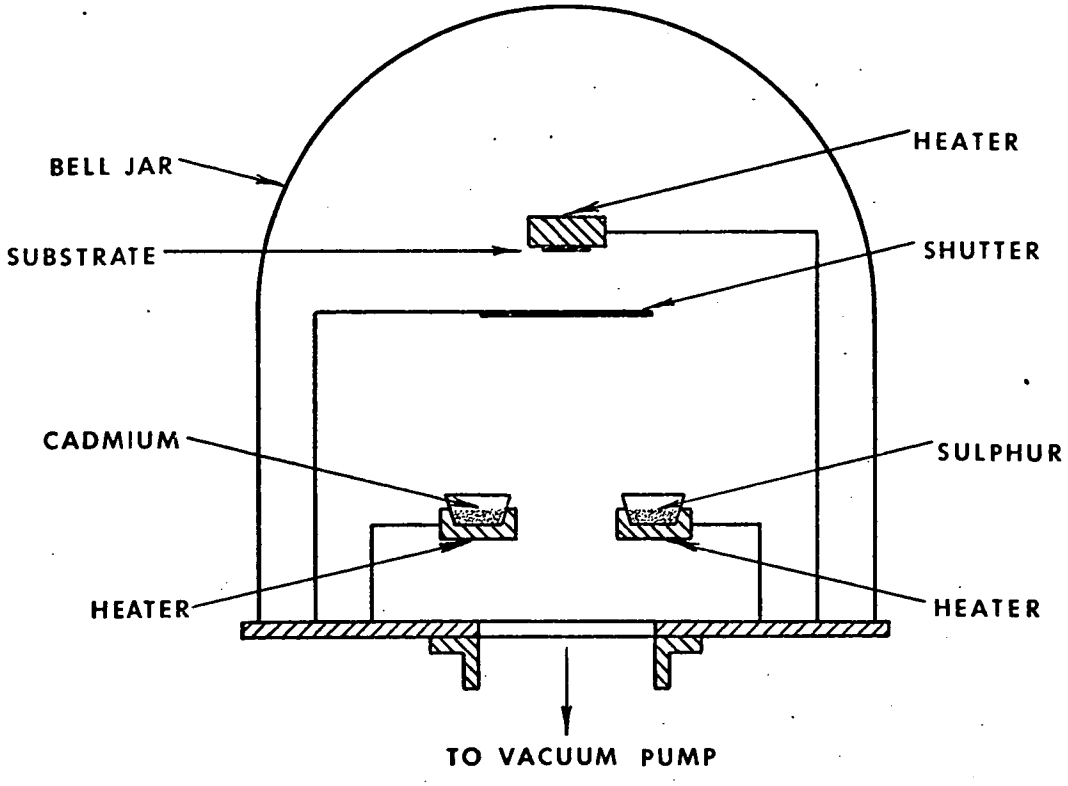


FIG 2.4.1.

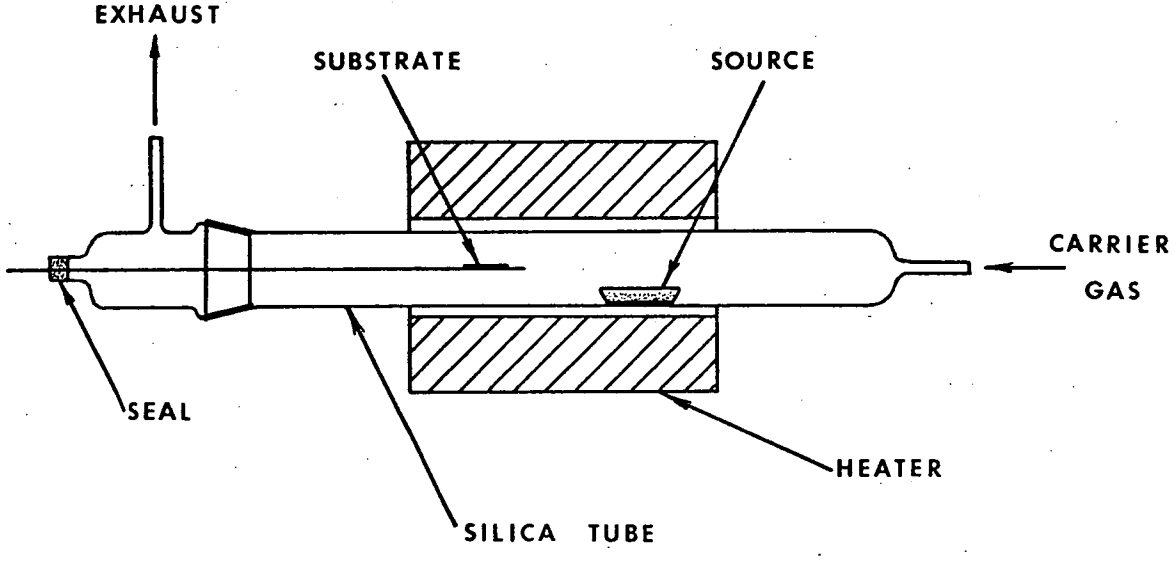


FIG 2.4.2.

of monosource films frequently at the expense of degraded piezoelectric properties.
De Klerk and Kelly have found that over a substrate temperature range of 50°C to 200°C neither cadmium nor sulphur would condense independently, hence ensuring only depositions of cadmium sulphide within this temperature range.

Evidence will be presented later to show that preferential deposition elsewhere in the apparatus may be an important factor in preventing growth.

Other variations include growth from the vapour phase at atmospheric pressure, Fig.2.4.2, by hydrogen transport [96,97,98,99], and by nitrogen transport [100]. Capella [101] has grown epitaxial films by the reaction :

$$H_2S + CdC\ell_2 \longrightarrow CdS + 2HC\ell \qquad (2.4.1.)$$

and Jacobs and Hart [102] by the reaction :

$$H_2S + Cd \longrightarrow CdS + H_2 \qquad (2.4.2.)$$

at a pressure of 10 torr. Polycrystalline epitaxial deposits have been obtained by these methods but little information relating to their stoichiometry is available.

In sputtering [103] the more complex growth conditions resulting from the presence of charged particles and vapours at relatively high pressures generally result in less well ordered films. Lichtensteiger et al [104] have prepared p-type material by diode sputtering methods using an

atmosphere of argon doped with phosphine.

An interesting investigation into growth of cadmium sulphide films by sulphidation of an existing cadmium film was performed by Hecht [105] et al, who obtained on glass substrates homogeneous films comparable in crystallinity and resistivity with evaporated films. An earlier attempt to produce cadmium sulphide films by a similar method was made by Mollwo [106]. Thermal flexibility is somewhat restricted in this method because of the need to maintain the entire deposition apparatus at a high temperature to prevent spurious condensation of sulphur.

Of particular importance in the production of photosensitive layers is the sintering process [107,108], Fig. 2.4.3, and the chemical spray process [109], Fig. 2.4.4.

In the quest for a production system capable of yielding cadmium sulphide films to meet the requirements defined in the first chapter the adoption of a vacuum method was favoured in view of the potential reduction on the substrate in numbers of adsorbed gas atoms which can result in a wide range of structural modifications in the film through their effect on surface mobility and their potential chemical reactivity.

2.5 INFLUENCE ON THE SUBSTRATE :

Evidence of some degree of orientation of

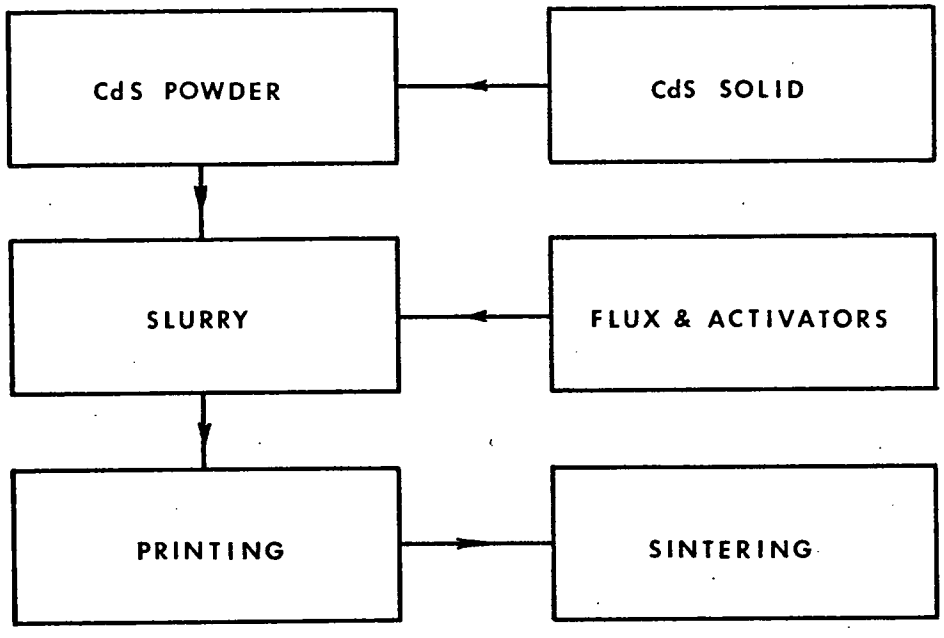


FIG 2.4.3.

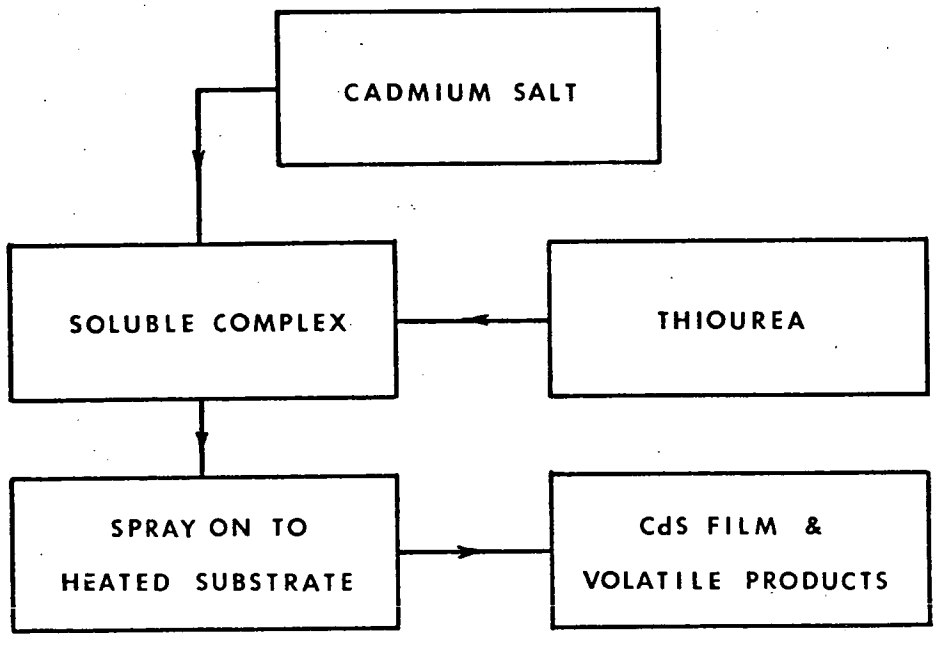


FIG 2.4.4.

cadmium sulphide films, even on amorphous substrates has frequently been noted[85, 86, 87,110,111]. The films range from amorphous to crystalline and the phase generally reported in polycrystalline films is the hexagonal phase which occurs generally with its [0001] axis arranged perpendicular to the substrate but randomly oriented in the other two directions. This situation is favoured by a larger binding energy between condensing atoms than exists between these atoms and the substrate. An increase in substrate temperature confers increased surface diffusion energy on the condensing species and thus extends the range of ordering. This is reflected in an increasing crystallite size with temperature, a phenomenon observed by several workers [112,113,114]. Such films usually also exhibit increasing crystallite dimensions with film thickness [115] presumably due to autoepitaxial effects. Experimental confirmation of this effect is presented in the fourth chapter.

Depositions on orienting substrates of monocrystalline nature aimed at promoting a more ordered structure have revealed the existence of polymorphic films [116,117,118]. Some doubt [119] exists as to the exact role of the substrate in influencing the preferred modification in view of the growth of cubic cadmium sulphide on hexagonal and even amorphous substrates at certain temperatures [120,121].

Structure variations are also sensitive to deposition rate and relative vapour pressures of the condensing species.

The occurrence of epitaxy reflects the influence of a substrate on its condensate. Atoms or molecules approaching a hypothetical perfectly amorphous substrate encounter a quasi-periodic potential field contributed by the substrate and subsequent to collision with the substrate may be adsorbed to contribute towards film growth, or re-emitted. Early stages of film growth are generally found to begin with the generation of isolated three dimensional islands or nuclei which are favoured by a decrease in the free energy of formation with increasing size. The formation of agglomerates of particles in islands is not necessarily a prerequisite for film growth since the contact angle between the over-growth, usually assumed to be a spherical cap for convenience, and the substrate may be zero for a substrate whose surface free energy exceeds that of the interface and overgrowth, for example the growth of lead on (111) plane silver [122]. Completely random conditions of deposition encouraged by a high deposition rate or low temperature may result in a similar situation through the condensate being "frozen" at the point of impact.

Islands may assume critical dimensions by surface diffusion of adsorbed monomer, by direct

monomer impingement from the vapour or by acceptance of a subcritical embryo from the vapour phase which becomes supercritical on adsorption. The former process is generally accepted and its operation may be treated according to the dimensions of the critical nucleus for example, the capillarity model of Hirth and Pound [123], or the atomistic approach of Rhodin and Walton [124]. Due to the small probability of an approaching atom finding itself directly in a potential well on the substrate surface, the process of surface diffusion may operate even on amorphous substrates where long range order is lacking.

In practice only approximations to a perfectly smooth clean and isotropic substrate surface are available and the nucleation process may be dominated by preferential nucleation on surface defects such as monatomic steps, or dislocations [125]. The presence of impurities or adsorbed gas on the surface is inevitable and their effects may be especially important if they are capable of forming a chemical compound with the condensate. Reid [126] for example has discovered variations in cadmium sulphide film structure purely due to ion bombardment of the substrate surface prior to deposition.

Since atomic surface mobility is an exponential

function of substrate temperature, it is reasonable to assume a critical dependence of film growth on this parameter. Control of surface diffusion by substrate temperature influences the initial formation of nuclei, their probability of coalescence and hence their apparently liquid like behaviour. Increased ordering of cadmium sulphide films with temperature on amorphous substrates has already been mentioned.

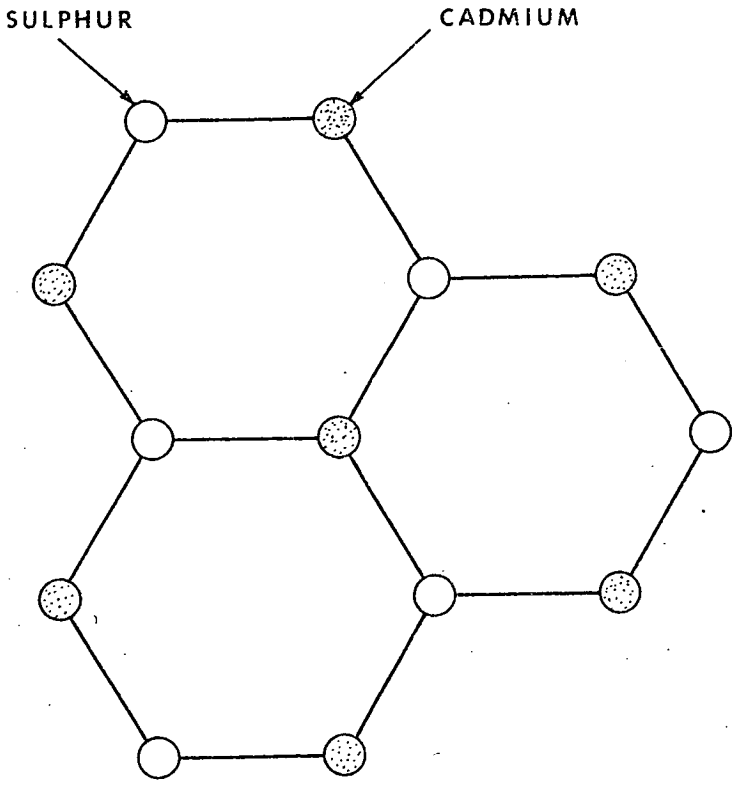
The introduction of a monocrystalline substrate imparts theoretically a periodicity to the surface potential field of the substrate, the object of epitaxial growth being to render this the dominant factor in influencing film growth. Considerable interest in epitaxial growth has been generated in recent years by the development of improved semiconductor devices, in particular the autoepitaxy of silicon and germanium.

Basic theories of epitaxy disagree on the relative importance of nucleation and subsequent growth processes, as well as on the nature of the initially nucleated deposit. The postulate of Frank and Van der Merwe [127] and Rhodin [128] that deposit atoms become arranged in regular surface potential wells of the substrate forming a pseudomorphic lattice on which subsequent layers approach gradually with increasing film thickness

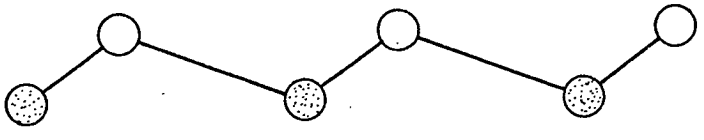
the correct lattice constants for the deposit fails to explain the occurrence of epitaxy at lattice misfits in excess of approximately 10%. The assumption of discrete nuclei formation in an atomic arrangement corresponding to the bulk lattice followed by coalescing growth of similarly oriented nuclei by Basset et al [129] is compatible with the observed occurrence of epitaxy at large misfits but places emphasis on orientation at the initial nucleation stage rather than on recrystallisation on a microscopic scale after initial nucleation. The latter view is favoured by Pashley [130] and experimental evidence supporting this view will be presented in Chapter 4. It seems likely that in view of the inevitable surface damage and disorder occurring in practice on the substrate, a regular periodic potential array is not viewed by the condensate but rather randomly distributed regions of good crystal structure interspersed with damaged regions. Ordered growth could occur on relatively undamaged regions and recrystallisation could proceed to adjust favourably the orientation of nuclei deposited in the intermediate regions since their binding to the substrate should be inferior. The ratio of damaged to undamaged sites would then be a major factor in the determination of the ease of microscopic recrystallisation, and crystallite size

obtainable on a particular substrate. Chopra [131] has shown that the influence of an orienting substrate may be obscured by an amorphous carbon film of 200 Angstrom thickness which suggests that substrate orientation may be readily obscured by a film which is not amenable to recyrstallisation. Further evidence in support of these theories is furnished by Chapter 4.

It is interesting to note that although lattice mismatch in the plane of the substrate is considered to be of importance in influencing epitaxy, little or no emphasis is placed on mismatch perpendicular to the substrate. It is postulated that this parameter may be of importance, particularly in the case of cadmium sulphide where a chemical reaction must occur at the substrate surface prior to growth of the compound. Experimental evidence in Chapter 4 confirms that epitaxy is most easily obtainable on an atomically highly textured substrate surface of sapphire. An analogy is proposed between the actions of vanadium pentoxide, which is a common catalyst for chemical reactions which it may influence by disturbing physically the reactants on its surface, and sapphire which possesses the same crystal structure. Comparative plans of various substrate planes employed in experimental work are presented in Figs. 2.5.1, — 2.5.4.

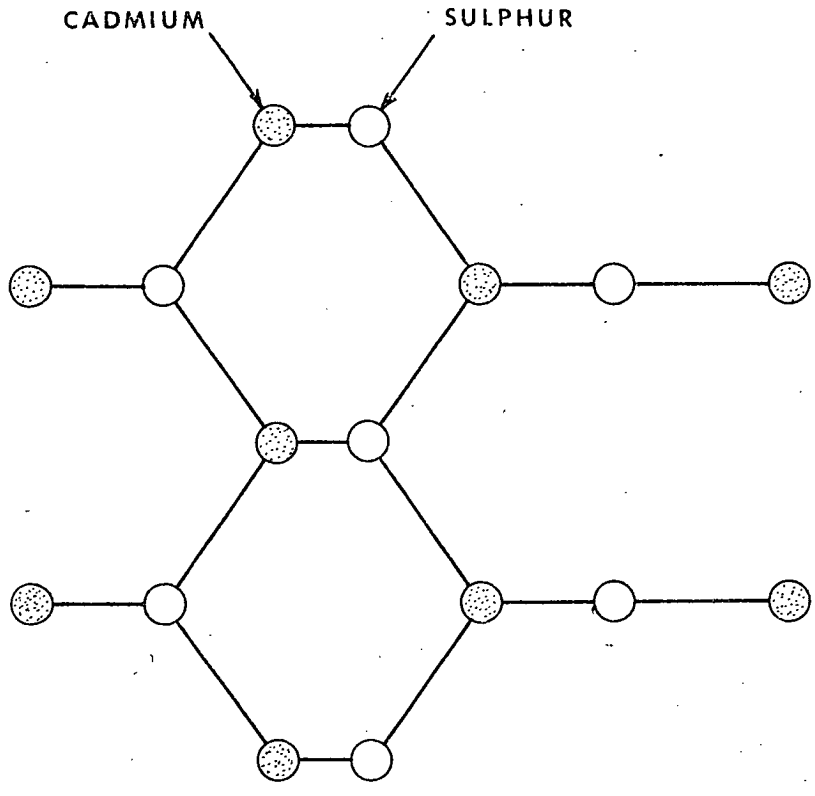


CdS (0001) PLANE

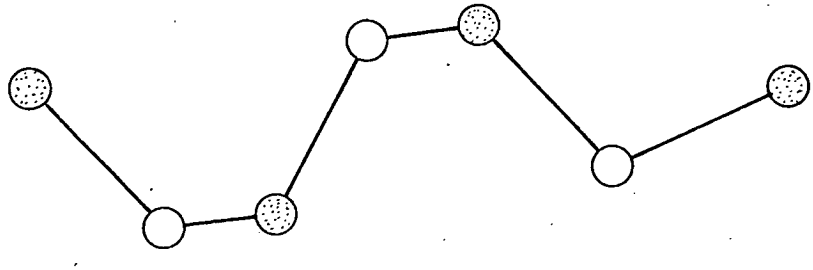


SECTION THROUGH CdS (0001) PLANE

FIG 2.5.1.

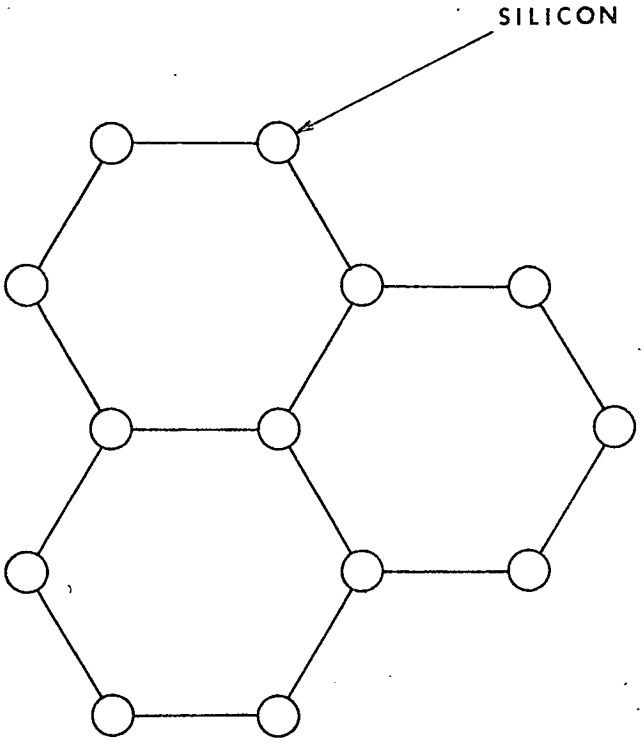


CdS $(10\bar{1}2)$ PLANE

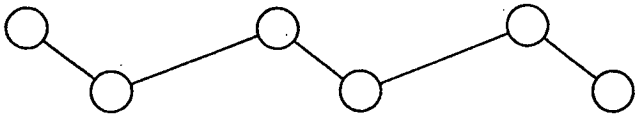


SECTION THROUGH CdS $(10\bar{1}2)$ PLANE

FIG 2.5.2.



SILICON (111) PLANE



SECTION THROUGH SILICON (111) PLANE

FIG 2.5.3.

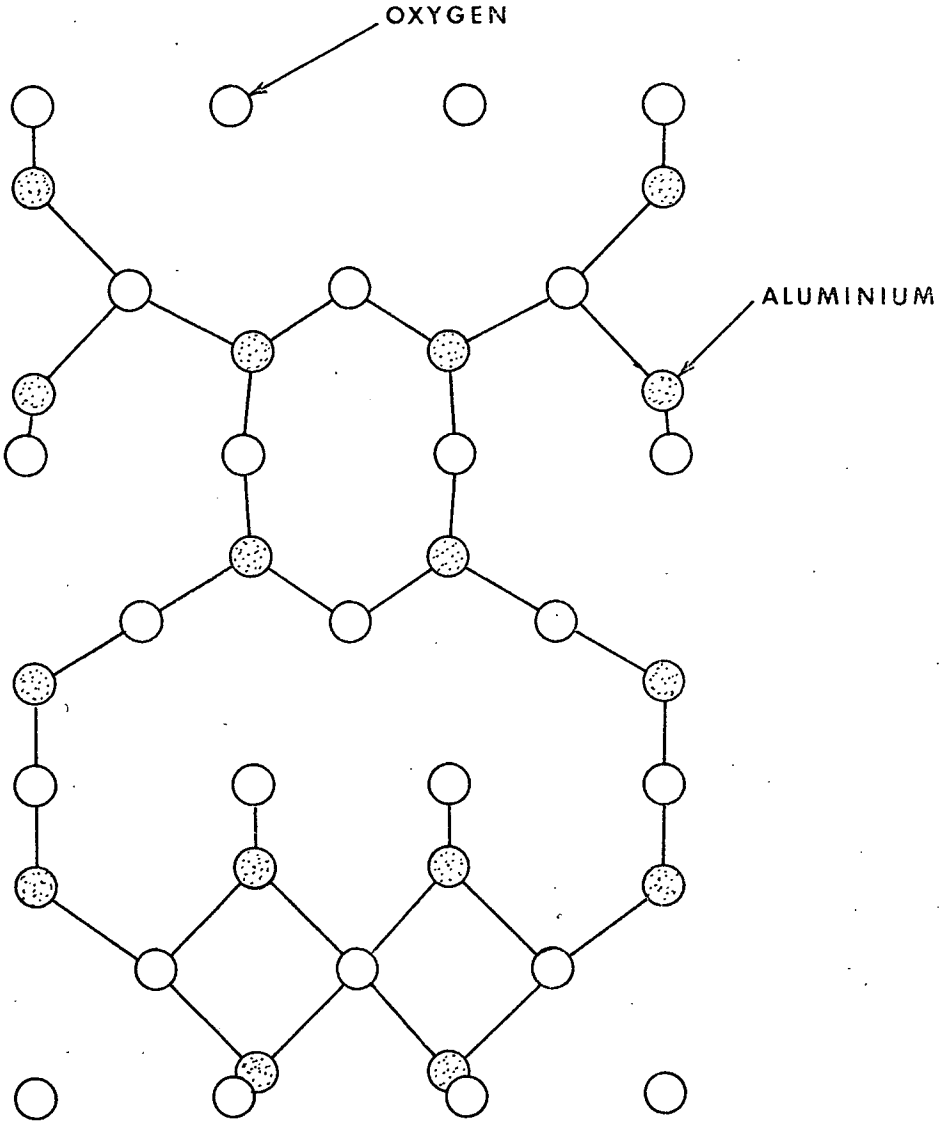

OXYGEN
ALUMINIUM
Al_2O_3 $(2\bar{1}\bar{1}0)$ PLANE
SECTION THROUGH Al_2O_3 $(2\bar{1}\bar{1}0)$ PLANE

FIG 2.5.4.

2.6 ACTIVATION AND RECRYSTALLISATION OF FILMS :

Activation is the process of incorporating impurities into a crystal for a specific purpose, usually to obtain or modify photoconduction or luminescence properties in which direct band to band transitions are relatively unimportant. Metals of Group I, for example copper, gold and silver, are often introduced as acceptors, or a non-metal from Group VII, usually chlorine, may act as a donor. Methods of dopant introduction include evaporation of dopants on to the film surface, firing the film in atmospheres of dopant, or addition of dopants to the source material prior to deposition. In view of the already complex interactions, which are not well understood, involved in preparing these films, such additional processes must inevitably suffer a lack of standardisation. Allied to the process of activation and developed from it [80] is the phenomenon of bulk recrystallisation, a process which is considered to be virtually independent of the substrate [115] and in common with other catalytic actions is not associated with a convincing theory explaining its underlying mechanism.

Experimental evidence indicates that recrystallisation occurs under conditions of heat treatment in vacuum [117, 132], heat treatment

in various gas atmospheres [133,134,135], and in a Group I metal induced catalytic process [91,115]. An attempt to combine essentially these methods was made by Böer Esbitt and Kaufman [136], and while increases in Hall mobility and crystallite size are available, the piezoelectric properties may be adversely affected by the resulting grain tilts of up to 25° away from the substrate normal of the [0001] axis.

It is felt that a concentration of effort at the deposition stage is perhaps a more elegant approach to the problems of improving film quality.

CHAPTER 3.

ADVANCES IN CADMIUM SULPHIDE FILM PRODUCTION TECHNIQUES.

3.1 IMPROVEMENTS IN FILM DEPOSITION TECHNIQUES :

Assuming the adoption of a vacuum deposition technique as described in paragraph 2.4, the production of layers containing a measure of excess cadmium must be expected since the adsorption process at the substrate is biased in favour of the cadmium species at substrate temperatures normally employed. Artificial enrichment of the vapour stream in the more volatile component by an independent sulphur source, pre-enrichment of the charge or by reversion to separate elemental sources, invokes an additional degree of freedom which requires precise control if reproducible results are to be attained. This presents a particularly difficult situation in the first case and to a lesser extent in the latter, in that although independent source temperature control is externally available, evaporation rates within the deposition chamber are mutually dependent. Some doubt also exists as to whether the high values of resistivity thus attainable are induced by improved stoichiometry, or by sulphur lattice imperfections. Moreover, little influence is exerted on other properties of cadmium sulphide thin films, such as their polycrystallinity, variable crystallographic orientation and polymorphic tendencies. Alternatively an increase in substrate temperature, (paragraphs 2.3 and 2.5), during deposition exerts

EX BIBL UNIV. EDINBURGEN

a beneficial influence on the film composition, the consequently enhanced mobility on the surface of the substrate which is enjoyed by the condensate being reflected in enlarged crystallite dimensions and a reduced density of intrinsic defects. A natural limiting factor in the elevation of substrate temperature is the attendant reduction in adsorption time by the substrate of the impinging species, which acts to suppress the growth rate and ultimately to prohibit continuous condensation. This commonly occurs at substrate temperatures in excess of 200°C in conventional monosource systems as shown in Fig. 3.1.1, and no serious effort appears to have been directed to significantly increasing this figure until Addiss [115], in pursuit of films suitable for recrystallisation studies, was forced to conclude that the most critical part of the process was the initial cadmium sulphide deposition.

To reduce excessive preferential condensation on the vacuum chamber outer walls at high substrate temperatures a small inner chamber, Fig. 3.1.2, radiantly heated by the source and substrate heaters was introduced, its effect being to encourage increased vapour pressure, the increase being most marked for the component of lowest condensation coefficient. The improved quality of films thus deposited at substrate temperatures between 200°C and 250°C permitted the observation of a catalytic recrystallisation process, which employed a Group I thin

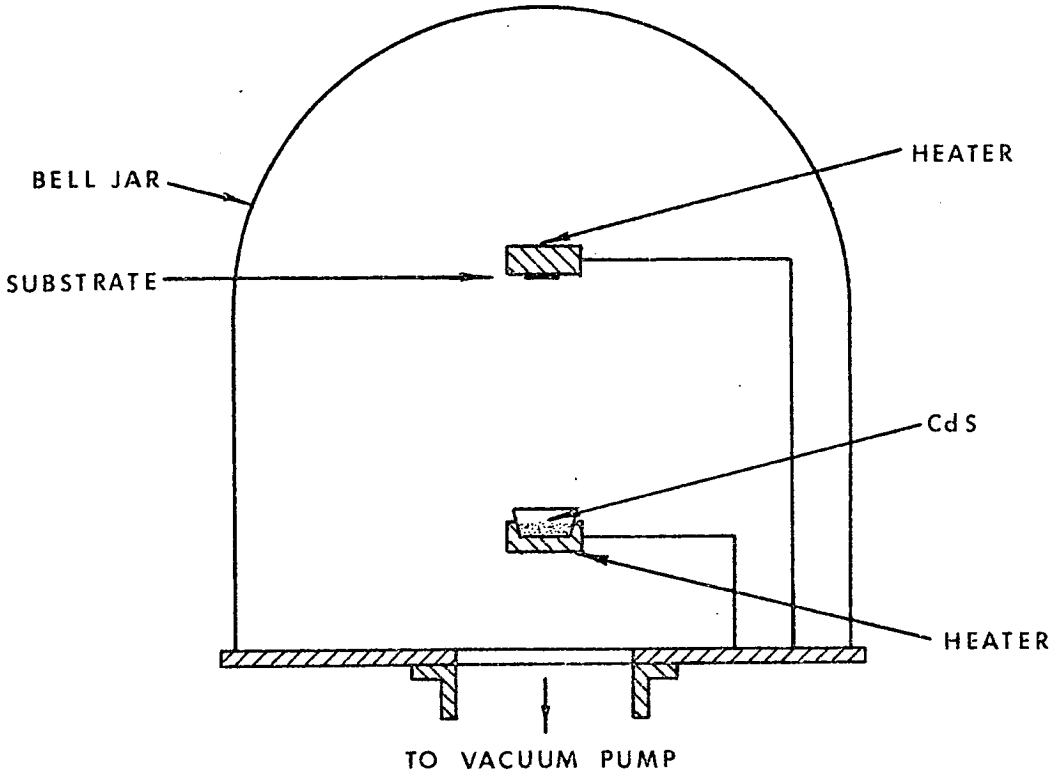


FIG 3.1.1.

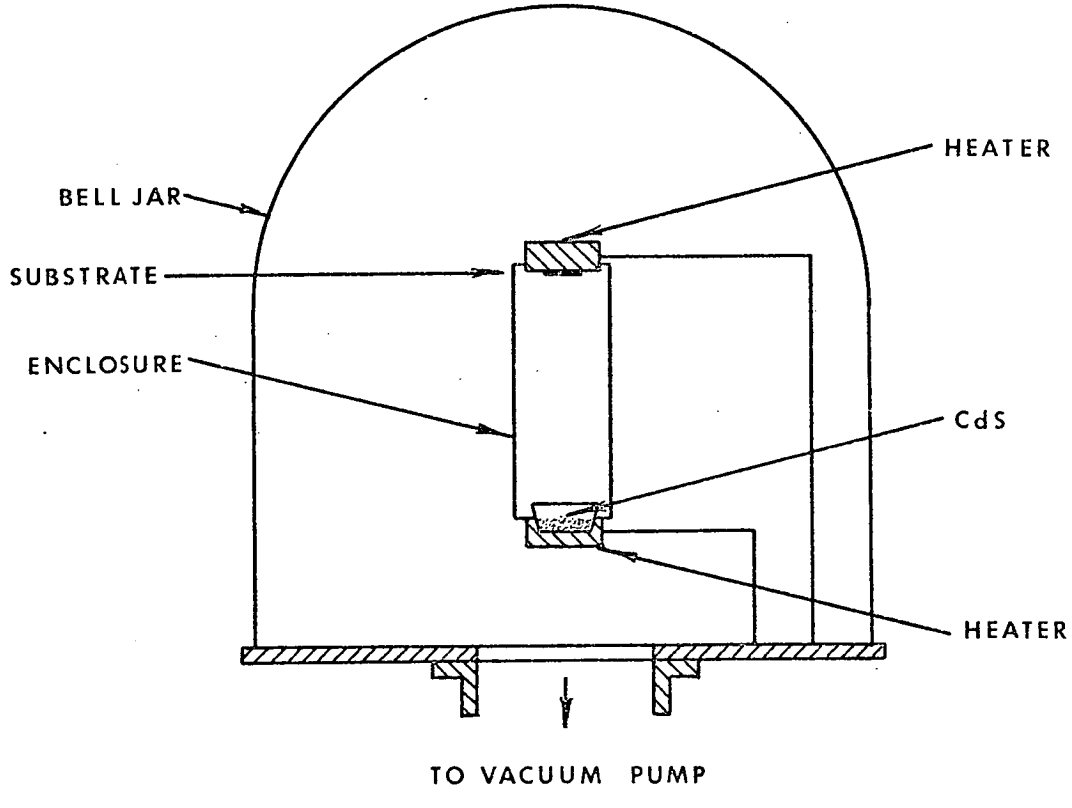


FIG 3.1.2.

metal film deposited on the surface, followed by heat treatment in an argon atmosphere. This could not be observed in films conventionally deposited at a substrate temperature of 150°C. A similar procedure enabled Brunnschweiler [137] to deposit single crystal films of cadmium selenide on mica at substrate temperatures of 200°C to 450°C and Reid's [126] adaptation, Fig. 3.1.3, in which a resistance-heated tantalum chimney combined the functions of substrate heater, holder and heated deposition chamber, permitted the deposition of good quality cadmium sulphide films on mica (muscovite) at similar temperatures. In both cases, initial nucleation demanded a source - substrate temperature differential in excess of that required for steady state deposition. This state was induced by depression of substrate temperature.

A different design approach exploiting the same principles was evolved by Hudock [138] in a system, Fig. 3.1.4, featuring a sublimation technique using near equilibrium conditions in ultra-high vacuum. Hall mobilities and resistivities of the films were found to be strongly influenced by the source impurity concentration and resistivity. Untreated films deposited at 2×10^{-10} torr background pressure on sapphire substrates at 450°C exhibited Hall mobilities of

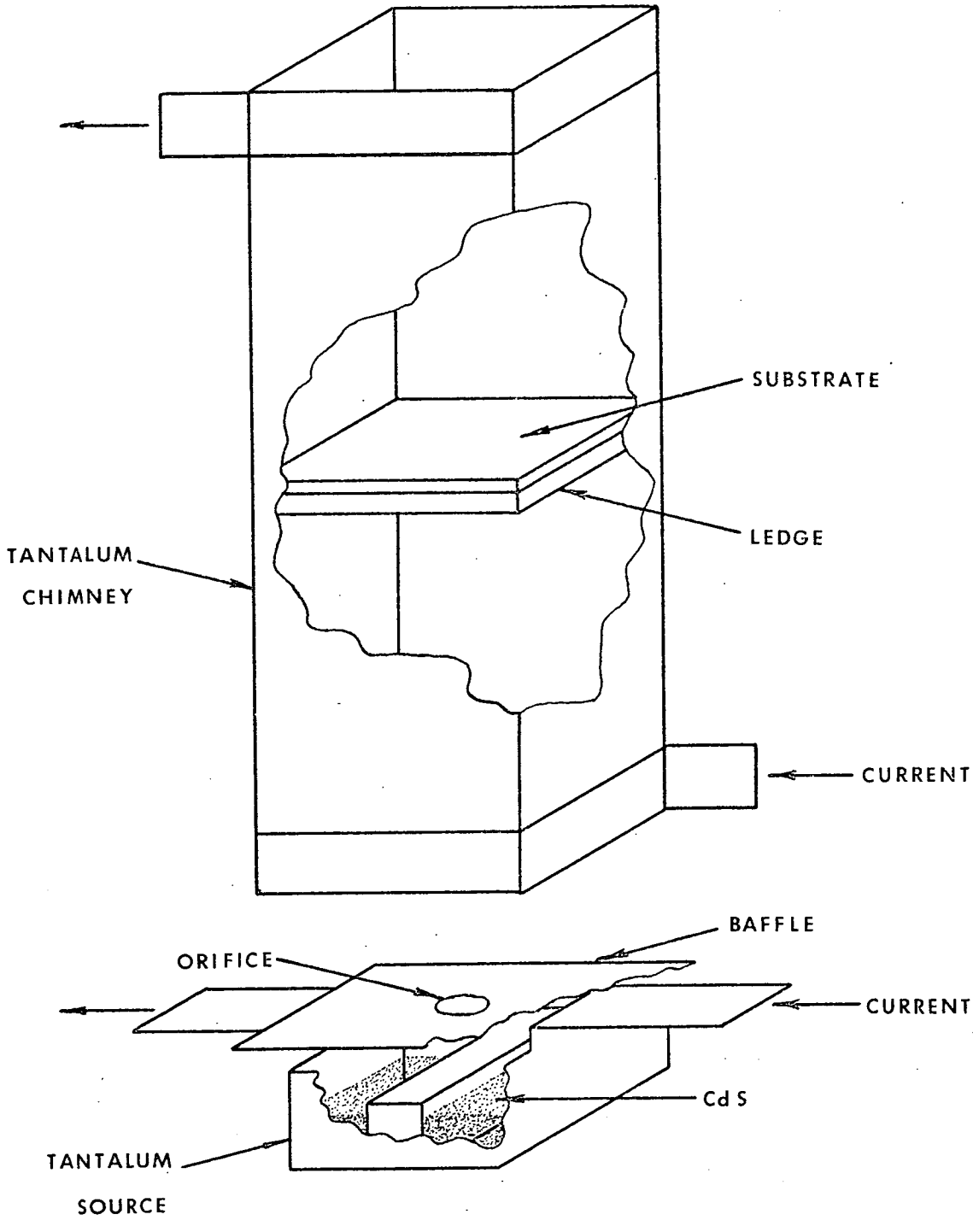

SUBSTRATE
LEDGE
TANTALUM
CHIMNEY
CURRENT
BAFFLE
ORIFICE
CURRENT
Cd S
TANTALUM
SOURCE

FIG 3.1.3.

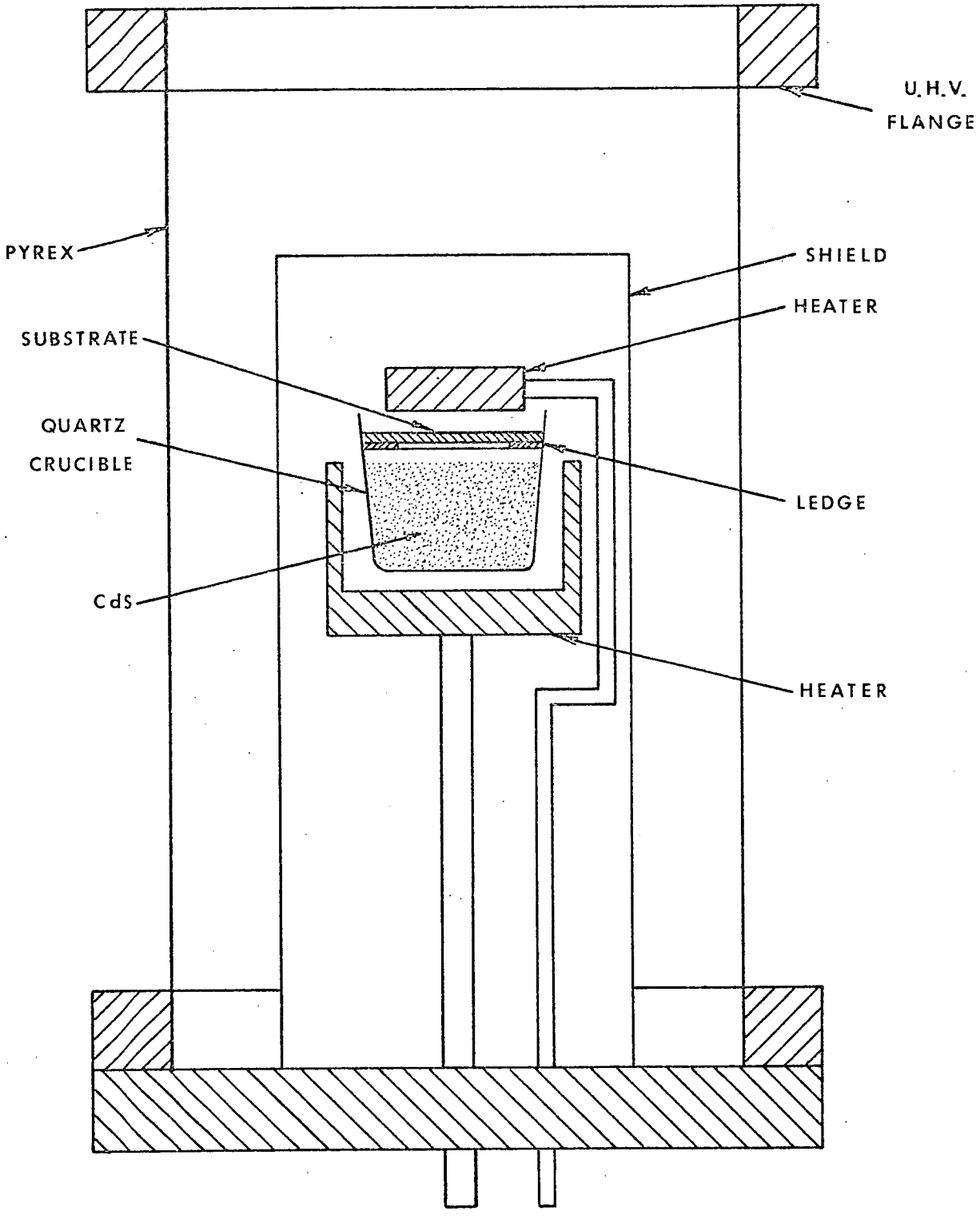

U.H.V.
FLANGE
PYREX
SHIELD
HEATER
SUBSTRATE
QUARTZ
CRUCIBLE
LEDGE
CdS
HEATER

FIG 3.1.4.

between 15 x 10^{-4} and 54 x 10^{-4} metre^2/volt sec whereas a background pressure of 10^{-7} torr reduced this to 5 x 10^{-4} metre^2/volt sec. This unusually pronounced pressure dependence can perhaps be related to the low source temperature of 475^{o}C employed, since the rate of component incidence on the substrate from such a source would be readily rivalled by residual gas incidence rates. Information on deposition rates is lacking and an assessment of charge stoichiometry based on the resistivity of 10^{-2} to 2 x 10^{2} ohm-metre suggests either cadmium biased or donor rich charge material. However, the inferiority of electronic grade powder to crystalline source material was clearly demonstrated. The film's [0001] axis was observed to grow perpendicular to the substrate face although no crystallographic orientation was quoted to define this face.

Further elevation of substrate temperature was investigated by Igarashi [139] in a system based on similar design criteria, Fig. 3.1.5. Epitaxial growth of hexagonal material with the [0001] axis oriented normal to the surface was observed on the (111) "arsenic face" of gallium arsenide at substrate temperatures in excess of 840^{o}C while polymorphic material was found to characterise layers deposited at less than 800^{o}C on this face. Information defining the source material is absent

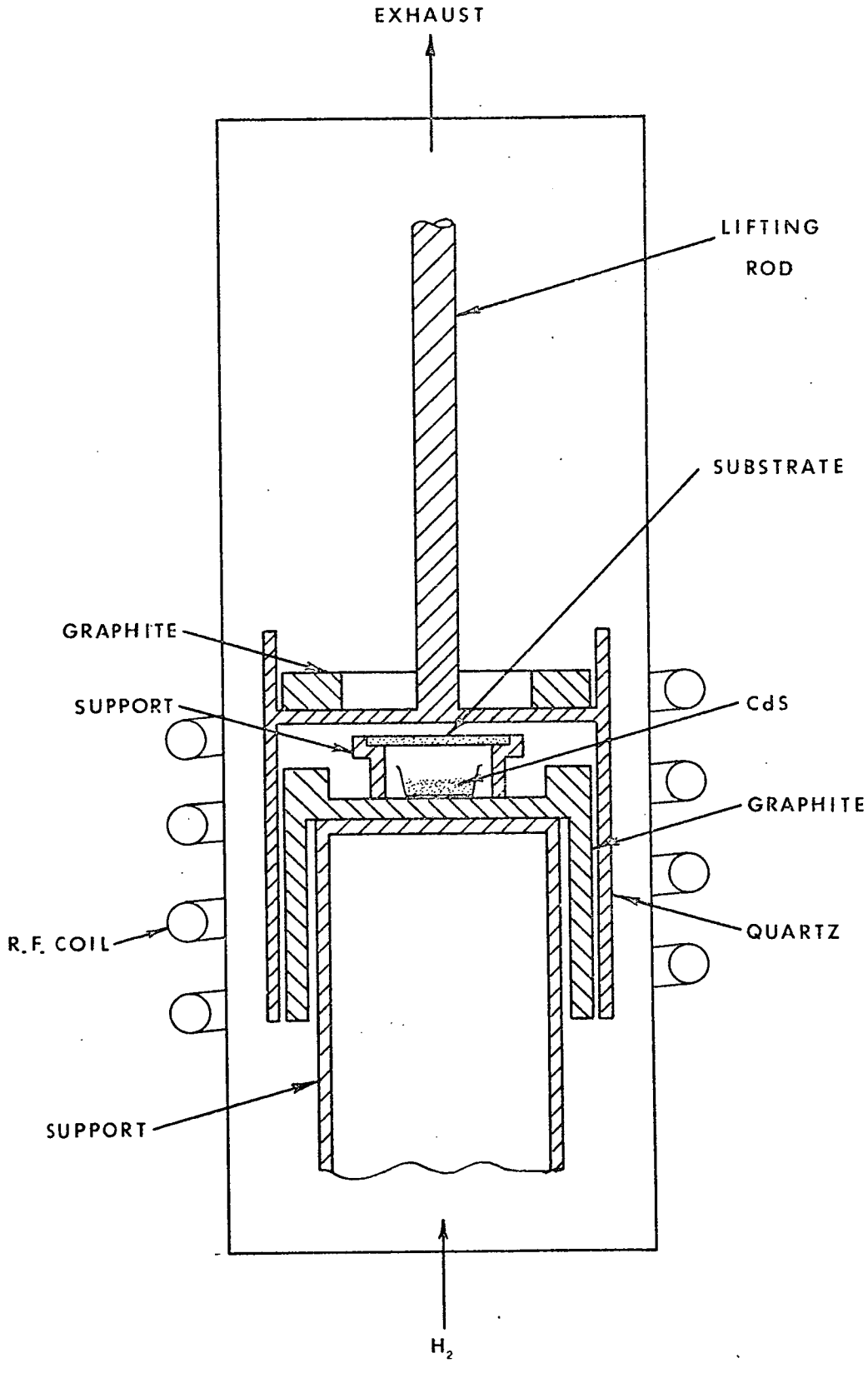

EXHAUST
LIFTING ROD
SUBSTRATE
GRAPHITE
SUPPORT
CdS
GRAPHITE
QUARTZ
R.F. COIL
SUPPORT
H_2

FIG 3.1.5.

and depositions were performed in an atmosphereof hydrogen at an undisclosed pressure. The presence of a reactive gas in this system would be expected to complicate the processes of nucleation and diffusion involved in epitaxy, as stated in the previous chapter.

3.2 VAPOUR PHASE GROWTH OF CADMIUM SULPHIDE BULK CRYSTALS :

Although conditions in film growth as the substrate temperature is raised bear an increasing resemblance to bulk crystal growth conditions, little effort has been directed to an application of knowledge gained from the latter process to the former in spite of the fact that its aim is usually to produce a film which resembles crystallographically, if not dimensionally, a bulk crystal.

Interest in II-VI bulk crystals preceded that in films by many years, being generated principally by their photo-conductive properties. The first sizeable synthetic II-VI crystals were produced by Lorenz[140] in a dynamic method which was followed by Frerichs [141,142] adaptation, Fig. 3.2.1, in which hexagonal phase platelet and ribbon type single crystals up to 2×10^{-2} metre in length with [0001] axes parallel to the platelet faces were produced by the reaction :

$$Cd + H_2S \longrightarrow CdS + H_2 \qquad (3.2.1.)$$

Modifications of Frerichs method have been used by several workers [143,144,145,146].

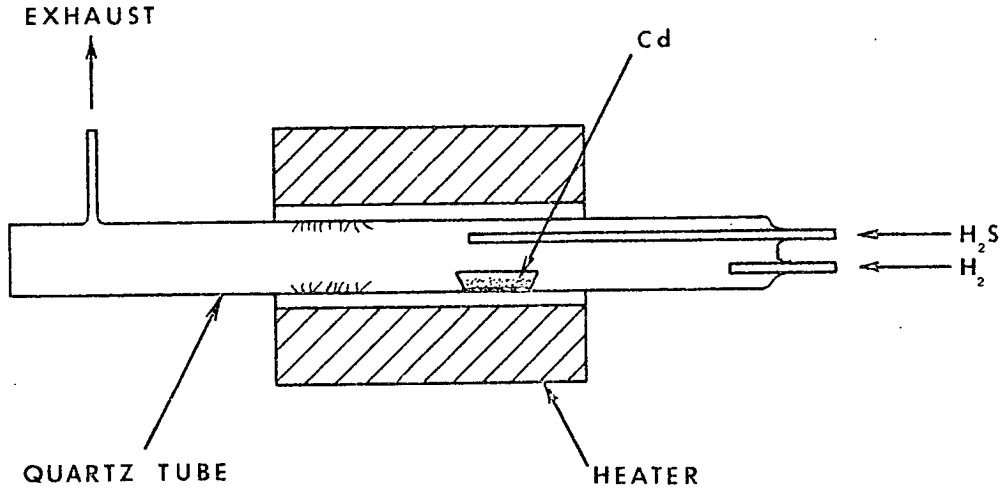


FIG 3.2.1.

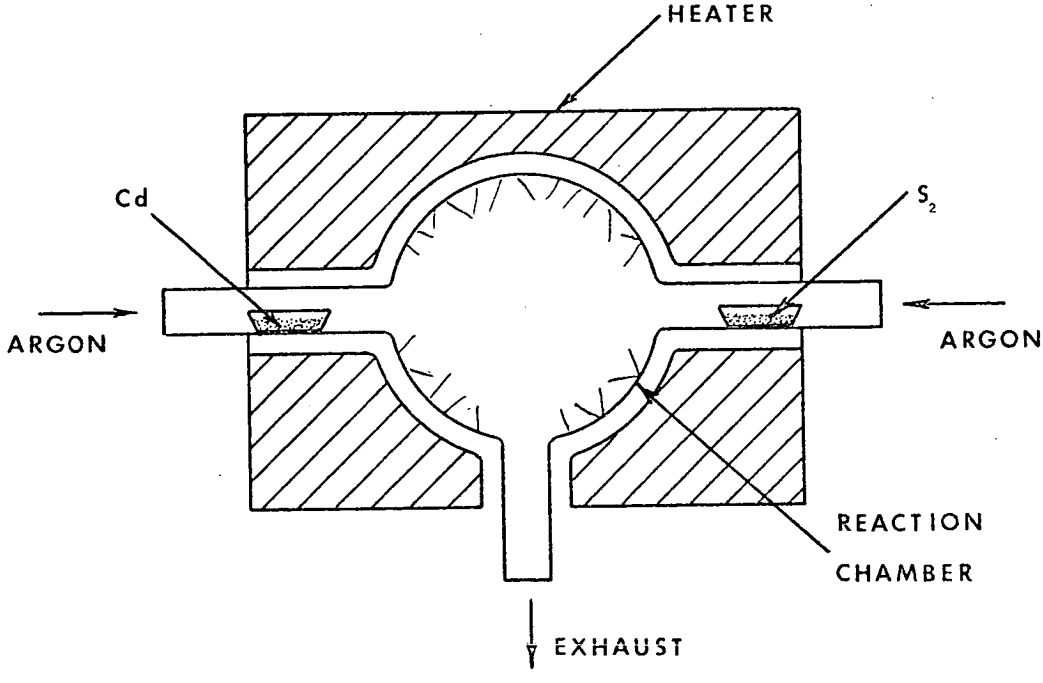


FIG 3.2.2.

A further modification by Bishop and Liebson [147], Fig. 3.2.2, employed separate cadmium and sulphur sources with argon as a carrier gas and may be considered as a non-vacuum co-evaporation technique preceding by some years the corresponding vacuum technique of Miller et al [92]. The principal attractive feature of dynamic systems is their ability to function without a preformed charge of the II-VI compound, which in many cases is not readily available in a high purity form. It tends, however, to be limited to growth of plate or ribbon type crystals and to overcome this Czyzak et al [148] developed a static method, in which the charge was sealed at the centre of a fused silica tube in an atmosphere of hydrogen sulphide. Nucleation occurred on the charge itself to yield hexagonal prismatic crystals which naturally tend to incorporate charge impurities. This technique was modified by Greene et al [149] to transfer nucleation from the charge to a seed plate, Fig 3.2.3, and by Fochs [150] to grow either platelets or needle-like crystals by adjusting the temperature differential between separate charge and crystal furnace elements.

The above static methods suffer an inherent lack of reproducibility in their results, in some measure due to the dependence of growth conditions on the purity and composition of the charge which in turn is difficult to measure and reproduce. A more

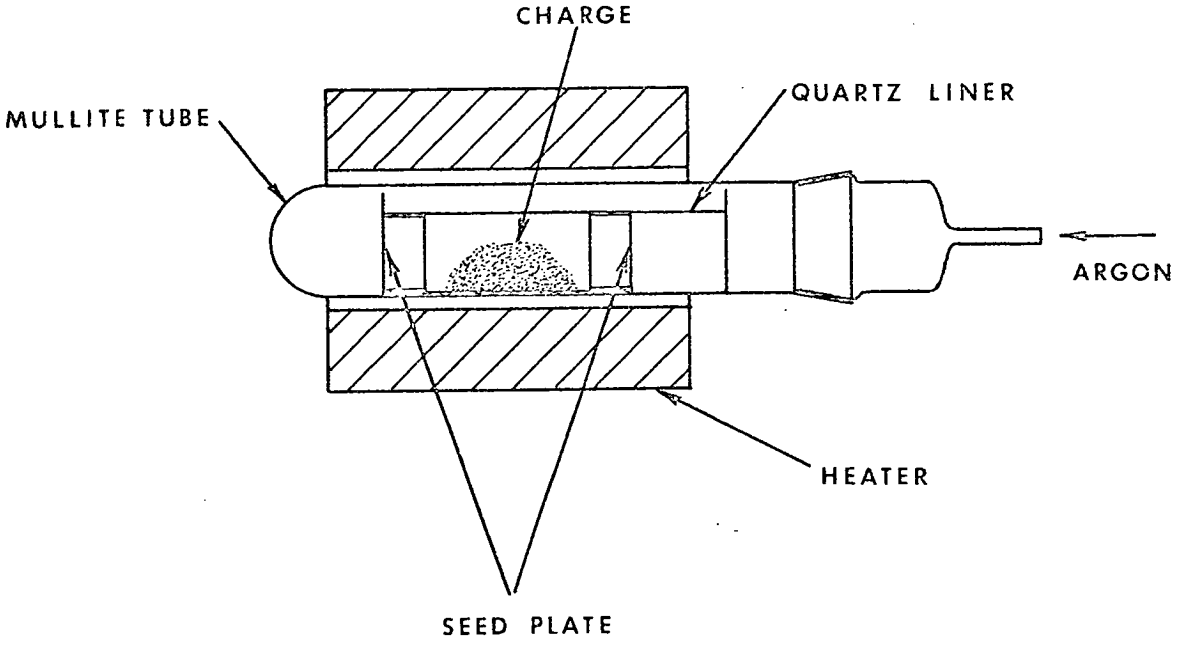


FIG 3.2.3.

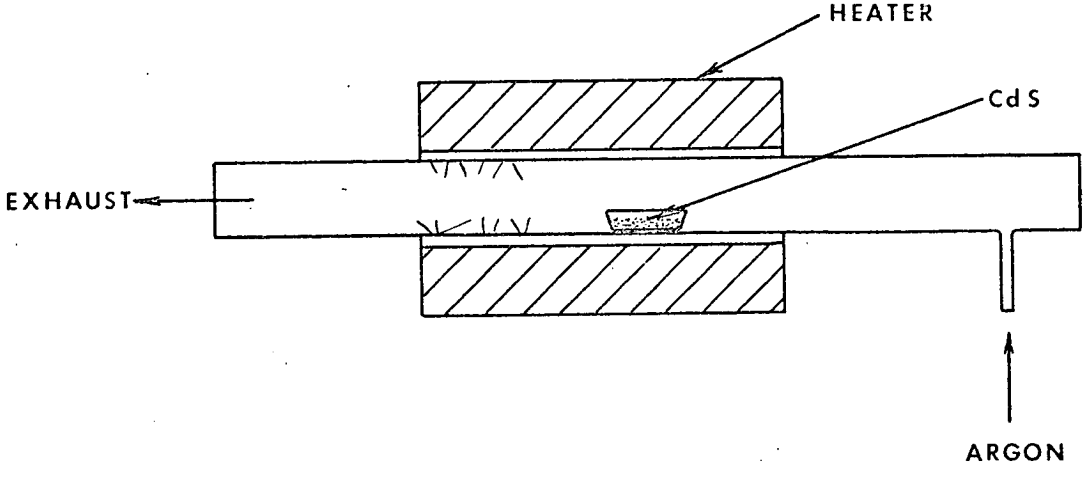


FIG 3.2.5.

controllable procedure was introduced by Piper and Polich [151] in which a fused quartz capsule, Fig.3.2.4, loaded with purified and sintered charge is heated in an argon stream at 1 atmosphere pressure with the crucible tip near the temperature profile peak. Escaping vapour seals off the capsule near the final temperature configuration in which the tip is cooled to induce nucleation thus confining the remainder of the charge. Excess of either component or volatile impurity is thus presented with an opportunity to escape before growth commences. Analogous to the sealed system of Fochs for needle and platelet growth is the inert gas transport system [152,153] shown in Fig. 3.2.5, which offers reduced sensitivity to volatile impurities in the charge.

A more convenient configuration based on the Piper and Polich method is described by Clark and Woods [154] and Fochs [155] et al, Fig. 3.2.6 in which a long tail communicating with the otherwise sealed growth chamber provides a condensation facility for excess cadmium or sulphur. In addition, a reservoir of either component in the tail section permits modification of partial pressures in the upper chamber by maintaining the tail at a controlled temperature.

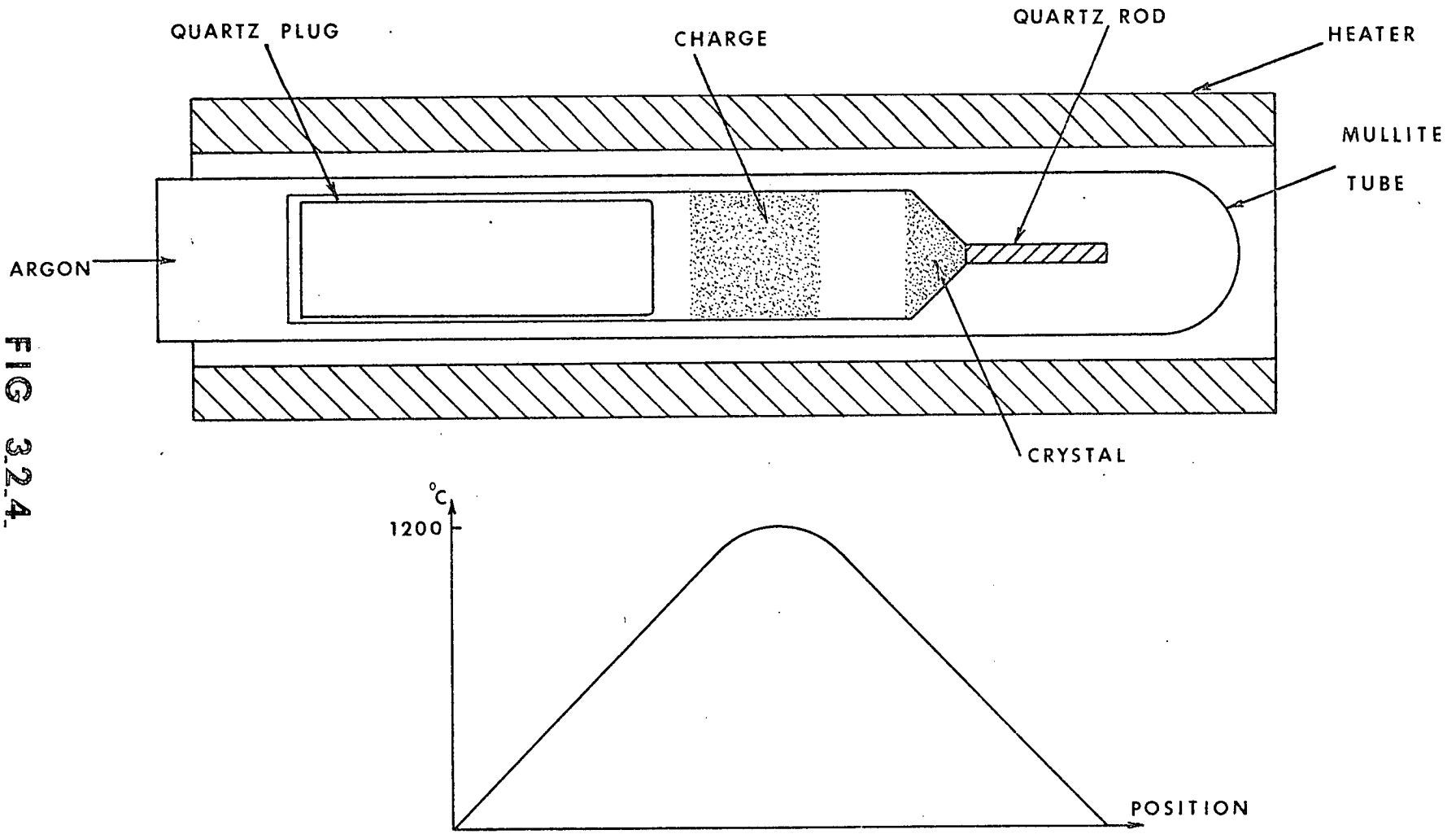

QUARTZ PLUG
CHARGE
QUARTZ ROD
HEATER
MULLITE
TUBE
ARGON
CRYSTAL
°C
1200
POSITION

FIG 3.2.4.

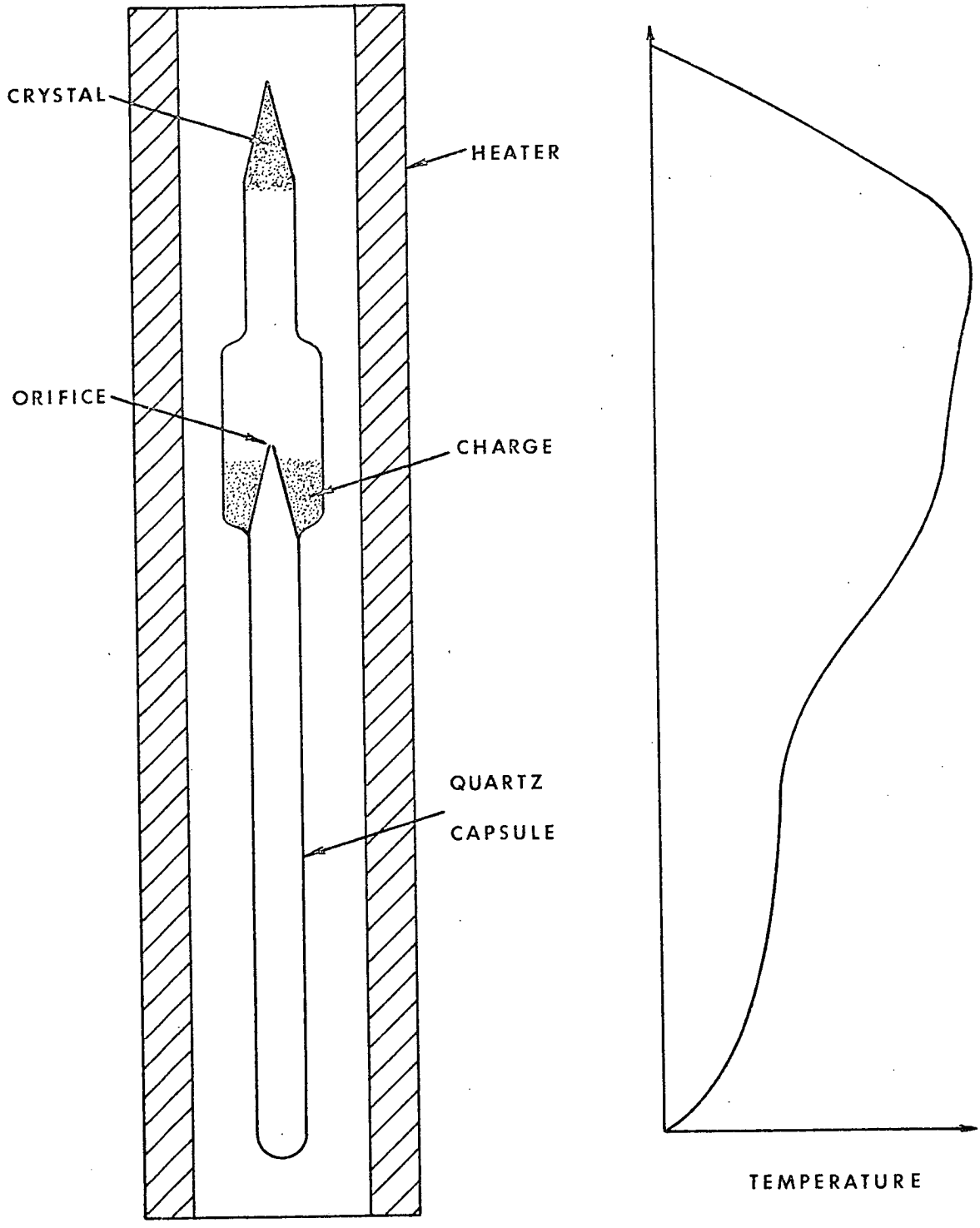

CRYSTAL
HEATER
ORIFICE
CHARGE
QUARTZ
CAPSULE
TEMPERATURE

FIG 3.2.6.

3.3 DESIGN CRITERIA - SYSTEM 1.

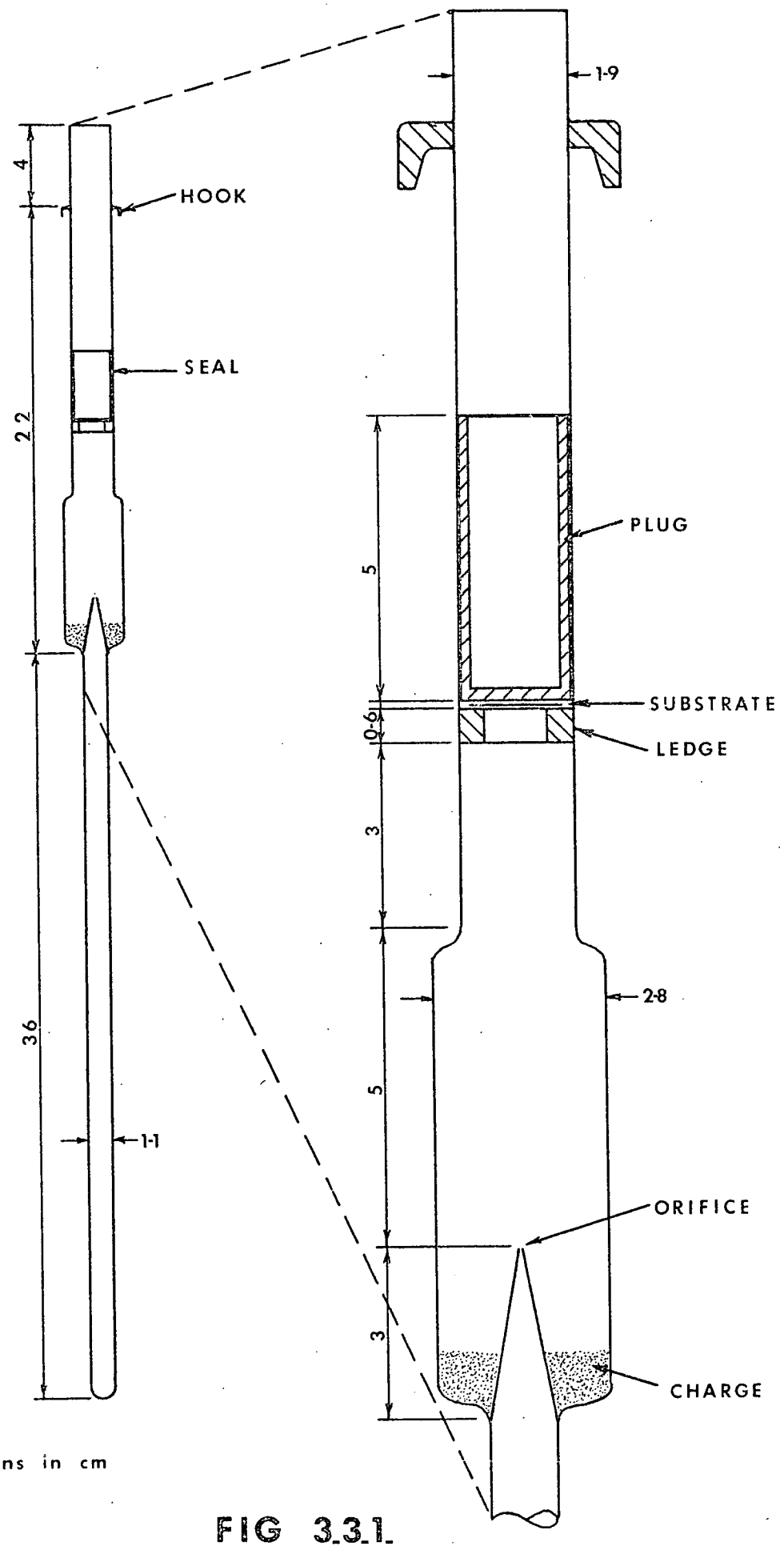
Bulk crystal synthesis experience has illustrated clearly the desirability of attaining an equilibrium of vapour pressures between source and growth face to influence the condensation process. This criterion excludes gas transport and open systems and hence practically all corresponding conventional thin film vacuum techniques. In direct conflict with this requirement is the instability of closed systems through their extreme sensitivity to small deviations from perfect stoichiometry or minute impurity concentrations in the charge. Each new design represents an attempt to resolve this conflict by exerting some measure of control over the patently unstable equilibrium.

The main corresponding implications for film growth systems are that desirable features should include vapour equilibrium between charge and substrate combined with some command of this equilibrium situation. Subsidiary requirements involve a high substrate temperature which, since it is compatible with high surface mobility of the condensate, is likely to promote epitaxy in conjunction with a high purity stoichiometric charge contained in a non-reactive environment to restrict equilibrium disturbances. This also excludes most conventional thin film vacuum techniques

It is interesting to note that some improvements in conventional film systems have been ascribed to such reduction in environmental reactivity, for example, electron beam heating of the charge [156].

In order to gain experience with such an idealised system the design shown in Fig. 3.3.1 was evolved. It features a twin chamber construction with a small communicating orifice as the vapour equilibrium control mechanism and is constructed in transparent fused quartz.

Phase diagrams for cadmium sulphide are not yet available in complete form, only the Cd-CdS liquidus being reported since the remainder of the phase diagram is rendered virtually inaccessible by enormous sulphur pressures, but the principle of operation may be explained by reference to typical pressure versus composition, Fig. 3.3.2, and temperature versus composition, Fig. 3.3.3, sections on a hypothetical phase diagram. On raising the temperature to T, the gas in equilibrium with solid material has a composition represented by point A. Location of point A on the corresponding pressure versus composition section, Fig. 3.3.2, reveals that the vapour phase is in equilibrium with solid and that the compound loses predominantly sulphur species until points A and D become coincident. At this point the system has attained a pressure minimum, P_{min}, and since the solid and vapour have



All dimensions in cm

FIG 3.3.1.

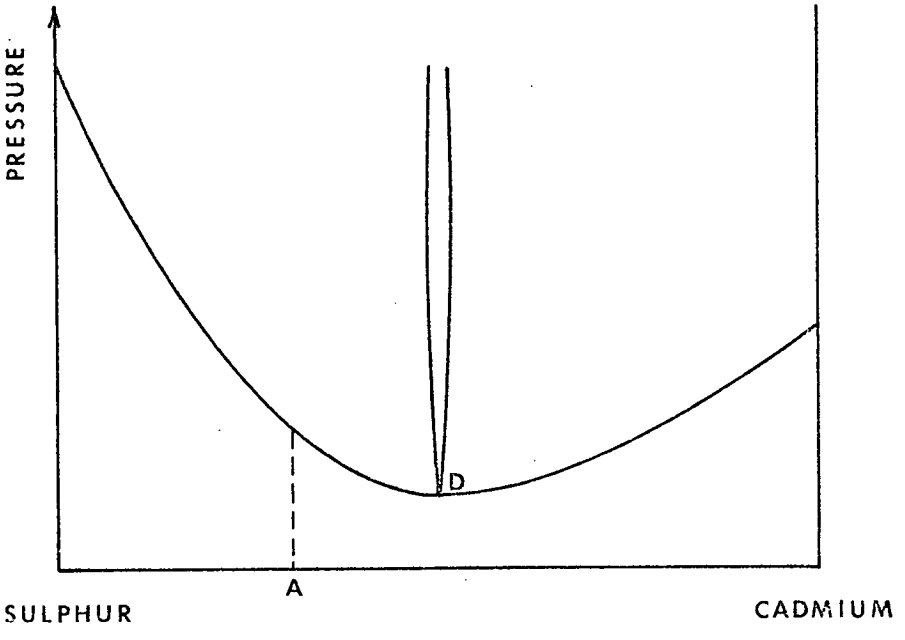


FIG 3.3.2.

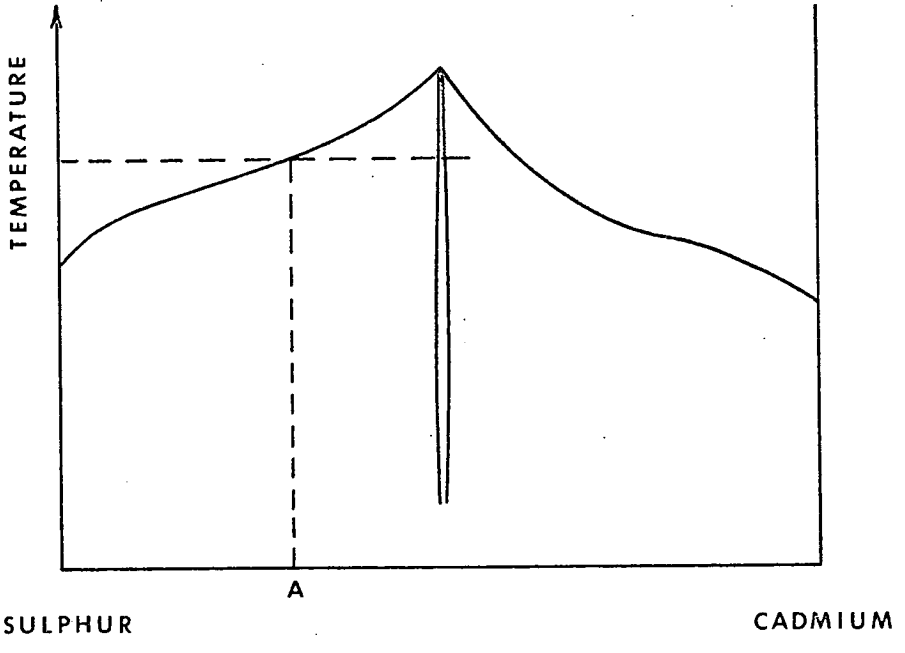


FIG 3.3.3.

identical compositions, evaporation may continue without further changes in composition until, theoretically, the entire charge has been consumed. In practice, sublimation would be terminated prior to exhaustionof the charge to limit extraction of less vclatile impurities. At the P_{min} point the vapour and solid, compositions need not be perfectly stoichiometric, but commensurate with the characteristic sensitivity of elemental vapour pressures to solid composition, only small deviations from stoichiometry are required to attain the P_{min} condition. Access to this condition offers,in theory, one constraint on the otherwise variable equilibrium point. Three distinct modes of operation are possible. In the first, a low tail temperature which permits condensation in the tail of cadmium, sulphur and cadmium sulphide results in equilibrium control by the P_{min} condition; in the second, tail temperature is in excess of that which permits condensation in the tail of species at P_{min}, in this case equilibrium is controlled by tail temperature; in the third, dopant is introduced into the tail and equilibrium is controlled by the dopant material and the tail temperature. The first mode is favoured since it involves fewer variables and hence should be more reproducible. It is also convenient in that the P_{min} condition relaxes requirements of mechanical strength on the capsule

and permits construction in fused quartz of 1 mm wall thickness. An estimation of total internal capsule pressure may be made by assuming that the following reaction occurs ;

$$\underset{\text{(Solid)}}{2\ CdS} \rightleftharpoons \underset{\text{(gas)}}{2Cd} + \underset{\text{(gas)}}{S_2} \qquad (3.3.1.)$$

Only components of the reaction which are in the gaseous phase need be taken into consideration in a mass action relationship [157], and

$$K = \frac{[Cd]^2[S_2]}{[CdS]^2} \qquad (3.3.2.)$$

where K is an equilibrium constant for the reaction and the square brackets represent concentrations. A pure condensed phase has, of course, a certain vapour pressure but this is constant at a given temperature and the term [CdS] is meaningless. The reaction involves simply a colligative property of the compound. It is convenient to introduce an equilibrium constant K_p, which is a function of temperature, where ,

$$K_p = [Cd]^2\ [S_2] \qquad (3.3.3.)$$

The total vapour pressure in the capsule, P_T, is given by ;

$$P_T = P_{cadmium} + P_{sulphur} \qquad (3.3.4.)$$

The condition for a minimum in P_T is that :

$$\frac{\partial P_T}{\partial P_{cadmium}} = \frac{\partial P_T}{\partial P_{sulphur}} = 0 \qquad (3.3.5.)$$

From (3.3.4) $P_T = P_{cadmium} + \frac{K_p}{(P_{cadmium})^2}$ (3.3.6)

and $\frac{\partial P_T}{\partial P_{cadmium}} = 1 - \frac{2K_p}{(P_{cadmium})^3}$ (3.3.7)

(3.3.7) vanishes when ,

$$P_{cadmium} = 2^{\frac{1}{3}} K_p^{\frac{1}{3}} \qquad (3.3.8)$$

Similarly $$\frac{P_T}{P_{sulphur}} = 1 - \frac{K_p}{2(P_{sulphur})^3} \qquad (3.3.9)$$

(3.3.9) vanishes when $P_{sulphur} = (\frac{1}{2})^{\frac{2}{3}} K_p^{\frac{1}{3}}$ (3.3.10)

Thus it follows that at the P_{min} point,

$$P_{cadmium} = 2P_{sulphur} = 2^{\frac{1}{3}} K_p^{\frac{1}{3}} \qquad (3.3.11)$$

and $$P_{min} = \frac{3}{2} \times 2^{\frac{1}{3}} K_p^{\frac{1}{3}} \qquad (3.3.12)$$

K_p and P_{min} are plotted as functions of temperature in Figs. 2.2.1 and 3.3.4, respectively [54, 158].

It has been tacitly assumed that the P_{min} condition is attained by removal via the communicating orifice of excess cadmium or sulphur from the vapour in the upper chamber, and that selective flow characteristics of the orifice itself do not exert any influence on this condition. It is unlikely that this condition will hold exactly since the diffusion of species through a small orifice is subject to Graham's Law and consequently the rate of diffusion through the orifice of S_2 molecules is 1.33 times that of cadmium atoms for equal pressures of each species at the orifice high pressure side. In order to attain an orifice dependent equilibrium the flow rate of S_2 molecules must be half that of cadmium atoms. Thus the equilibrium condition is :

$$P_{cadmium} = 2.66\ P_{sulphur} \qquad (3.3.13)$$

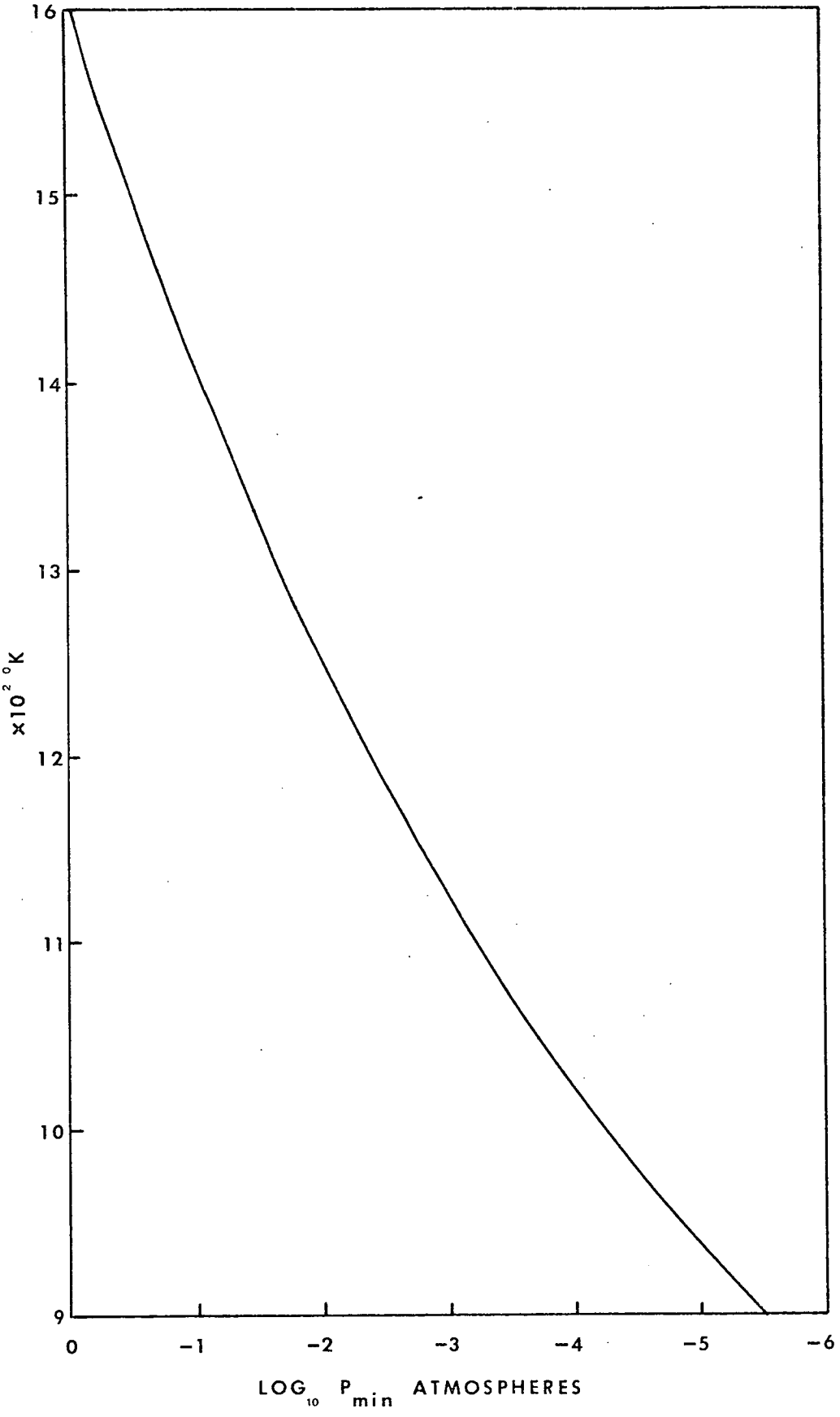


FIG 3.3.4.

It would be naïve to attempt a prediction of the final equilibrium position but it is likely that a high flow rate via the orifice would bias the equilibrium point towards Eqn. (3.3.13)and a low flow rate would favour Eqn. (3.3.11). Equation (3.3.13) assumes S_2 molecules in the vapour phase and would require modification in the presence of other molecular associates.

3.4 DEPOSITION PROCEDURE - SYSTEM 1.

Thermal demands imposed by the apparatus of Fig. 3.3.1,on a high temperature furnace are quite distinct from those of bulk crystal growth, mainly as a consequence of the comparatively short growth cycle which is initiated and terminated by insertion and withdrawal of the capsule from the furnace. Long-term stability is thus of less importance than the ability to raise the inserted capsule quickly to an operating temperature of approximately 1150^{o}C and maintain this for a short period. Since the capsule has considerable thermal capacity, this demand must be satisfied through specific design features of the heating system. Two options are available, the first comprising a heating element of low thermal inertia coupled to an elaborate temperature control system, the second comprising a heating element of a thermal inertia which greatly exceeds that of the capsule. In this way, the temperature control system may be simplified. In view of the inherent unreliability

of low inertia elements at such elevated temperatures the use of low voltage high inertia elements is favoured and, since this invokes the latter option, a furnace construction, as shown in Fig.3.4.1, of high thermal inertia is compatible with the stated requirements. Adjustment of the axial temperature profile ,Fig.3.4.2,by critically dimensioned thermal insulation ensures that a gently increasing temperature is maintained for a short distance above the charge in order to prevent condensation in the communicating orifice and that a high axial temperature gradient exists at the substrate surface in order to limit constitutional supercooling.
A relatively simple but unusual solid state system of control (Appendix 1) controls the upper zone temperature automatically using a platinum-platinum 13% rhodium thermocouple placed in the heating element. The lower zone is controlled manually. Access to a temperature profile of the form prescribed is essential if the system is to operate at all.

Fused quartz capsules were etched in dilute hydrofluoric acid after manufacture, flushed with doubly distilled water and blown dry with a jet of filtered nitrogen gas prior to storage in a heated drying cabinet. The hydrofluoric acid etch stage of this cleaning procedure was later replaced by a period of immersion, exceeding one hour, in a

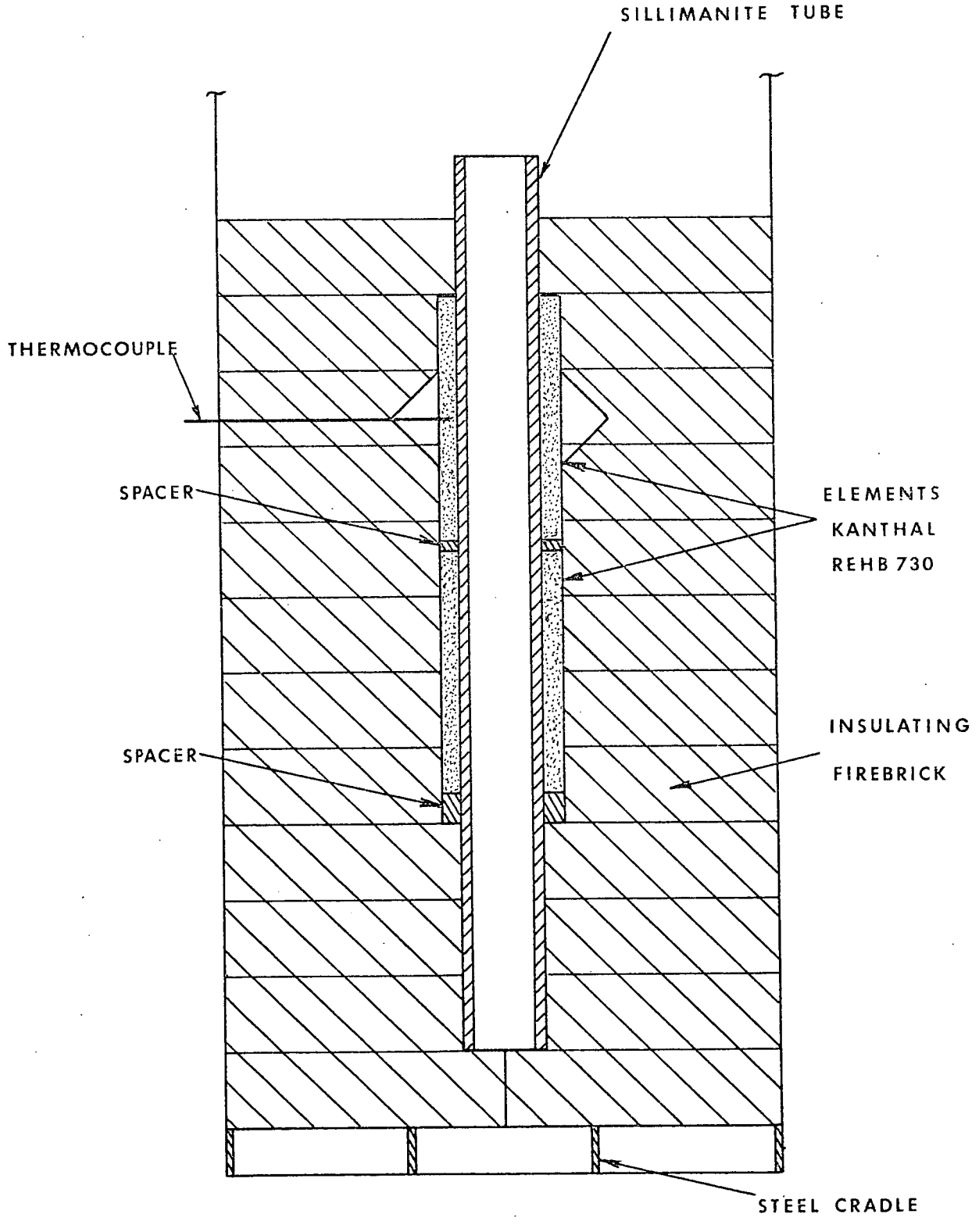

SILLIMANITE TUBE
THERMOCOUPLE
SPACER
SPACER
ELEMENTS
KANTHAL
REHB 730
INSULATING
FIREBRICK
STEEL CRADLE

FIG 3.4.1.

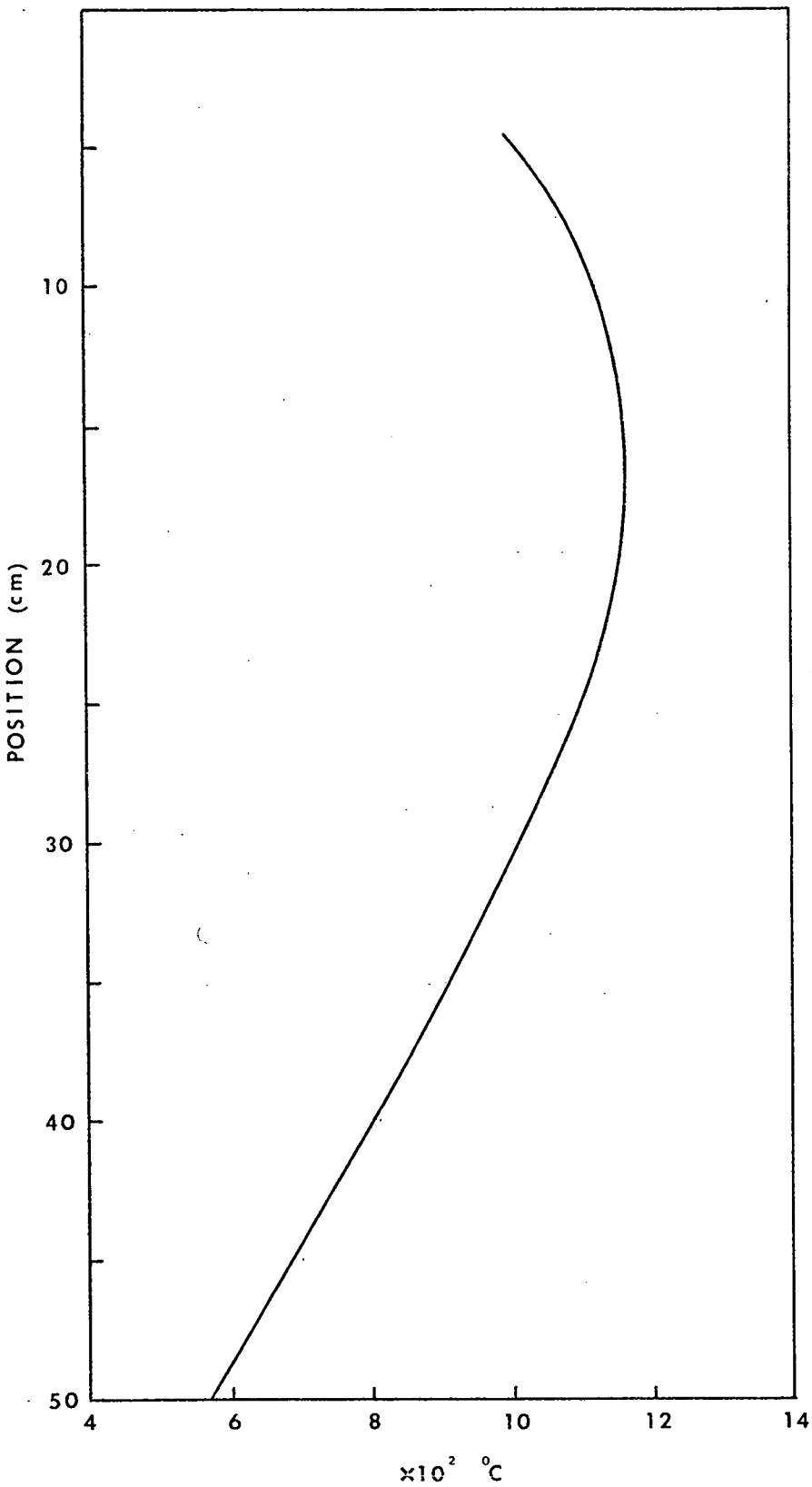


FIG 3.4.2.

boiling solution of a high purity alkaline detergent.* To delay the onset of devitrification, handling of capsules without gloves subsequent to cleaning was avoided.

In all cases the charge material consisted of high purity cadmium sulphide ** prepared by an ion exchange process, homogeneous precipitation and a final sublimation stage at 1050°C [159]. This process yielded small random shaped crystals with an impurity specification :

Copper and Silver	0.5 ppm.
Silica	5 ppm.
Chloride and Sulphate	5 ppm.

To minimise scatter of the charge material, loading was performed through a fused quartz loading tube temporarily inserted into the upper chamber and in order to limit diffusion of species, sealing of the capsule was performed under an absolute internal argon pressure of 80 torr using the arrangement of Fig. 3.4.3(a) initially. This arrangement was abandoned in favour of Fig. 3.4.3.(b) to combat difficulties experienced in collapsing the capsule neck above the substrate which also tended to fly from its ledge under the influence of argon flushing. The latter design, by incorporating a small pre-set flow of argon in the pumping manifold during the

---

* "Decon 75".

** Supplied by the General Electrical Company Limited, Wembley, Middlesex. This material is no longer available.

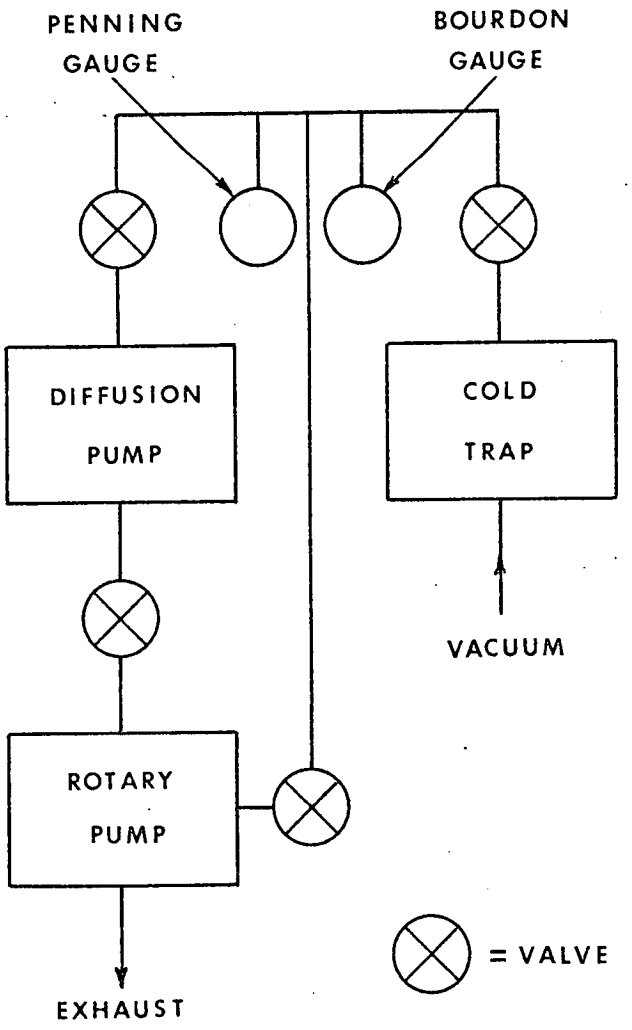
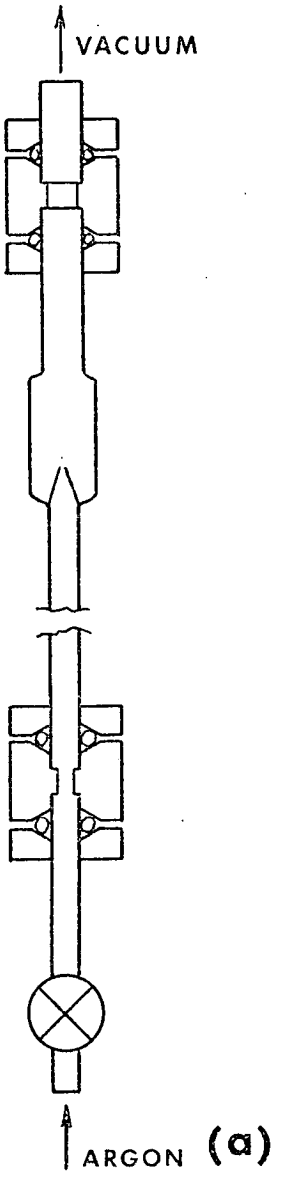
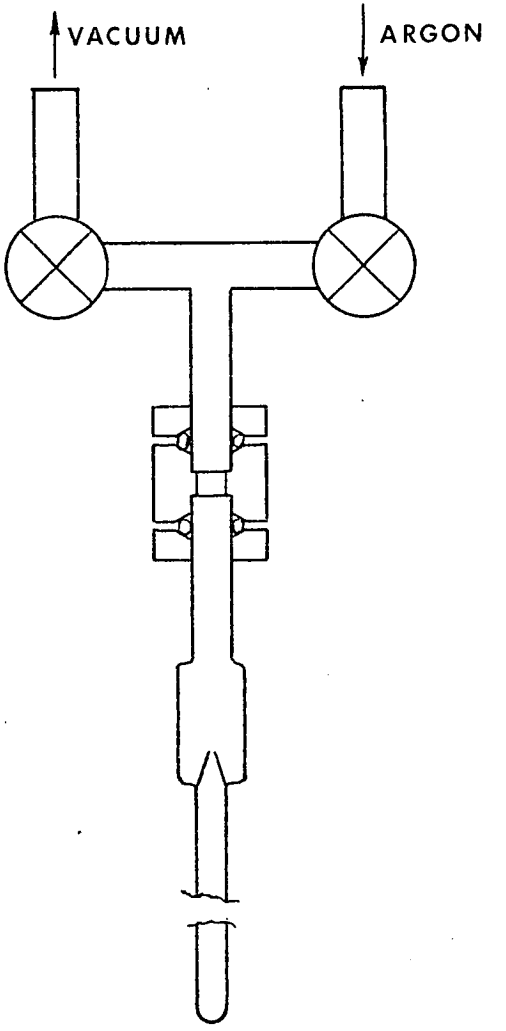

PENNING
GAUGE
BOURDON
GAUGE
DIFFUSION
PUMP
COLD
TRAP
VACUUM
ROTARY
PUMP
EXHAUST
= VALVE

FIG 3.4.3.


VACUUM
ARGON

(a)


VACUUM
ARGON

(b)

sealing operation ensured consistent argon sealing pressures of 80 torr absolute, in addition to assisting in the removal of silica subliming from the collapsing seal. Prior to final sealing, the capsule internal pressure was reduced to 10^{-4} torr followed by admission of 99.995% argon to atmospheric pressure. This flushing process was then repeated several times. Substrates were of silicon (111) plane scribed and broken from 10^{-2} ohm metre slices. The cleaning procedure adopted was as follows :

1) Suspend slice in a fused quartz basket and ultrasonically clean in trichloroethylene for 5 minutes.

2) Ultrasonically clean in acetone for 5 minutes.

3) Ultrasonically clean in doubly distilled water for 5 minutes.

4) Repeat step 3 in fresh doubly distilled water.

5) Immerse in a 10% hydrofluoric acid solution for 2 minutes.

6) Rinse in doubly distilled water for 5 minutes.

7) Ultrasonically clean in doubly distilled water for 5 minutes to remove surface deposits from stage (5) which could otherwise prove troublesome since they did not yield to simple rinsing.

8) Store under doubly distilled water until ready for use. Prior to insertion into the capsule, substrates were blown dry by a filtered nitrogen supply.

In accordance with the theories of epitaxial deposition presented in the previous chapter, this substrate orientation was expected to be compatible

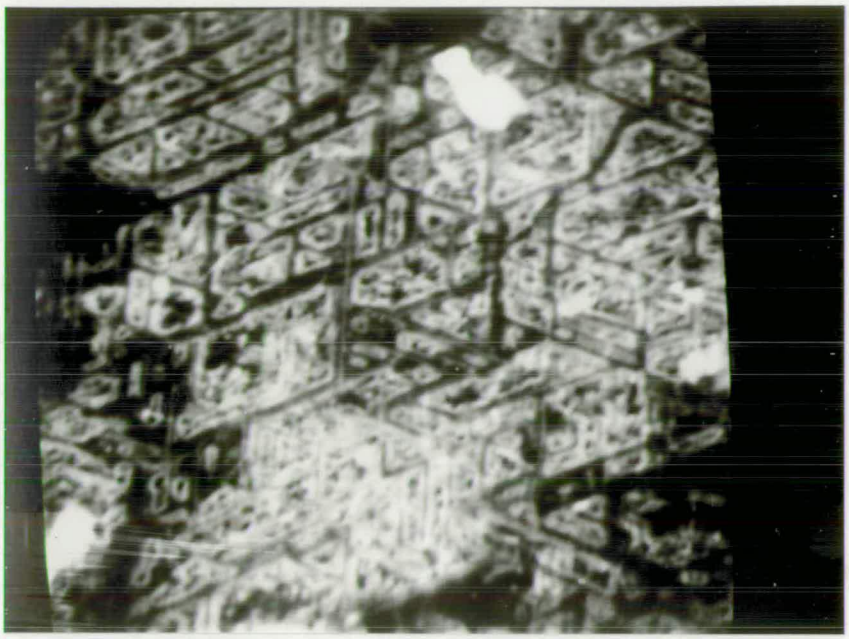
with the growth of (0001) plane cadmium sulphide, Figs. 2.5.1, and 2.5.3.

3.5 RESULTS FOR SYSTEM 1.

An initial series of depositions was performed by lowering the capsule into the furnace until the substrate position coincided with the maximum temperature region. This position was maintained for five minutes, to allow the charge to equilibrate with its vapour, and growth was then initiated by raising the capsule until the charge temperature exceeded that of the substrate by 15°C.

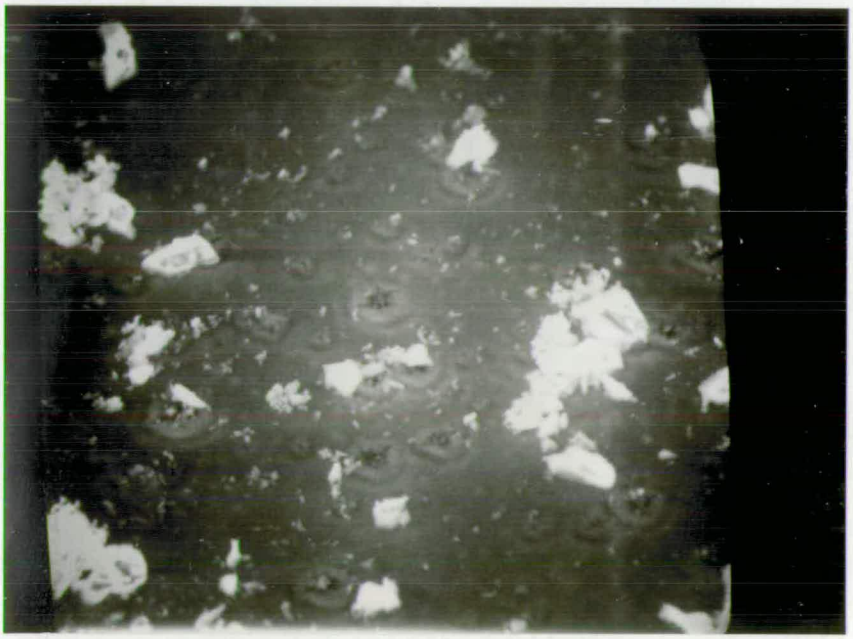
In all cases, temperatures were inferred from the furnace profile shown in Fig. 3.4.2, and capsule position. Deposition was terminated by withdrawal of the capsule after twenty minutes at the growth position. Depositions were characterised by cloudy films, off-white in colour, as shown in Figs. 3.5.1, and 3.5.2. The growth rate was virtually zero. The appearance of the charge changed from small lemon yellow random crystallites to a more consolidated mass slightly darker in colour with a matt surface finish and in the lower chamber yellow deposits were visible over a range of positions corresponding to temperatures of 640°C - 845°C. Some droplets of cadmium were observed near the lower end of this chamber at a position corresponding to a temperature of 150°C.

Subsequent experiments were performed with the addition of two platinum-platinum 13% rhodium



- FIG. 3.5.1 -

Magnification 6200.



-FIG. 3.5.2 -

Magnification 600.

thermocouples, Fig.3.5.3, in an effort to monitor more closely the charge and substrate temperatures. A typical plot of these temperatures is presented in Fig.3.5.4. Source-substrate temperature differentials of $2^{o}C$ - $20^{o}C$ were investigated although the growth rate remained at virtually zero and could not be sensibly correlated with temperature measurements except for the onset of crystallite growth at approximately $15^{o}C$ source-substrate temperature difference. The results did, however, indicate a marked dependence on the substrate surface condition, Figs. 3.5.5, 3.5.6, and 3.5.7 were obtained from deposits produced under identical conditions, but on substrates cut from different slices. Specimens from each slice were examined in an electron microscope for channelling patterns which are sensitive to surface condition [160] This revealed a much higher degree of surface damage in the substrates of Figs. 3.5.5, and 3.5.6, compared with that of Fig. 3.5.7. Mass spectographic investigation of the residual atmosphere in a capsule prior and subsequent to a deposition revealed strangely a large increase in carbon content. It is postulated that the carbon source is the silicon substrate. This phenomenon has been observed by other workers [161] and is thought to originate from polishing material embedded in the silicon surface.

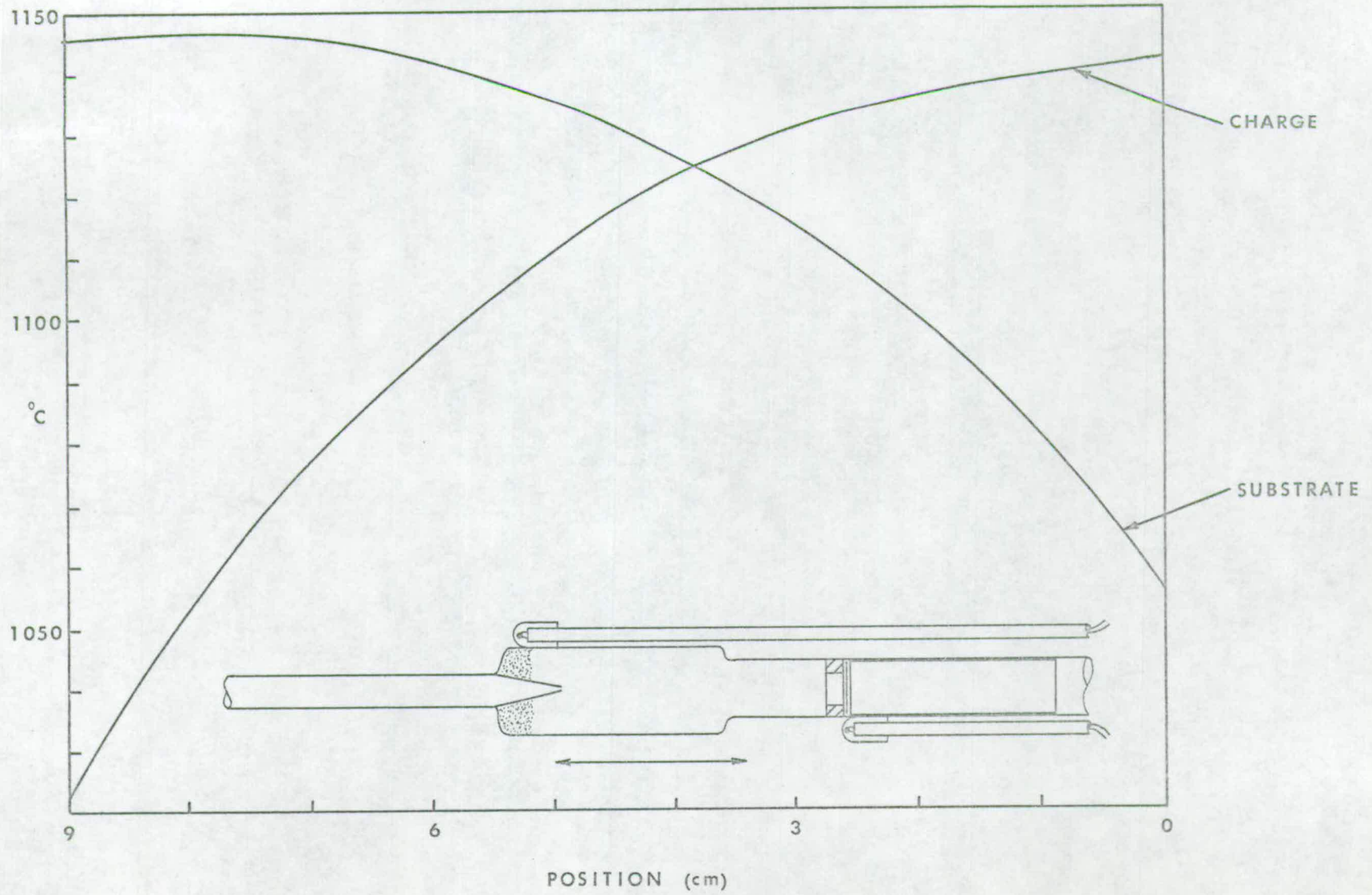


FIG 3.5.3.

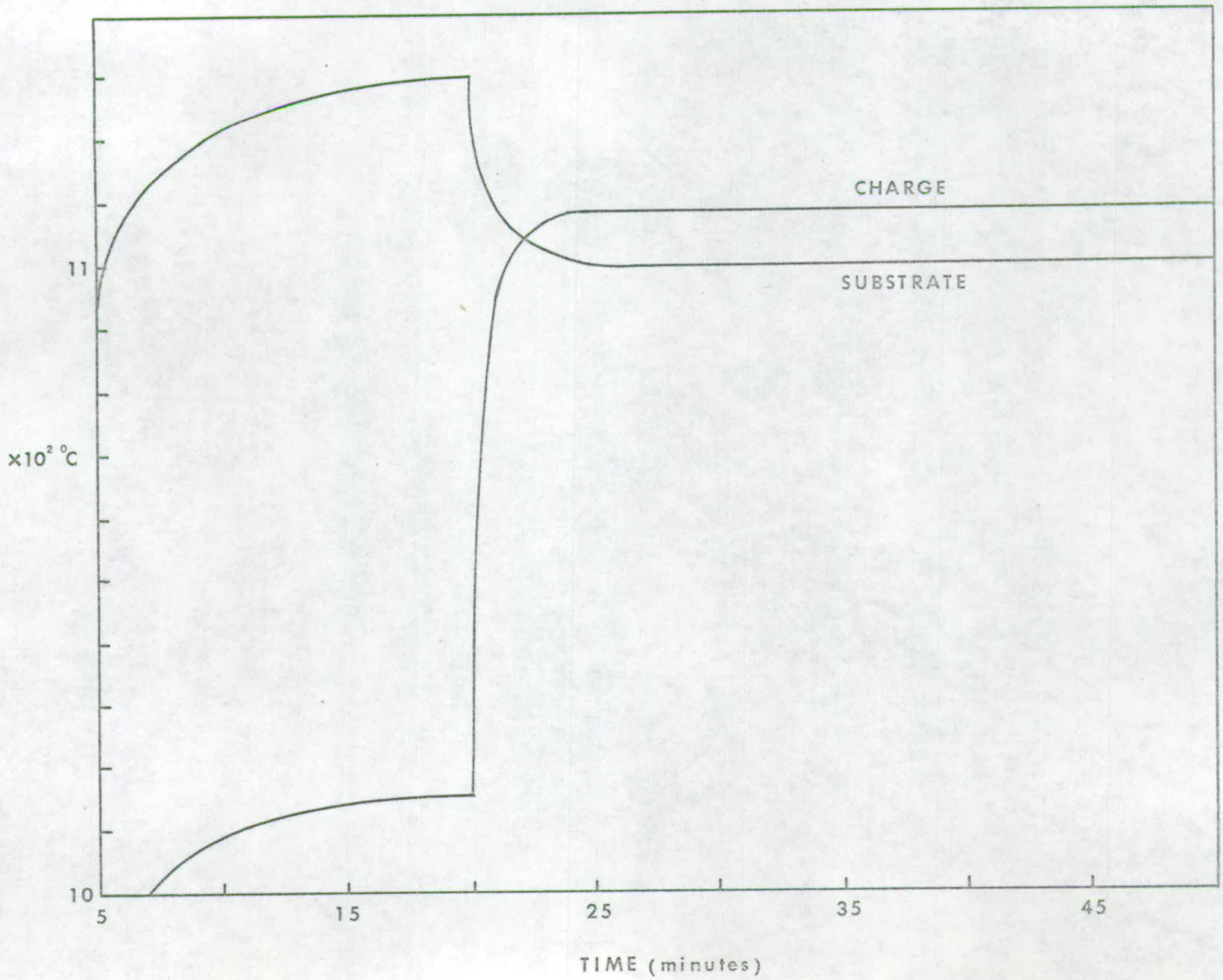


FIG 3.5.4.



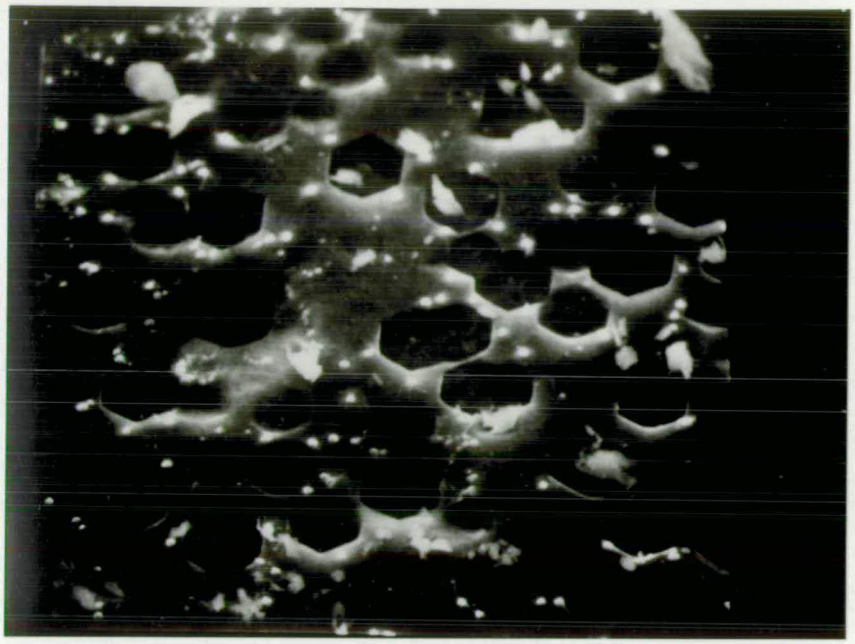
- FIG. 3.5.5. -

Magnification 200.



- FIG. 3.5.6 -

Magnification 1200.



- FIG. 3.5.7. -

Magnification 2000.

CHAPTER 4.

DESIGN AND OPERATION OF A DEPOSITION SYSTEM TO PRODUCE SINGLE CRYSTAL FILMS OF CADMIUM SULPHIDE.

4.1 DESIGN CRITERIA - SYSTEM 2.

Logical investigation of factors contributing to the low growth rate observed in the prototype system was impeded by the presence of indeterminate and inaccessible variables which included, in particular, the capsule residual atmospheric composition at the instant of sealing off and the presence within the capsule of volatile products of reaction which are active during a deposition in influencing the natural vaporisation or condensation processes.

Water vapour at high temperature within the reaction chamber may promote the formation of hydrogen sulphide and sulphur dioxide both of which engage active components of the desired reaction in an inactive form. This effect is particularly serious in view of the inefficiency of less elegant vacuum systems in removing water vapour which is introduced by such numerous and basic mechanisms as, adsorbtion on the charge crystallites and on the capsule walls, in addition to extraction from the fused quartz itself on heating. That the latter process has considerable influence on electronic properties of the condensate has been demonstrated by Fochs[155]. Moreover, whereas effects of adsorbtion on the

charge crystallites and on the capsule walls may be alleviated by a bakeout under vacuum of the capsule and its contents prior to sealing, re-inclusion of water in the quartz is fundamental to most conventional sealed systems since sealing is usually performed by a flame process, involving an oxygen-propane or oxygen-hydrogen reaction which itself results in water vapour diffusion into the material [162], subsequent to bakeout. A secondary effect of flame sealing is introduction of subliming silica into the growth chamber close to the substrate where it may condense, with detrimental effect, on the freshly prepared surface.

In addition to the undesirable chemical effects, several mechanical deficiencies emerged. Extraction of the substrate after a deposition involved cutting open the capsule neck with a consequent ingress of silica particles which necessitated discarding the charge material and cleaning of the entire apparatus, including the tail section which also required cutting and resealing.

The design of system II, Figs. 4.1.1, - 4.1.5, was evolved specifically in an effort to eliminate the chemical and mechanical imperfections of the prototype system. It features a twin capsule configuration, an inner reaction chamber communicating via a small orifice of 0.15 mm diameter with a large outer chamber which may either be pumped continuously or filled to any desired pressure with an inert gas

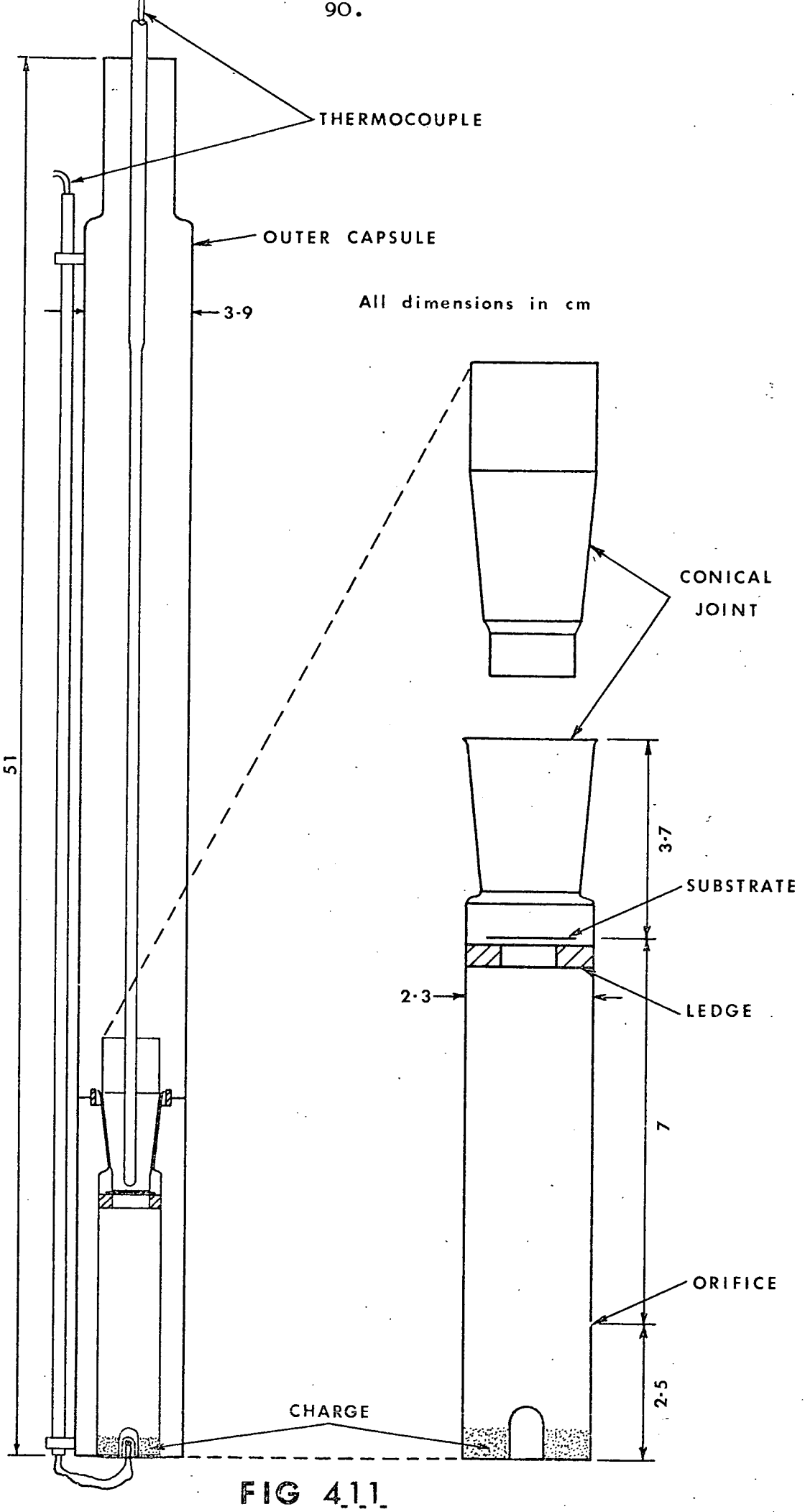

THERMOCOUPLE
OUTER CAPSULE
All dimensions in cm
3·9
51
CONICAL JOINT
3·7
SUBSTRATE
2·3
LEDGE
7
ORIFICE
2·5
CHARGE

FIG 4.1.1

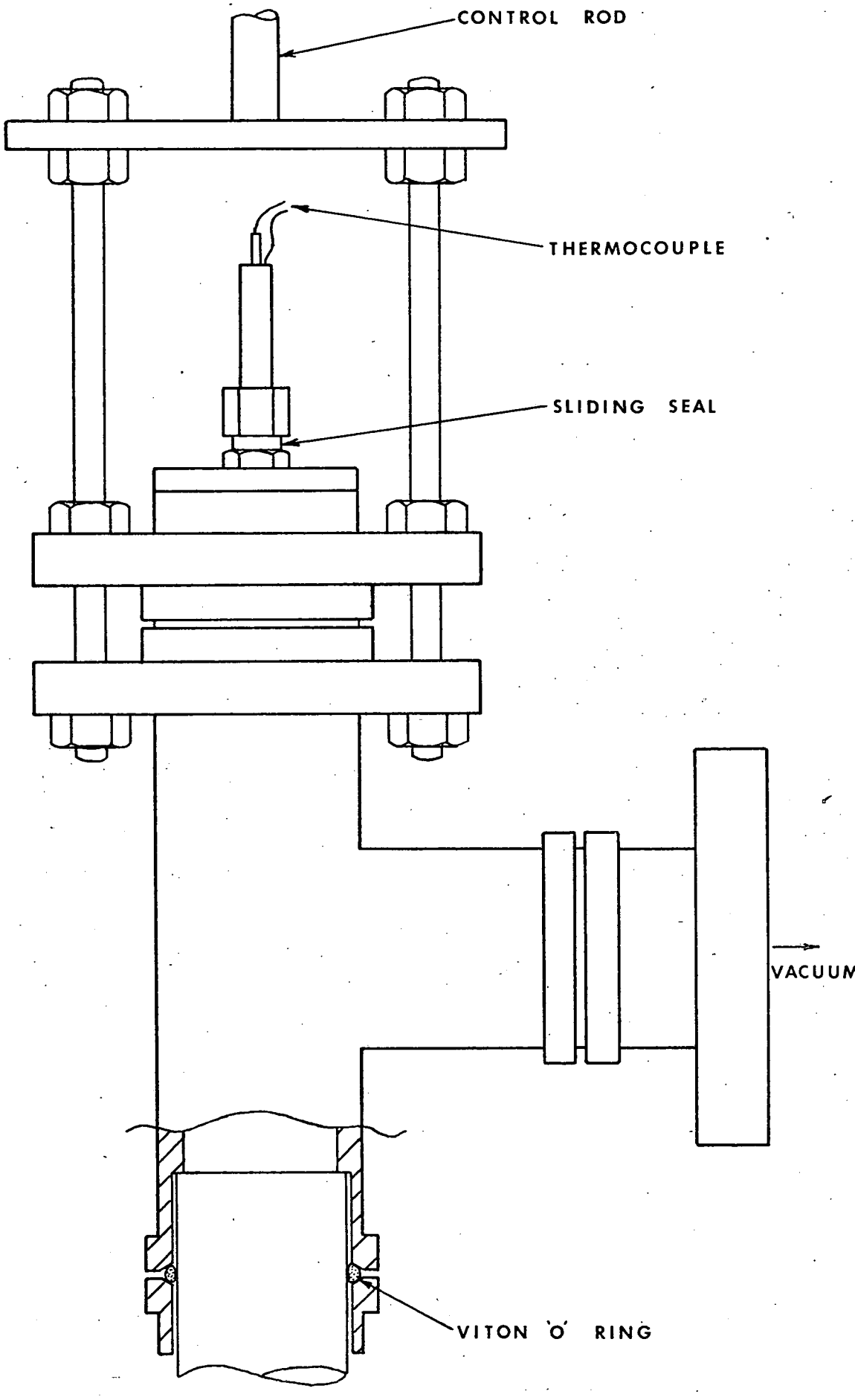


FIG 4.1.2.

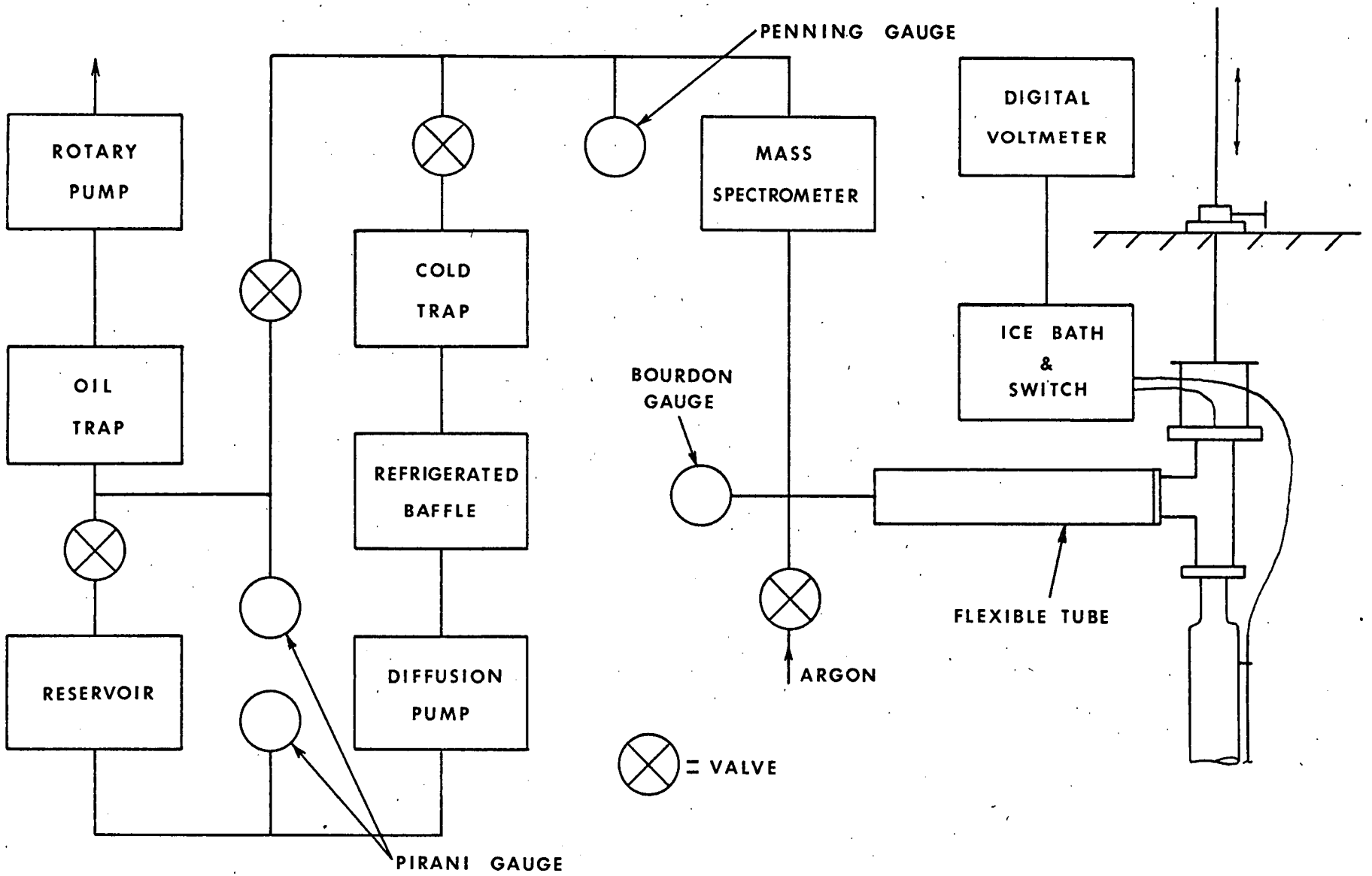
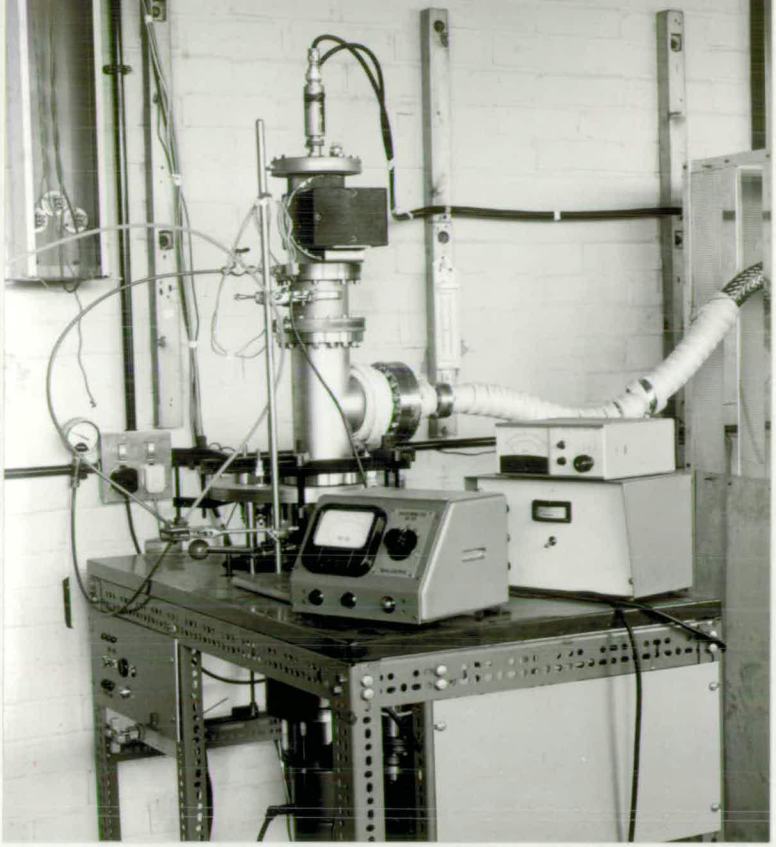
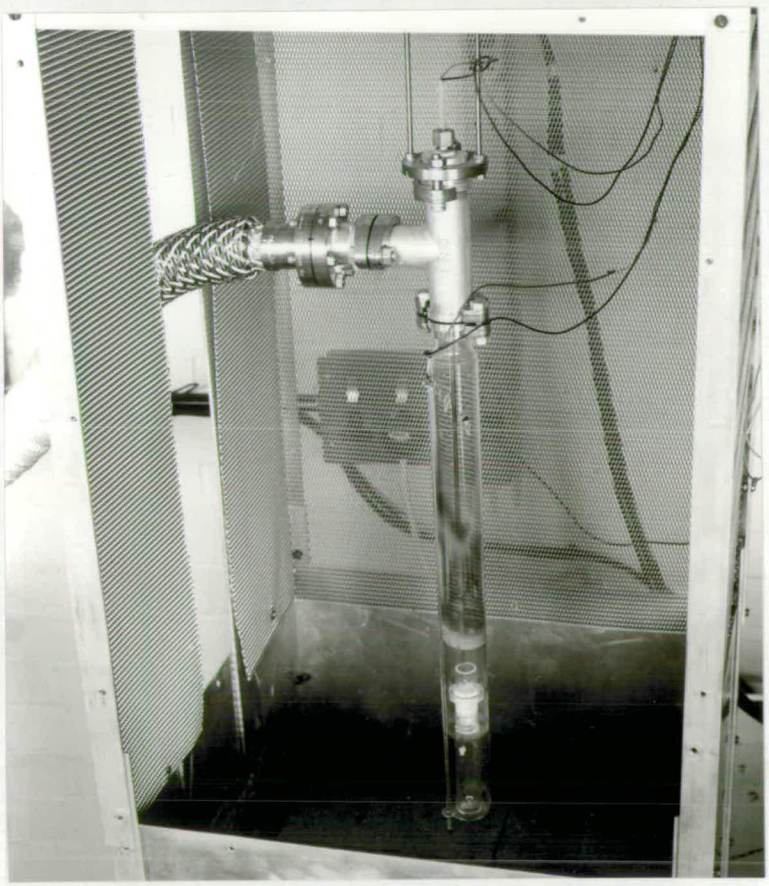

PENNING GAUGE
ROTARY PUMP
OIL TRAP
RESERVOIR
COLD TRAP
REFRIGERATED BAFFLE
DIFFUSION PUMP
PIRANI GAUGE
MASS SPECTROMETER
DIGITAL VOLTMETER
ICE BATH & SWITCH
BOURDON GAUGE
FLEXIBLE TUBE
ARGON
= VALVE

FIG 4.1.3.



- FIG. 4.1.4. -
General View of Deposition Apparatus



- FIG. 4.1.5. -
Capsules and Furnace

to control the film growth rate by influencing the diffusion process.

The inner capsule incorporates a conical joint seal above the substrate, this serves the purposes of positively locating the substrate, providing a simple substrate loading facility and,in the interests of safety,it provides a facility for automatic release of any excessive pressure in the reaction chamber which might be caused by faulty charge material or a blockage in the communicating orifice. It eliminates the necessity for flame treatment of the capsule at any time subsequent to manufacture, thus capsules may be thoroughly baked under vacuum before being raised to operating temperature.

The outer capsule, in effect, forms a bakeable vacuum chamber and provides for the removal of volatile impurities from the charge during both bake-out and deposition. In addition it permits access for mass spectrographic analysis of products evolved from the reaction chamber. The charge and substrate temperatures were continuously monitored by platinum-platinum 13% rhodium thermocouples positioned centrally at charge level and as near as possible to substrate level.

Complementing the capsule assembly is a three-way coupling providing connection via bakeable flexible stainless steel bellows to the vacuum pumping and mass spectrometer apparatus. All internal and sealing surfaces in the coupling were finely polished

to reduce surface area and accurate registration of capsule position in the furnace is provided by a calibrated sliding rod which is locked in alternative positions for bakeout or deposition. A vacuum of 10^{-7} torr is readily available at the flexible bellows.

4.2 DEPOSITIONS ON SILICON SUBSTRATES :

Prior to deposition, the inner and outer capsules were cleaned and dried by a procedure similar to that employed for the previous system. Loading of the charge material into the inner capsule and preparation of the (111) plane silicon substrate also followed a procedure similar to that employed in the previous system.

After assembly of inner and outer capsules, pumping was maintained under bakeout conditions with the capsules partially inserted into the furnace for at least twelve hours before initiating the reaction by further lowering the assembly into the furnace. Deposition was terminated by extraction of the assembly. Typical profiles of temperature versus time and temperature versus position are presented in Figs.4.2.1, and 4.2.2. respectively.

Initial attempts at deposition using the temperatures indicated in Fig. 4.2.1 yielded heavily etched substrates, Fig. 4.2.3. This etching was found to be caused by the charge vapour since by reducing the charge-substrate temperature differential the degree of etching could be reduced, Fig.4.2.4, and finally

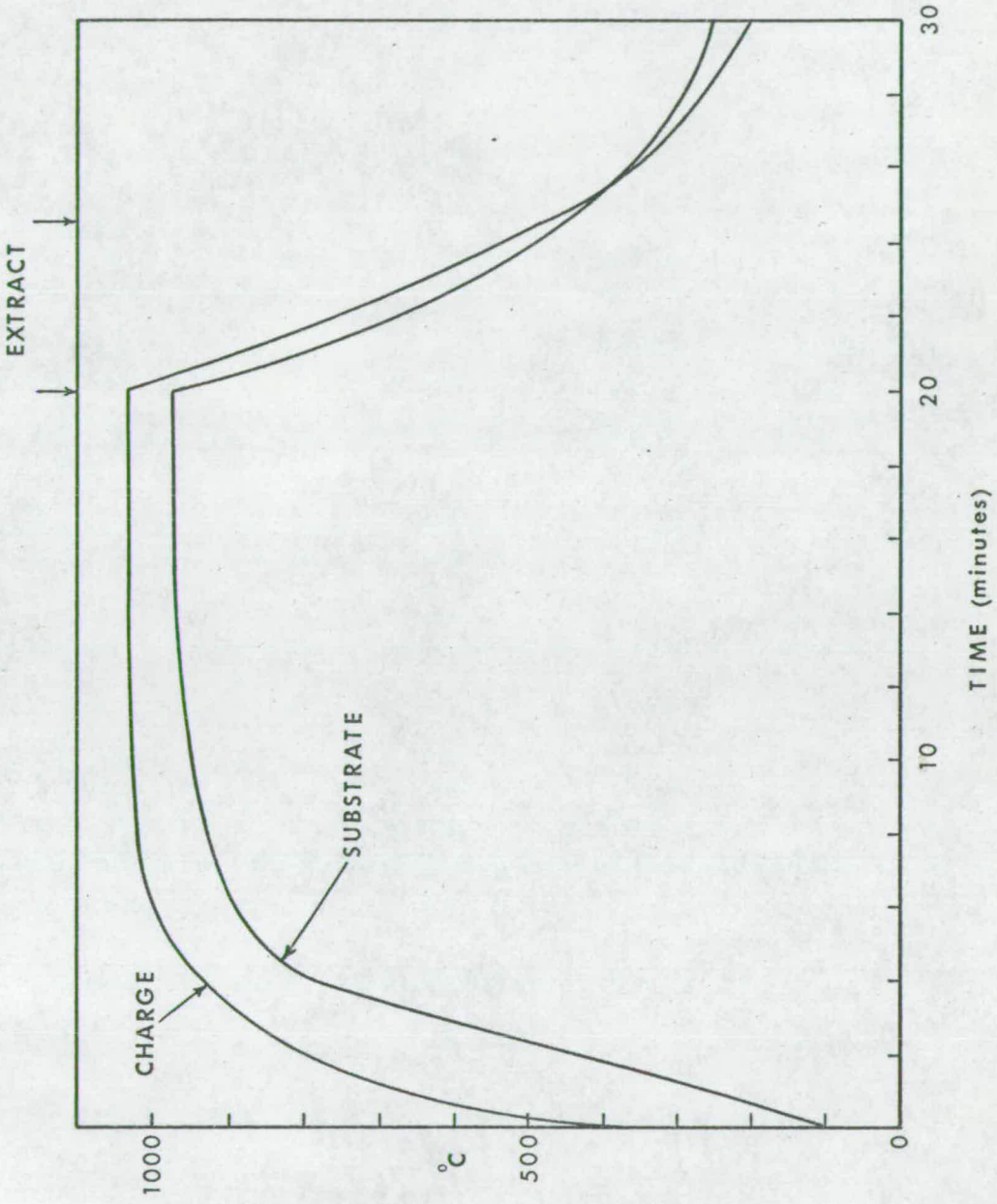


FIG 4.2.1.

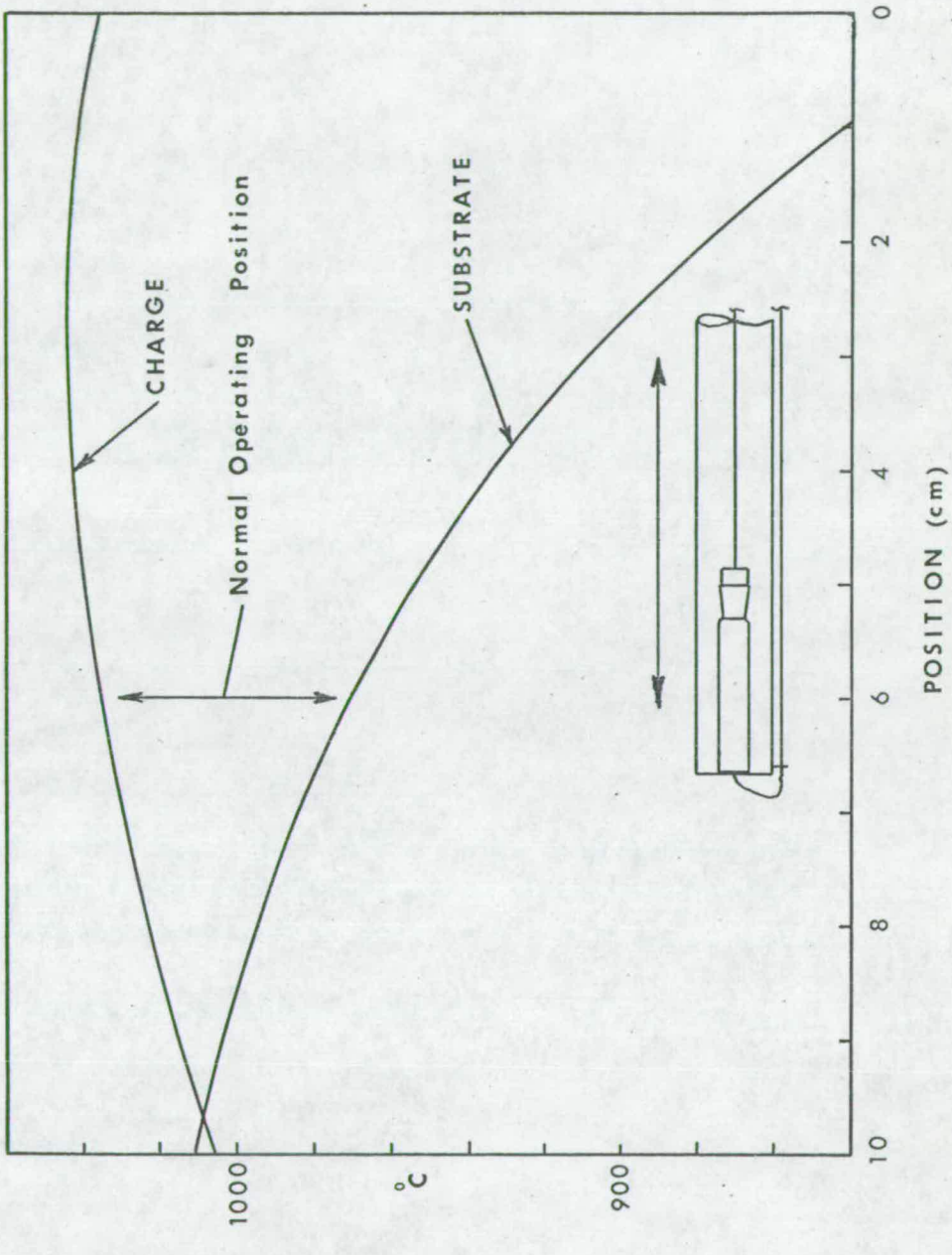
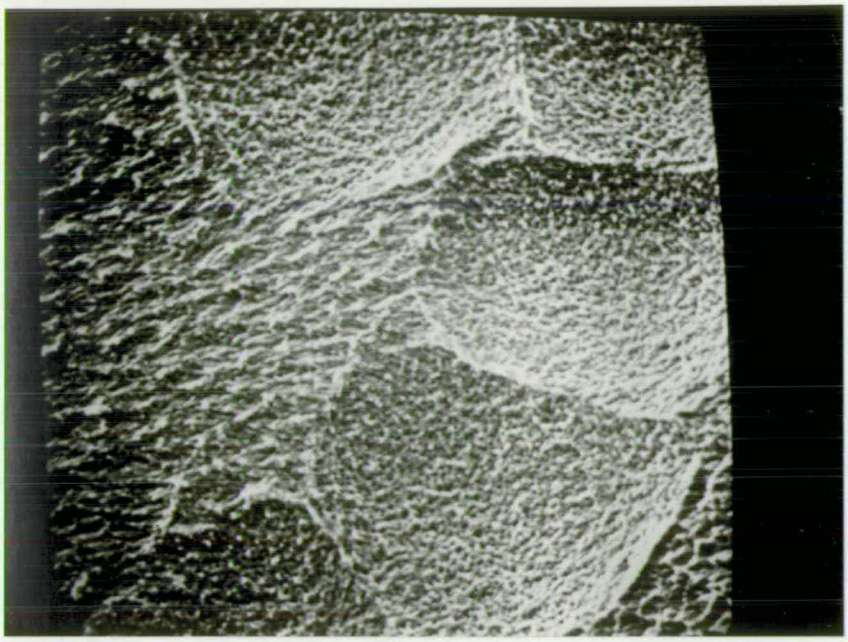
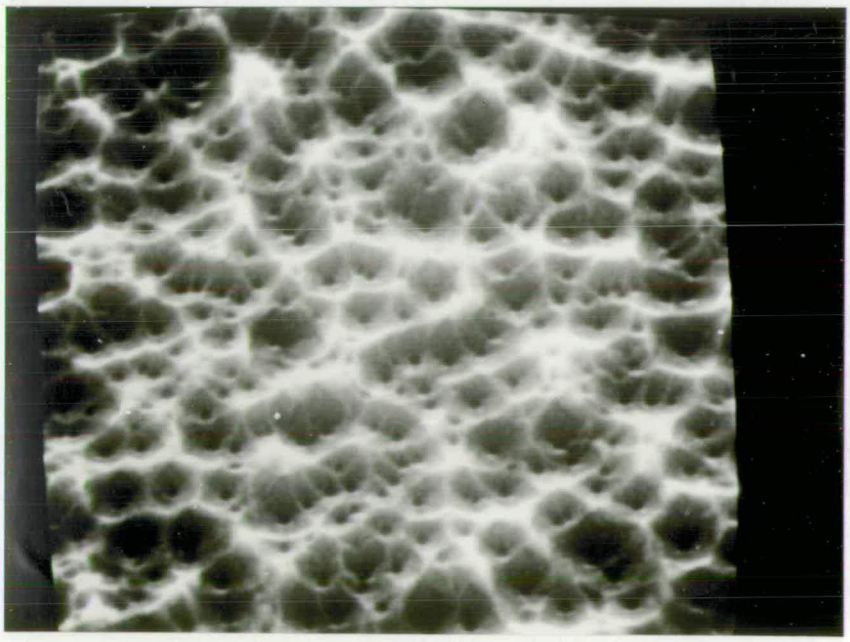

CHARGE
Normal Operating Position
SUBSTRATE
1000
°C
900
0
2
4
6
8
10
POSITION (cm)

FIG 4.2.2.



- FIG. 4.2.3. -

Magnification 240.



- FIG. 4.2.4. -

Magnification 4000

prevented. It appears that the formation of silicon sulphide rather than cadmium sulphide was favoured at the substrate, resulting in annular deposits of silicon, cadmium sulphide and cadmium on the outer capsule with decreasing temperature. In accordance with the principle of Le Chatelier, the more vigorous removal of sulphur-silicon reaction products compared with the prototype system would be expected to encourage the reaction to proceed in this direction since by inference from the hypothetical silicon-sulphur phase diagram [163] the products of the silicon-sulphur reaction remain in the gaseous phase under conditions where products of the cadmium-sulphur reaction form the solid phase.

At this point, investigations of depositions on silicon substrates were terminated in favour of similar studies on sapphire (α corundum) substrates which are less reactive than silicon.

4.3 DEPOSITIONS ON SAPPHIRE SUBSTRATES :

Initial tests employed mechanically polished substrates of α corundum $(10\bar{1}2)$ plane. Before insertion into the reaction chamber each substrate was subjected to a cleaning procedure which comprised :

1. Ultrasonic cleaning in trichloroethylenefor 5 minutes.
2. Rinse in acetone.
3. Ultrasonic cleaning in acetone for 5 minutes.
4. Rinse in isopropyl alcohol.
5. Ultrasonic cleaning in isopropyl alcohol for 5 minutes.

6. Rinse in doubly distilled water.
7. Dip in cold concentrated hydrochloric acid for 15 minutes.
8. Rinse in doubly distilled water.
9. Ultrasonic cleaning in doubly distilled water for 2 minutes.
10. Repeat (7) in fresh doubly distilled water.

Substrates were blown dry with a jet of filtered nitrogen immediately prior to use and a bakeout pumping and deposition procedure identical to that described in 4.2 was employed. Mass spectrographic analyses performed before and during deposition, Figs. 4.3.1 and 4.3.2 respectively, indicated little change in composition of the atmosphere reaching the pumping system and no traces of gaseous products of reaction could be detected.

A high growth rate was immediately evident, layers 1.3×10^{-3} metre in thickness being produced in a single deposition indicating an average growth rate of 4×10^{-3} metre /hour. Optical examination of the layers in addition to revealing their blatantly polycrystallinenature, confirmed in accordance with the ideas of Chapter 2 and other workers [115], an increasing crystallite size with distance from the substrate as shown in Figs. 4.3.3 and 4.3.4.

In order to encourage a growth rate more compatible with film production, the source-substrate temperature differential was reduced to $10C^{o}$. Although this action curtailed average growth rate to 0.8×10^{-3}

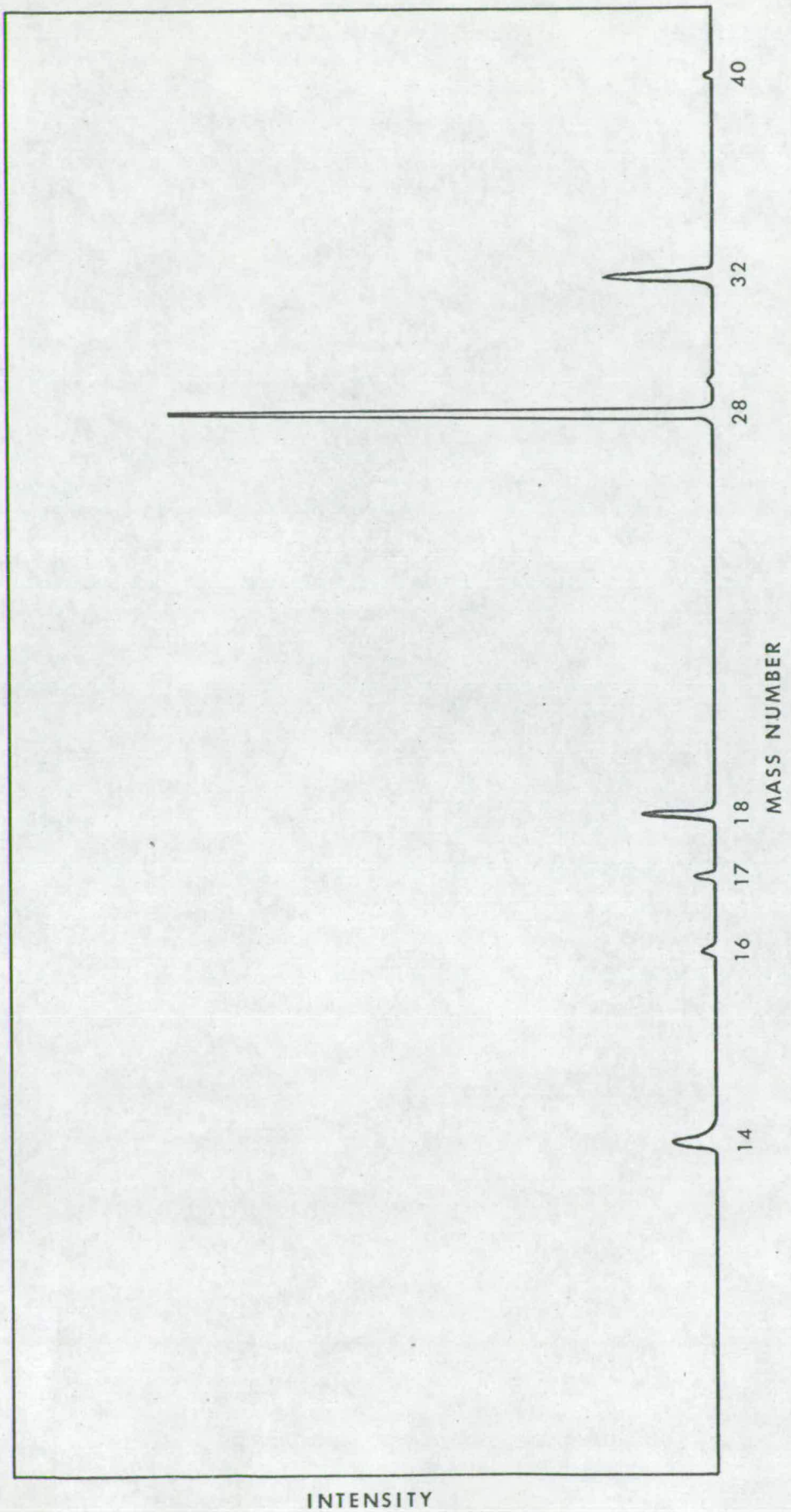


FIG 4.3.1.

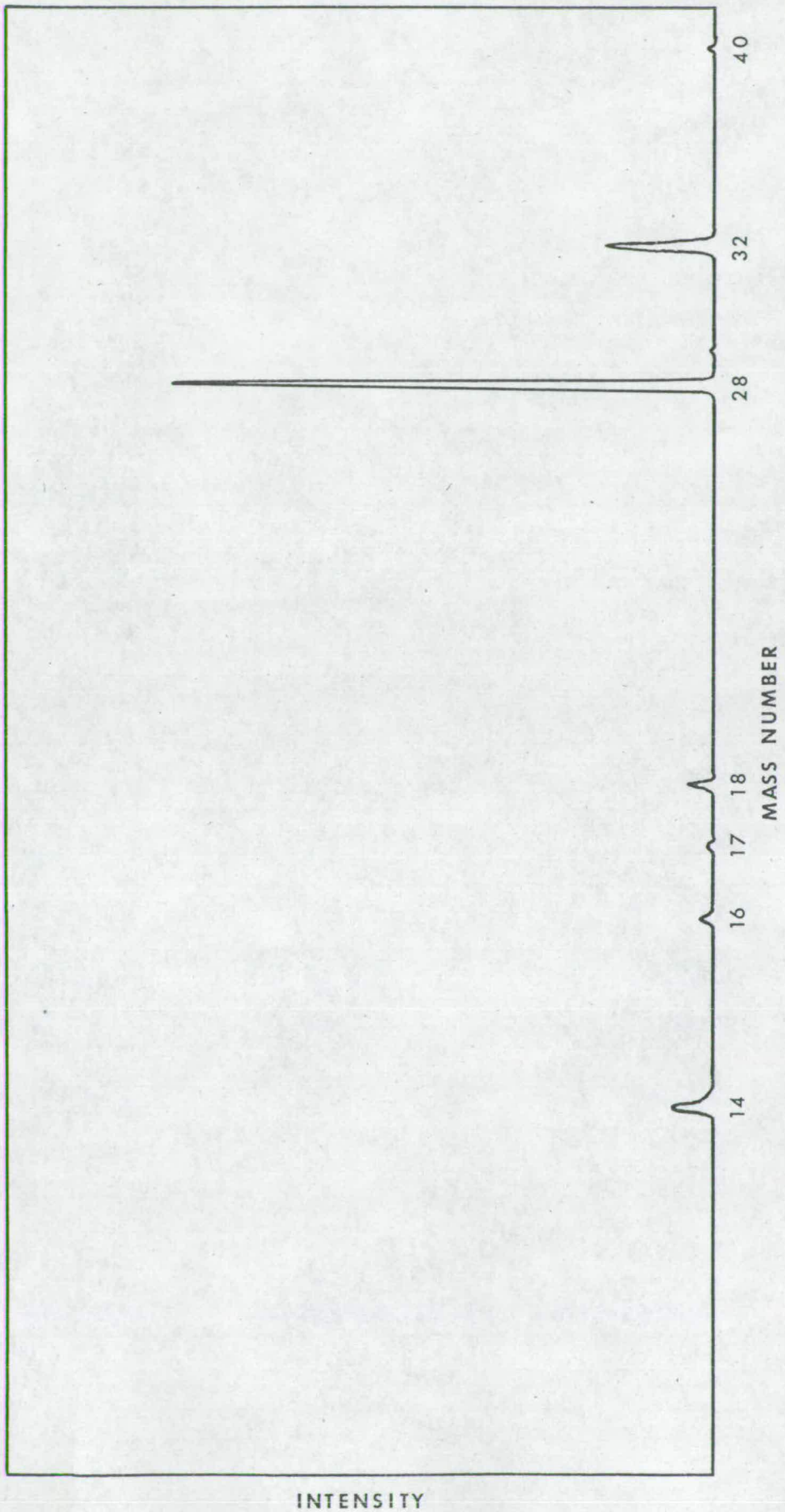
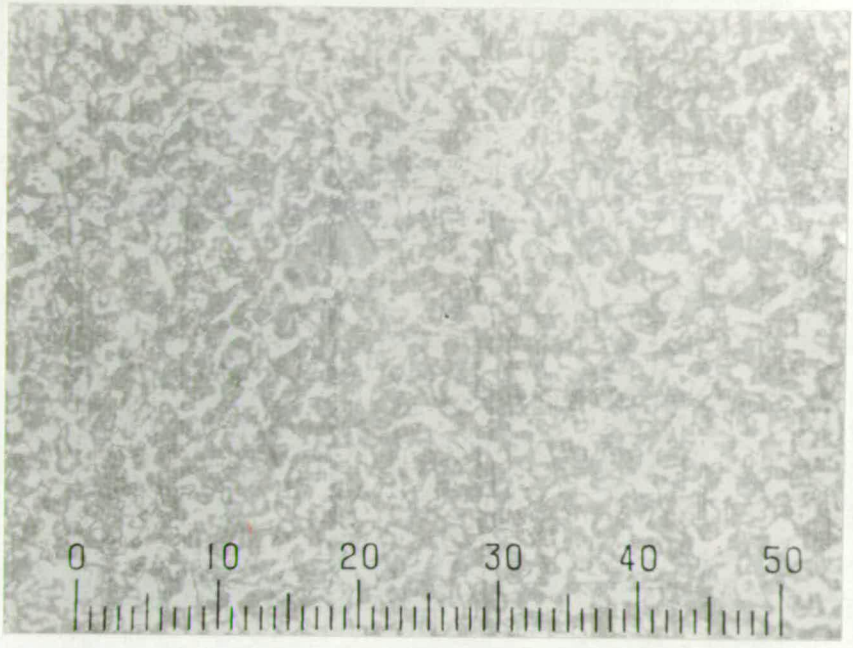
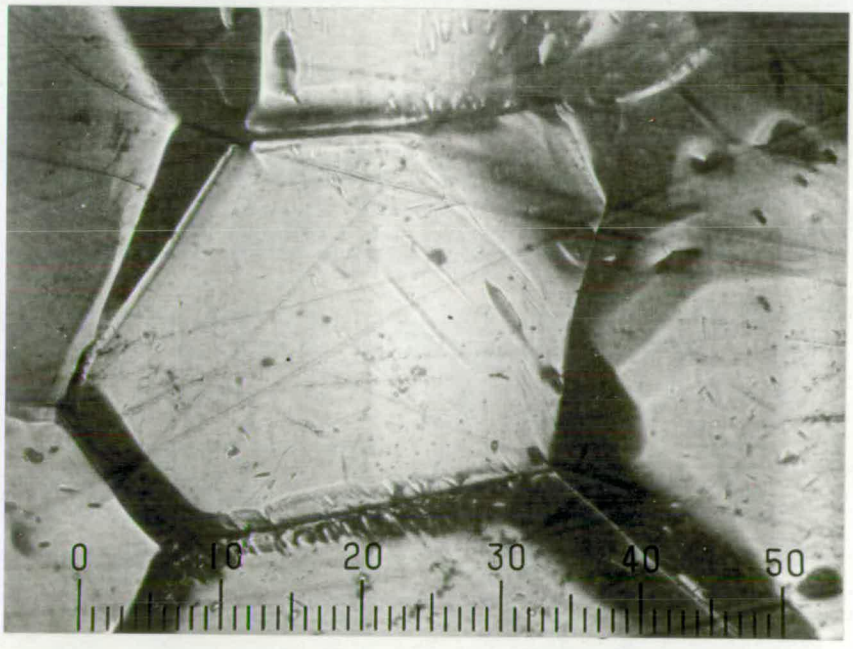


FIG 4.3.2.



- FIG. 4.3.3. -

Substrate Face.
10 microns/ division.



- FIG. 4.3.4. -

Growth Face.
10 microns/ division.

metre /hour, it highlighted a hitherto unsuspected radial substrate temperature gradient, by yielding convex layers tapering in thickness to zero near the substrate edge. In view of the relatively high thermal conductivity of sapphire and 0.5×10^{-3} metre thickness of substrates employed, attempts to smooth the substrate radial temperature gradient by further increasing the substrate thickness were not considered.

Exploration of reduction in charge temperature to inhibit the rate of sublimation revealed that acceptable deposition rates could thus be obtained, although this procedure naturally imposed an undesirable restriction on the maximum substrate temperature which could be employed.

4.4 THE EFFECTS OF SYSTEM PARAMETERS ON EPITAXY :

As a comparison with conventional deposition systems employing relatively low substrate temperature a series of depositions was performed under the thermal conditions defined by Fig. 4.4.1 on mica (muscovite) and sapphire substrates. Mica substrates were cleaved prior to insertion into the reaction chamber, and sapphire substrates were subjected to the cleaning procedure outlined in 4.3. In both cases deposition on the substrate was effectively terminated within approximately ten minutes by preferential deposition on the walls of the inner capsule. The deposition front propagated downwards

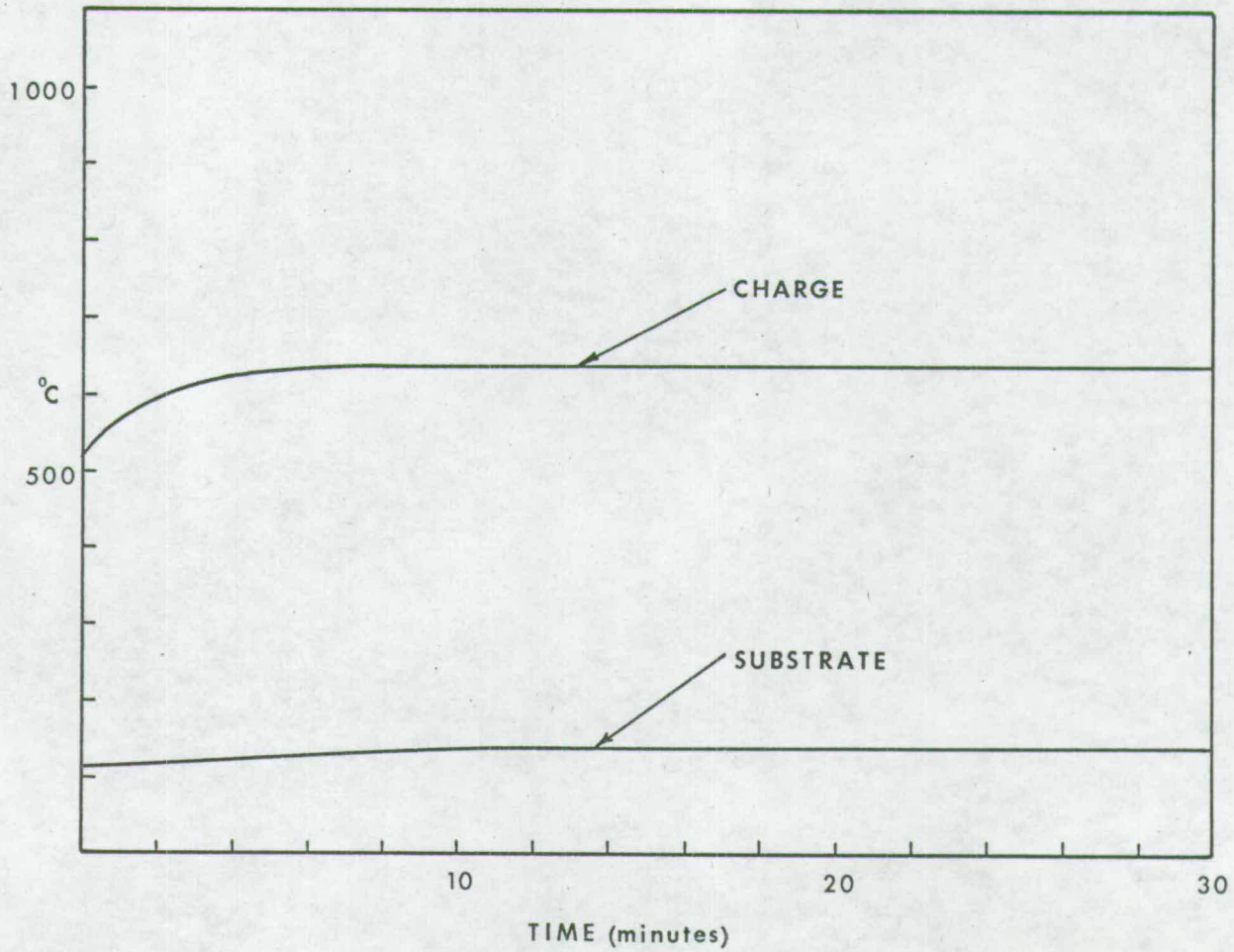
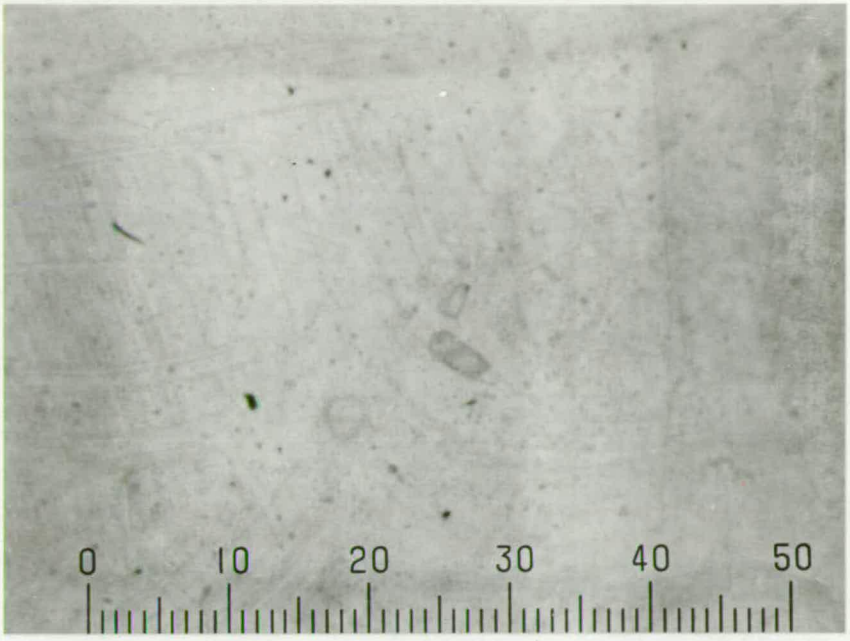


FIG 4.4.1.

from substrate level at approximately 3×10^{-3} metre /minute finally reaching the charge level. On mica, shiny continuous layers were formed with no structure in or on the surface except for mica cleavage steps and glancing angle X-ray diffraction showed distinct continuous polycrystalline arcs representative of those from crystallites of less tha 0.1 micron . The corresponding films on sapphire were optically similar, reproducing the polished structure of the substrate. The broad diffuse arcs obtained from glancing angle X-ray diffraction indicated that the layers were more or less amorphous. Film thickness was approximately 3000 Å and the optically featureless films were lemon yellow in colour in spite of the low substrate temperature.

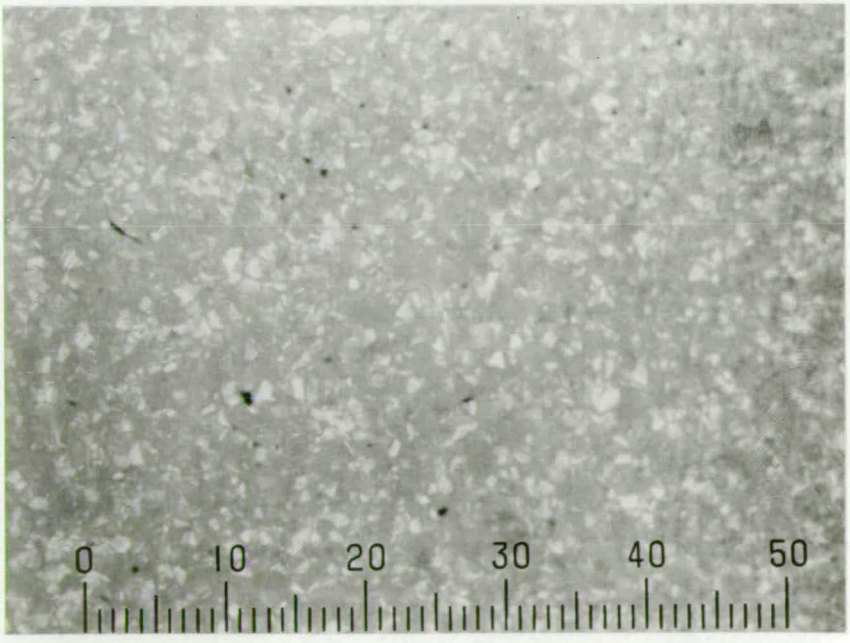
Figs. 4.4.2 - 4.4.6 demonstrate clearly the beneficial effect of increasing substrate temperature on crystallite size but in all cases large variations, up to 50:1, in grain size are evident, and at substrate temperatures in excess of 900°C the rate of increase in grain size was found to decrease rapidly. The layers obtained at temperatures in excess of 800°C can perhaps best be described as irregularly shaped agglomerates of fairly large crystallites. X-ray Laue back reflection revealedin all cases randomly oriented crystallites which are impossible to index Fig.4.4.7.



- FIG. 4.4.2 -

Substrate Temperature 600°C.

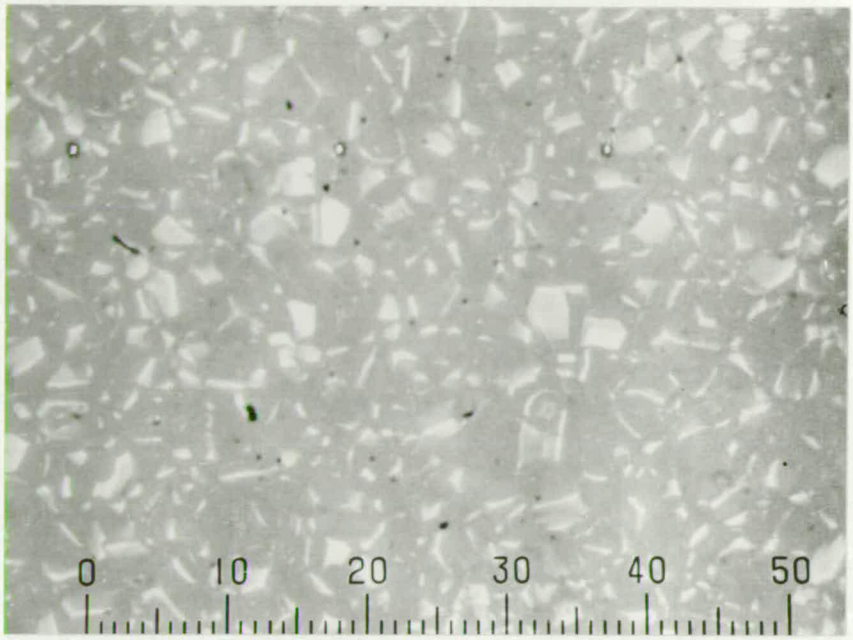
10 microns/division.



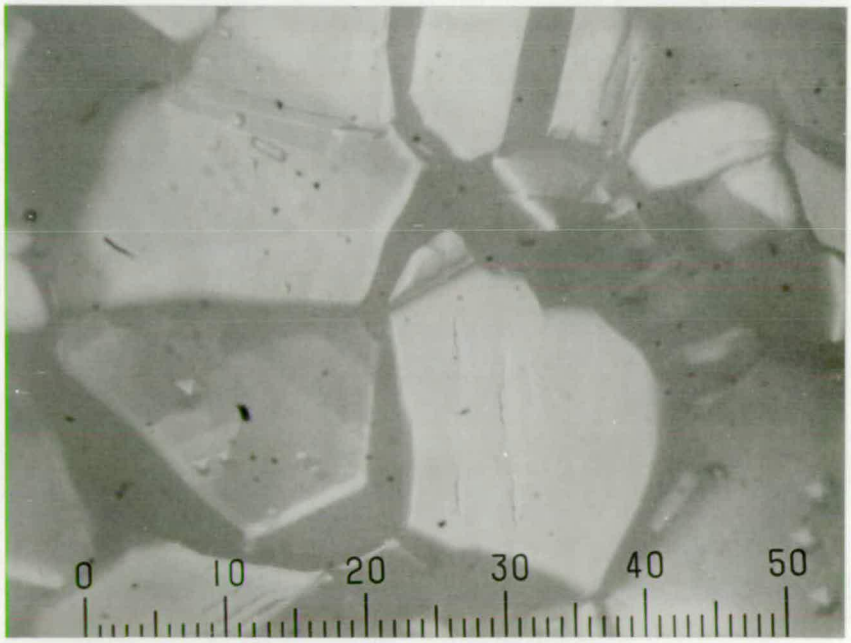
- FIG. 4.4.3 -

Substrate Temperature 675°C.

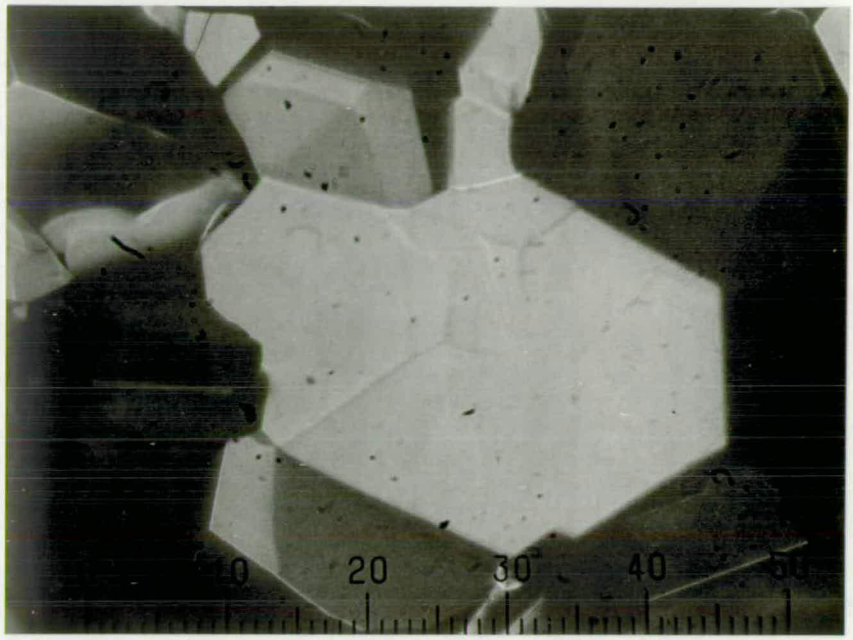
10 microns/division.



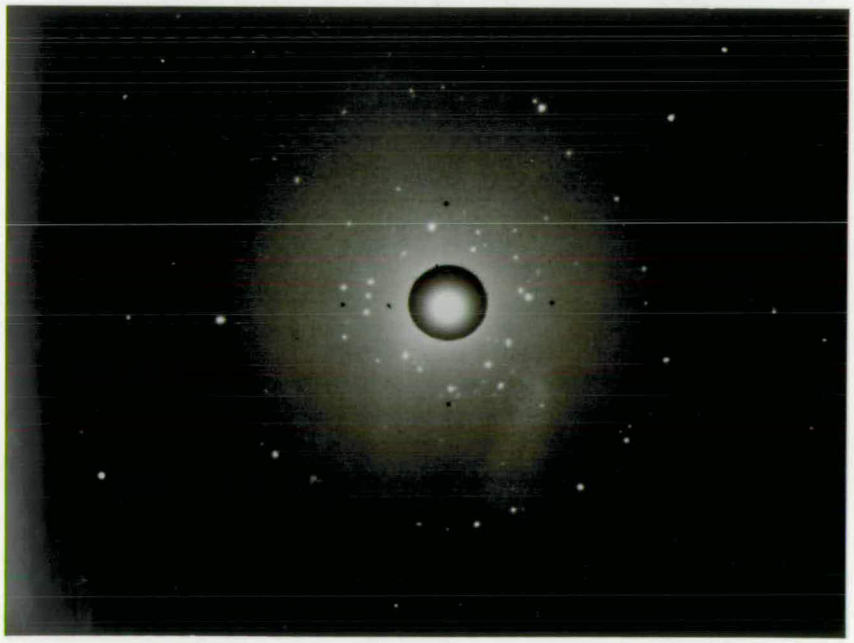
- FIG. 4.4.4. -
Substrate Temperature 750°C.
10 microns/division



- FIG.4.4.5. -
Substrate Temperature 825°C.
10 microns/division



- FIG. 4.4.6. -
Substrate Temperature 975°C
10 microns/division.

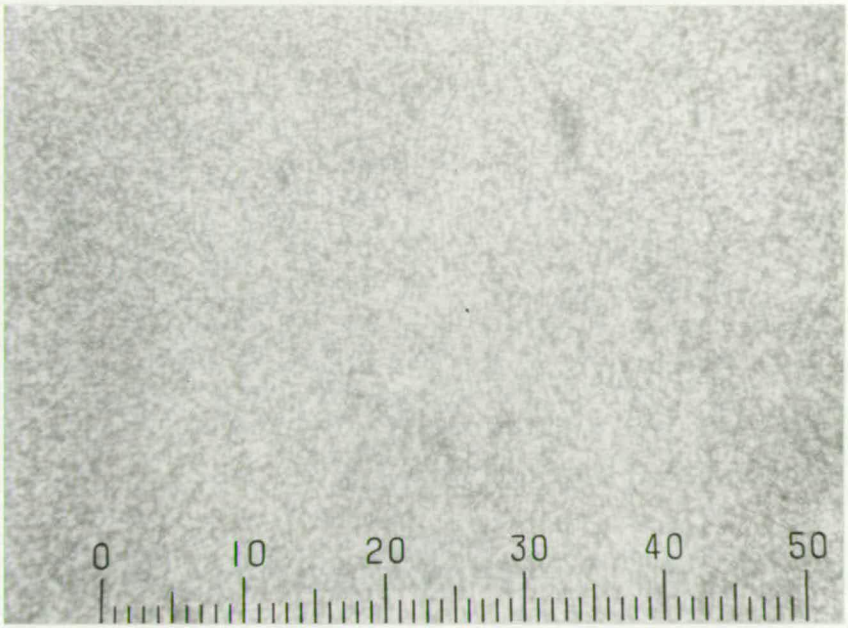


- FIG. 4.4.7. -

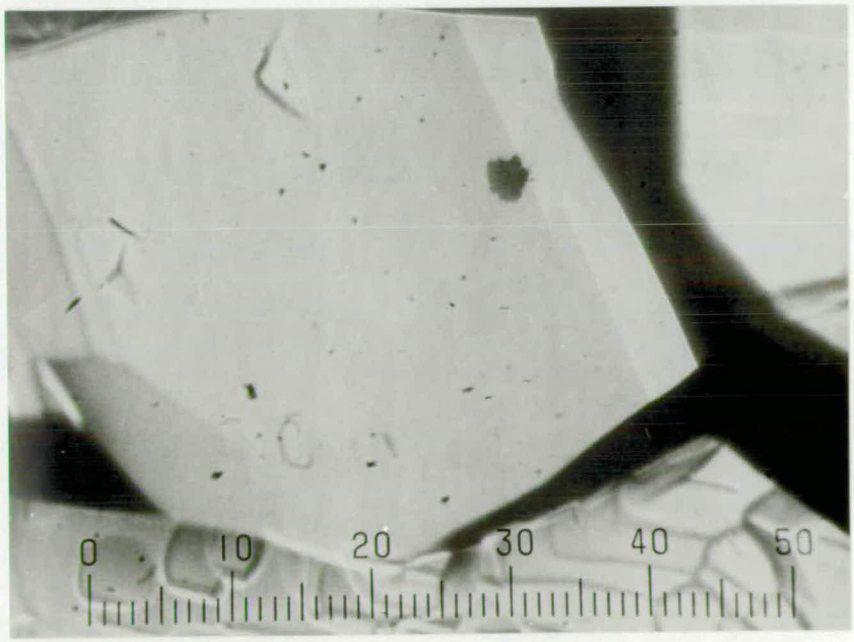
While clearly an improvement in crystallite size over films deposited conventionally at less elevated temperatures had been obtained, a suspiciously low degree of crystallite orientation was evident, and the existence of a barrier in dimensions was not commensurate with the situation of a deposit with increasing surface mobility seeking ever more favourable sites on the host lattice through microscopic recrystallisation at the nucleation stage. Tests encompassing a wide range of substrate orientations confirmed that at no temperature could crystallite dimensions or orientations be sensibly related to the host lattice orientation, nor were variations evident, indicating that the condensing deposit was either lacking a clear view of the host lattice or was failing to respond to this view. To test this theory, a programme of substrate chemical etching as described in 5.1 was initiated.

At substrate temperatures of 600°C, Fig.4.4.8, the effects of chemical etching in revealing the host lattice structure are not yet evident (compare Fig. 4.4.2), inferring that the condensate does not yet enjoy sufficient surface mobility to respond fully to the host lattice.

A more harmonious condensate-substrate system develops with increasing substrate temperature Fig.4.4.9. In addition the substrate orientation begins to influence the film.



- FIG. 4.4.8. -
Substrate Temperature 600°C
2.5 microns/division.



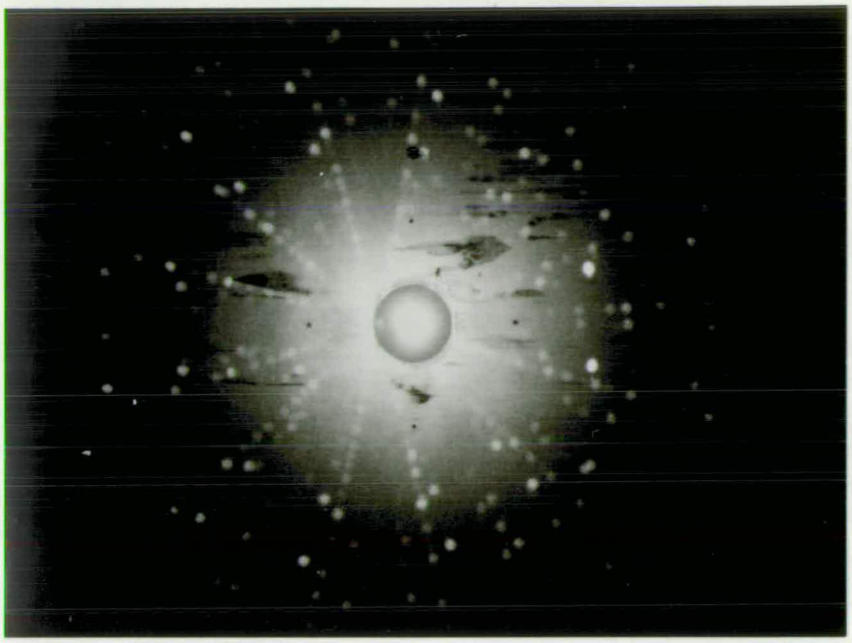
- FIG. 4.4.9. -
Substrate Temperature 850°C
10 microns/division.

Logically, according to the theory presented in the second chapter, further elevation of substrate temperature, with associated enhancement of surface mobility, must force an orientation dependent tendency towards single crystal films.

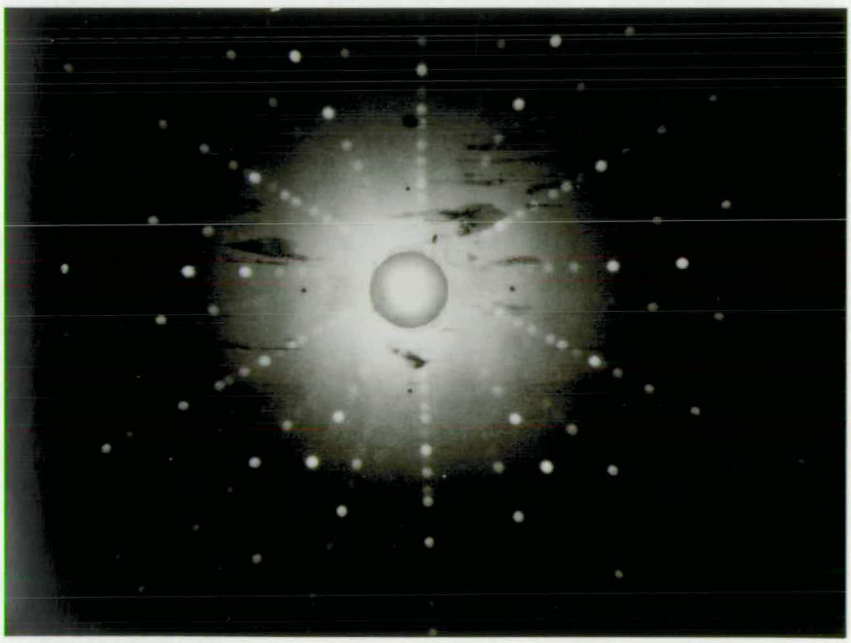
Depositions performed under thermal conditions defined by Fig.4.2.1 exemplify this process in X-ray back reflection Laue photographs, Figs.4.4.10 and 4.4.12. Specimen Laue back reflection photographs obtained from bulk single crystals of cadmium sulphide are presented by way of comparison in Figs. 4.4.11 and 4.4.13. The thickness of films examined was approximately 100 microns and the substrate material was Verneuil grown sapphire in all cases.

4.5 CONDITIONS FOR EPITAXIAL GROWTH :

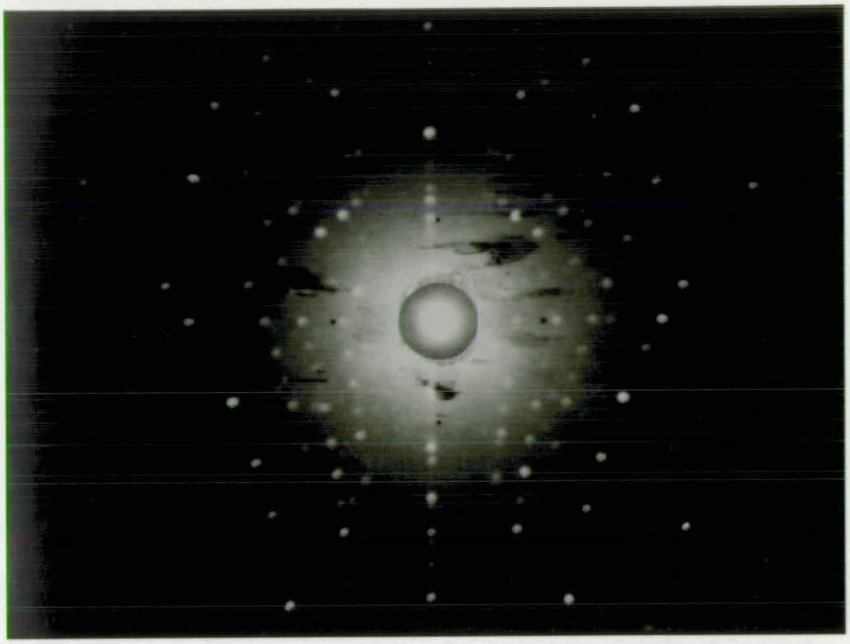
Mention has been made of the necessity to employ source-substrate temperature differentials of approximately 70°C to swamp radial substrate temperature gradients and of the ensu ing inconveniently high layer growth rates. Since reduction in charge, and hence substrate temperatures as a means of control is effective only over a limited temperature range below 850°C, at the more elevated temperatures required to yield single crystal films the introduction of an inert gas at a predetermined pressure to the apparatus as impediment to diffusion is an acceptable alternative.



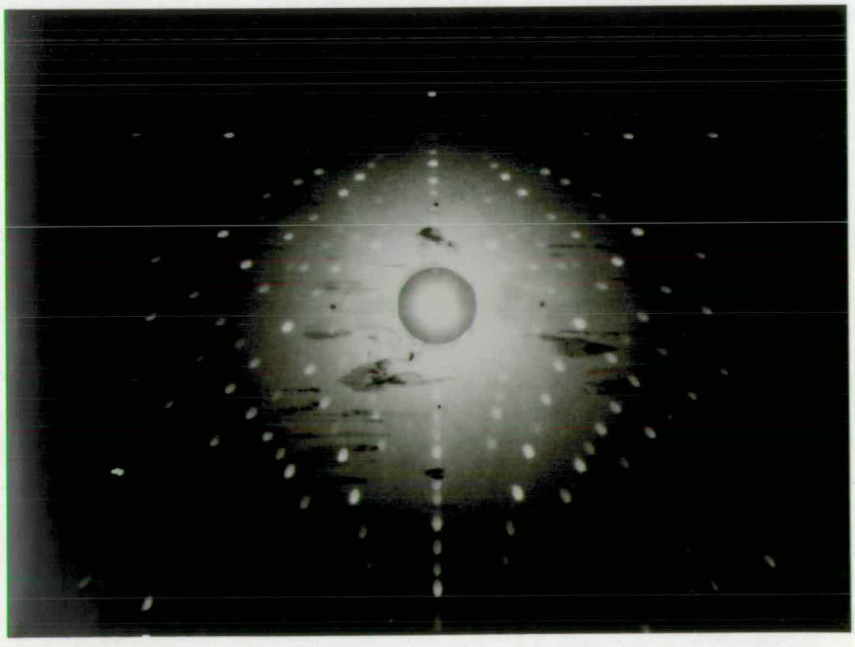
- FIG. 4.4.10. -
CdS 0001 Plane Film
on (10$\bar{1}$2) Plane Sapphire



- FIG. 4.4.11 -
CdS (0001) Plane
From Bulk Single Crystal.



- FIG. 4.4.12 -
CdS ($10\bar{1}2$) Plane Film
on ($2\bar{1}\bar{1}0$) Plane Sapphire.



- FIG. 4.4.13 -
CdS ($10\bar{1}2$) Plane
From Bulk Single Crystal.

Single crystal films as shown in Fig.4.4.12 were produced by charging the apparatus during bakeout prior to deposition with 99.995% argon to a pressure of 200 torr. This ensured a convenient average growth rate of 0.3×10^{-3} metre /hour. The dependence of growth rate on argon pressure is illustrated in Fig.4.5.1 and agrees reasonably with that observed by Toyama [164]. Reference to Fig. 4.2.1 reveals that in the initial stages of deposition the substrate temperature lags that of the charge. This is fundamental to the design of the apparatus and reflects simply the enhanced thermal transfer characteristics at the reaction chamber base which is in contact with the heated outer chamber. Obviously, the first few hundred angstroms of film are deposited at a substrate temperature of approximately 300°C and in order to investigate this preliminary layer, a deposition on a chemically etched substrate was quenched in the initial stages, Fig. 4.5.2, by rapidly withdrawing the apparatus from the furnace with simultaneous introduction of argon to a pressure of 600 torr. The resulting film, shown in Fig. 4.5.3 was similar to earlier low substrate temperature depositions on chemically etched and unetched substrates displaying a grain size of less than 1 micron in evidence that the grain structure of the film had not yet been significantly influenced.

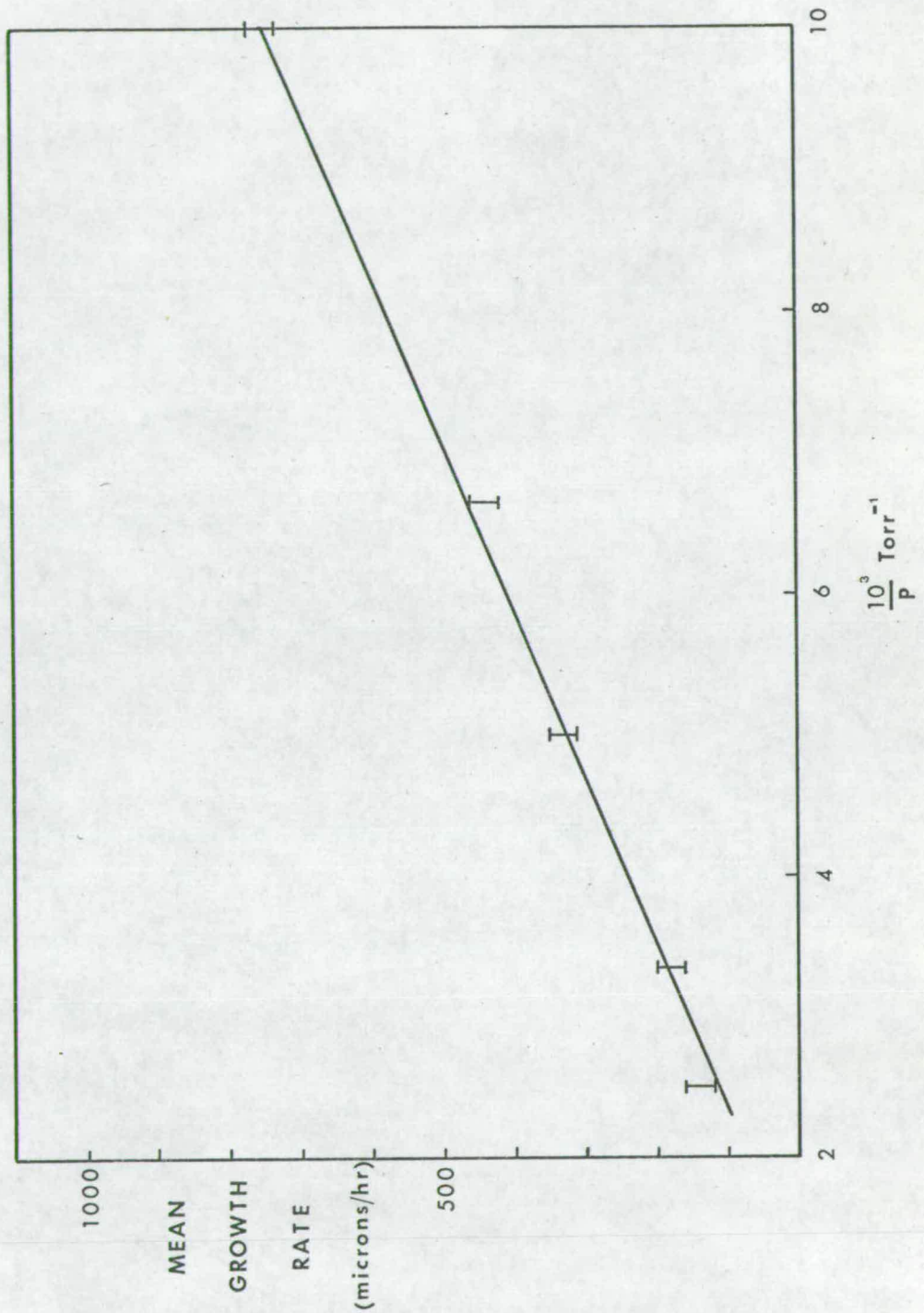


FIG 4.5.1.

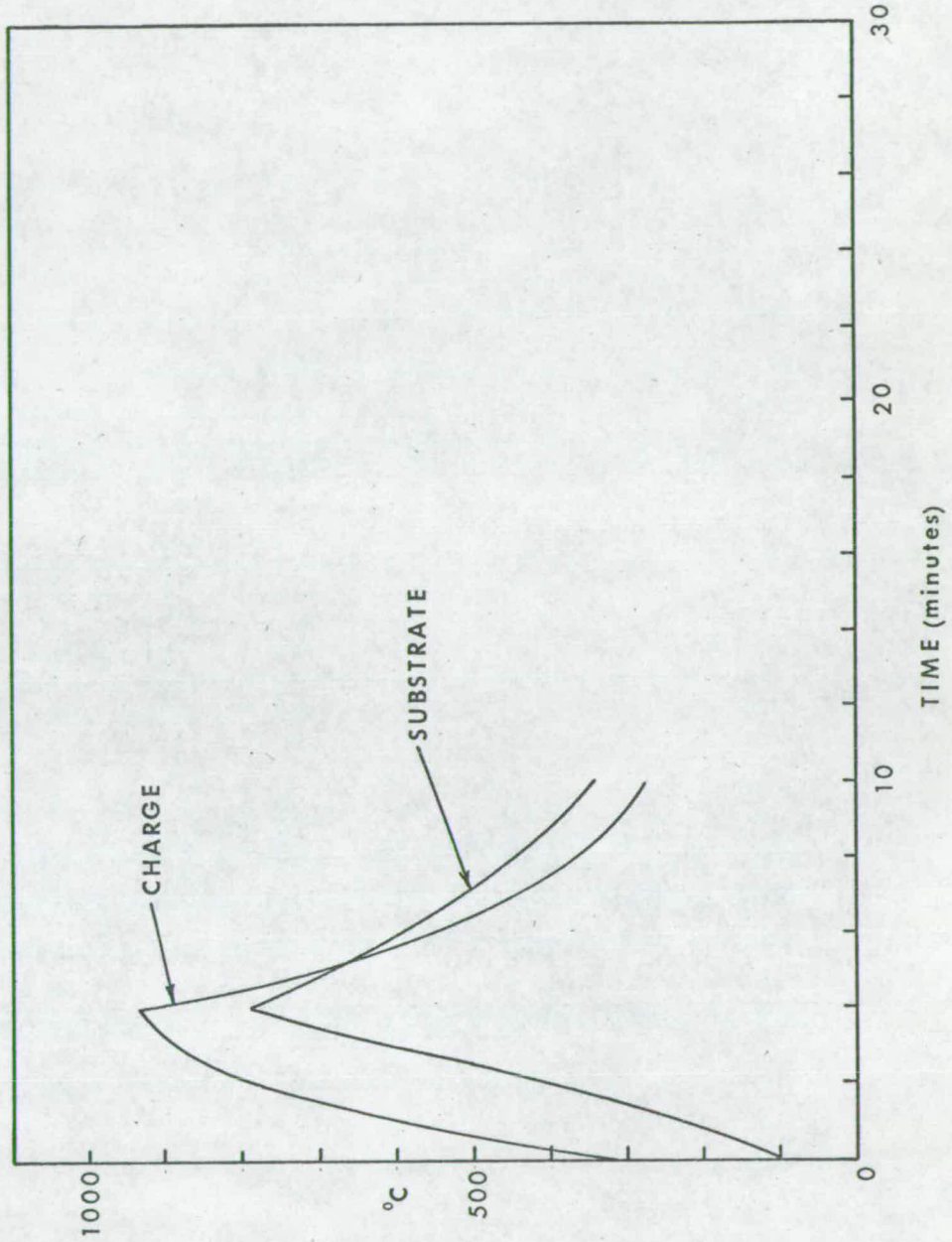
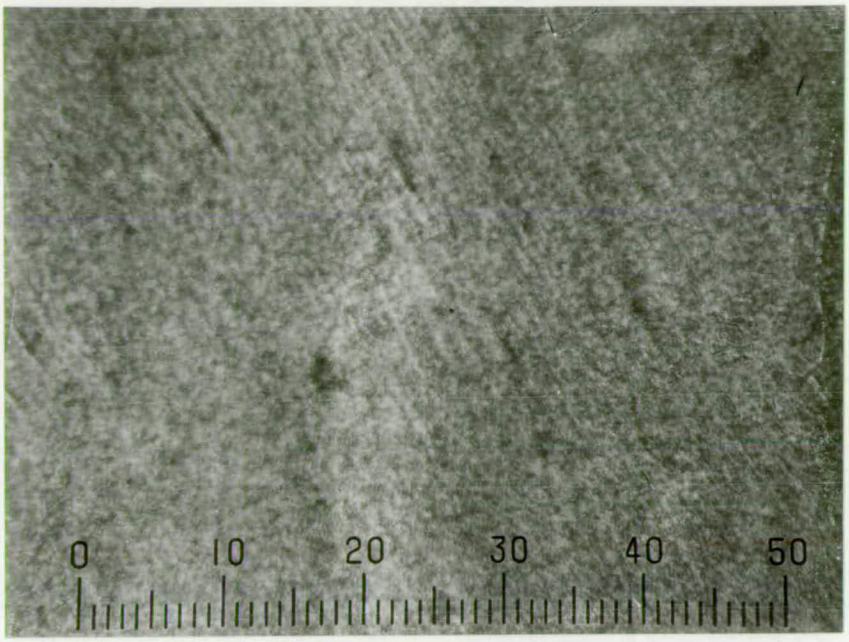
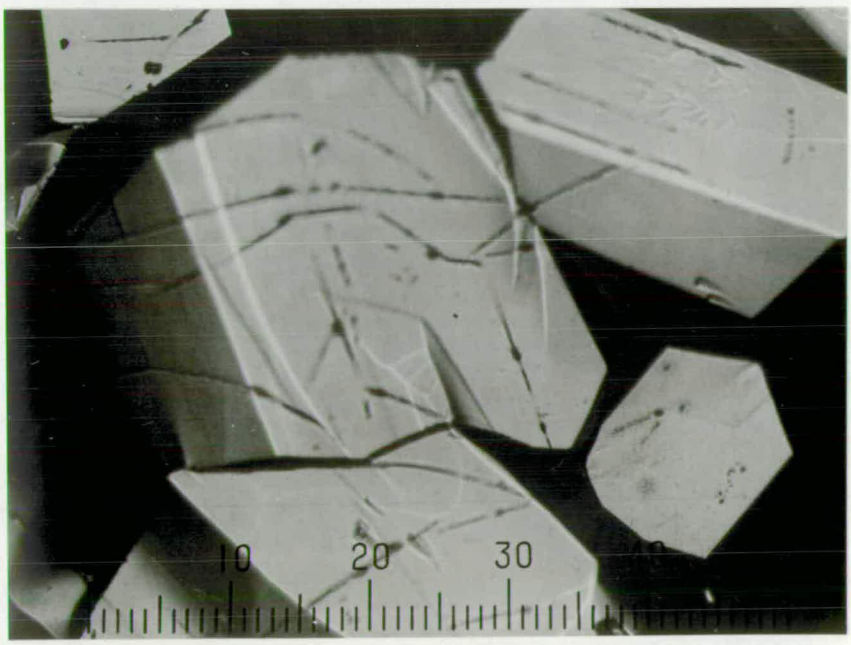


FIG 4.5.2.



- FIG. 4.5.3. -

2.5 microns/division.



- FIG. 4.5.5. -

10 microns/division.

Conversely, a series of depositions was performed in two stages, the initial stage being a deliberately prolonged low substrate temperature deposition, Fig.4.5.4 and the final, a normal high temperature growth. On chemically unetched substrates the results as shown in Fig. 4.5.5. were comparable with single stage high temperature depositions, and on chemically etched substrates the film comprised regions of striated crystallites as shown in Figs. 4.5.6 - 4.5.7 and 4.5.8.

These results indicate that recrystallisation plays an important role in the early stages of film growth, the initial deposition being of polycrystalline material which recrystallises on a microscopic scale only as the substrate temperature is raised, this process being seriously inhibited by further deposition of material at low temperature. The similarity of the initial layer of material to that grown on unetched substrates indicates that the initial nucleation process, while obviously not unimportant, does not yield single crystal epitaxial films unless supplemented by a favourable growth process. This appears to contradict some earlier theories of epitaxy [127,128,129], but is in agreement with Pashley [130].

Further evidence of the importance of the recrystallisation process was discovered in attempts to produce films by lowering the substrate temperature

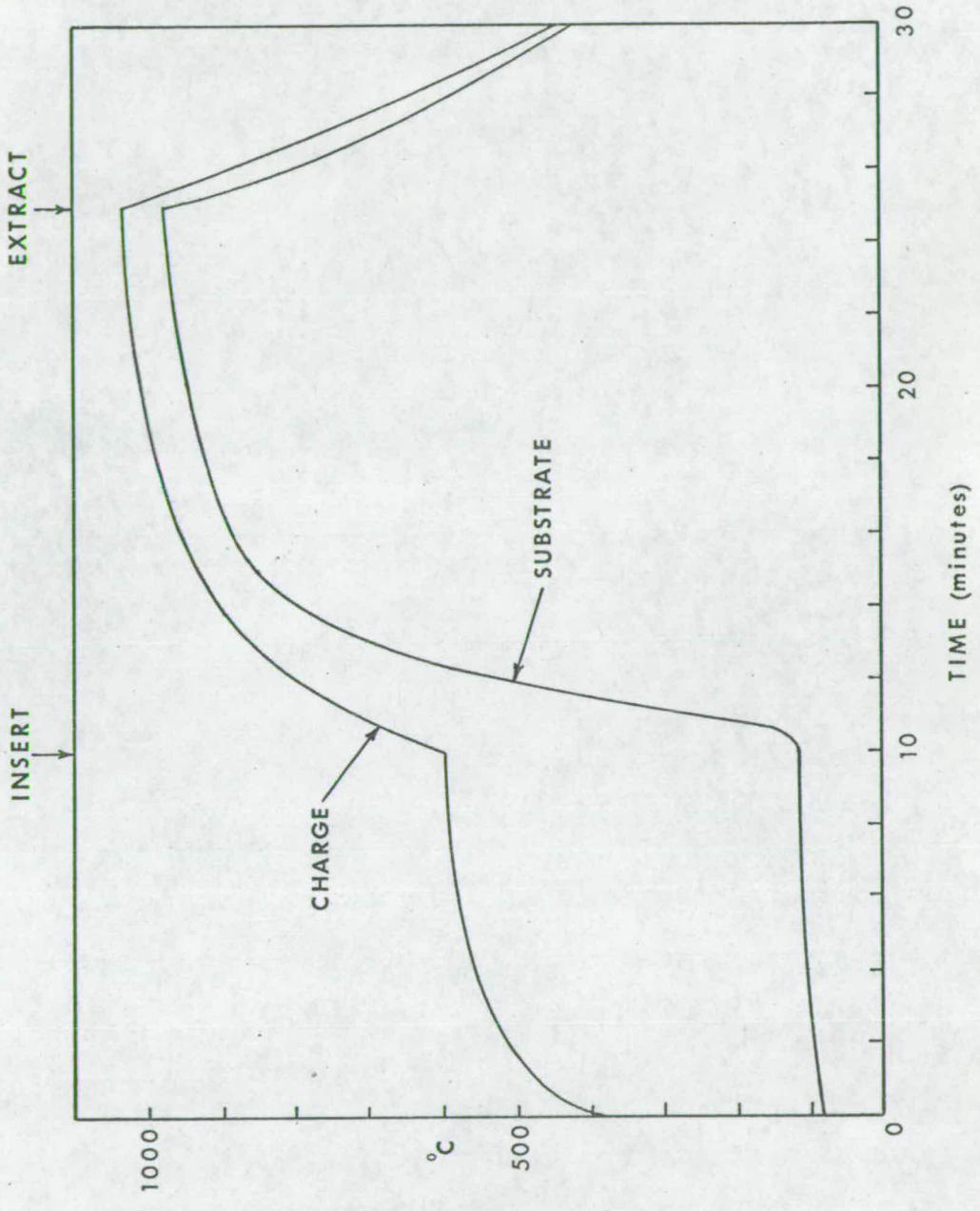
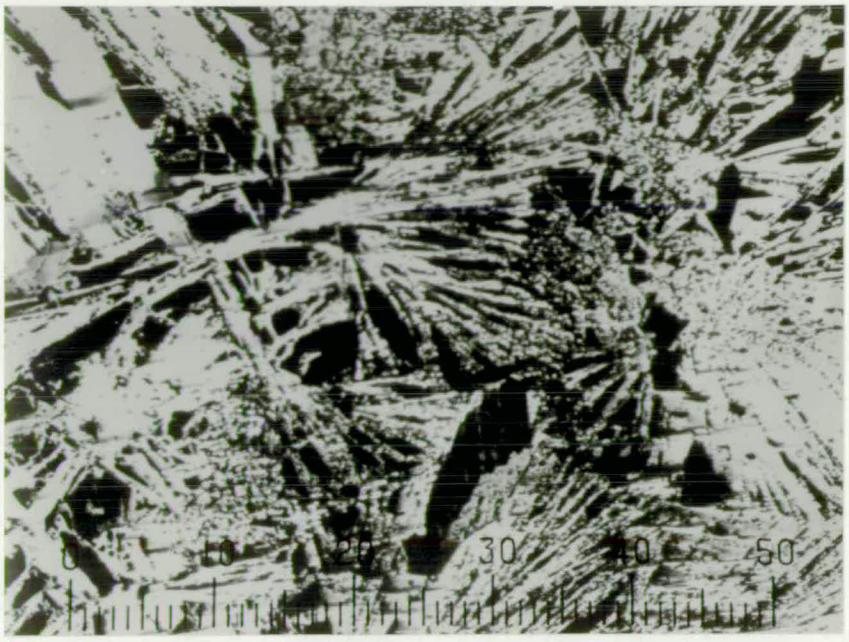
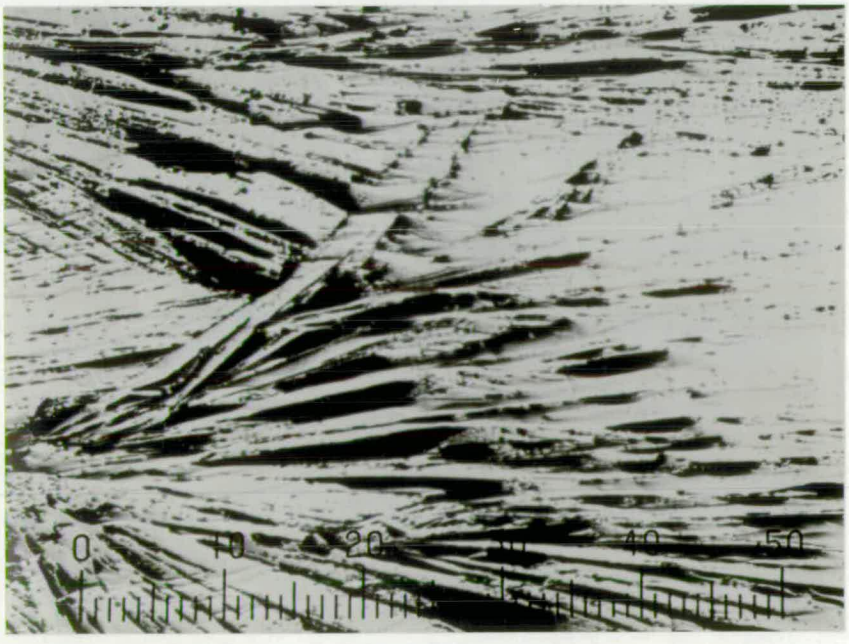

EXTRACT
INSERT
CHARGE
SUBSTRATE
1000
500
°C
0
10
20
30
TIME (minutes)

FIG 4.5.4.



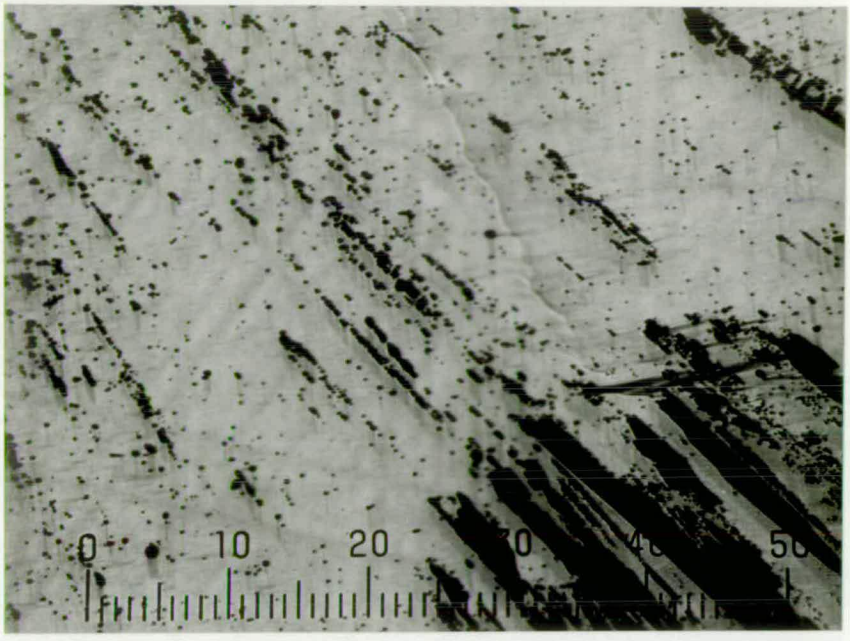
- FIG. 4.5.6. -

20 microns/division.



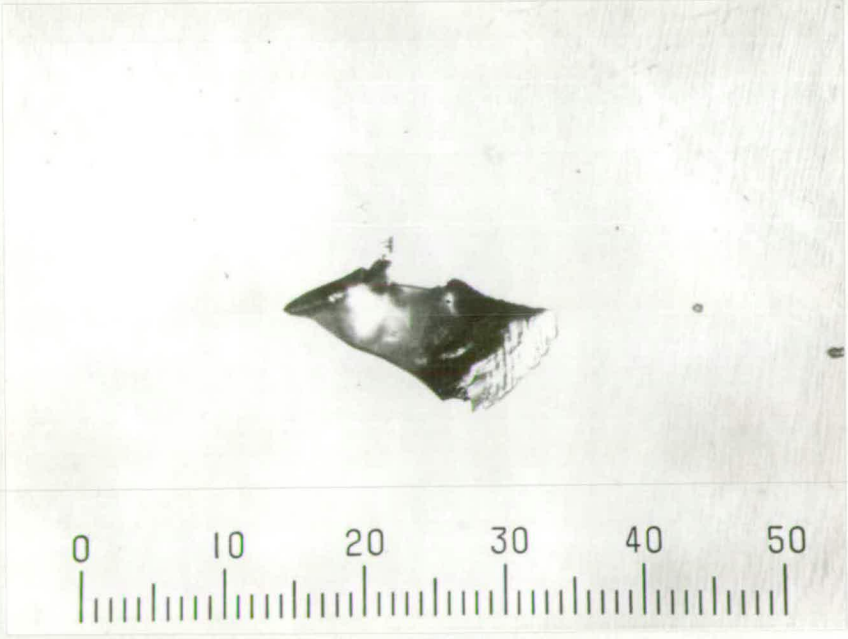
- FIG. 4.5.7. -

20 microns/division.



- FIG. 4.5.8. -

20 microns/division.



- FIG. 4.5.10 -

10 microns/division.

from a value exceeding that of the charge, Fig.4.5.9, thus initiating growth on a substrate free from prenucleated deposit. These failed to yield a film structure on both unetched and chemically etched substrates, Fig. 4.5.10, thus indicating failure of the substrate to accept condensing deposit consistently over its surface and adding weight to the theory that a regular periodic potential is not available at all points on the surface.

The appearance of imperfect regions of growth on some substrates had been noted with interest and when one substrate displayed, after chemical etching, a distinct line across its surface, Laue back reflection X-ray photographs were obtained from material on both sides of the line. These revealed single crystal sapphire on one side, as shown in Fig.4.5.11, and polycrystalline material on the other, Fig.4.5.12. This fortuitous substrate fault permitted observation of growth on different grades of substrate material in a single experiment and the result is displayed in Fig.4.5.13. The nature of growth depends heavily on substrate perfection presumably through the more widely spaced recrystallisation centres viewing relatively undamaged substrate material, which are available on poor quality substrates. As a consequence of this theory one would expect single crystal growth to occur at a lower temperature on more perfect substrate material, for example on Czochralsky grown material

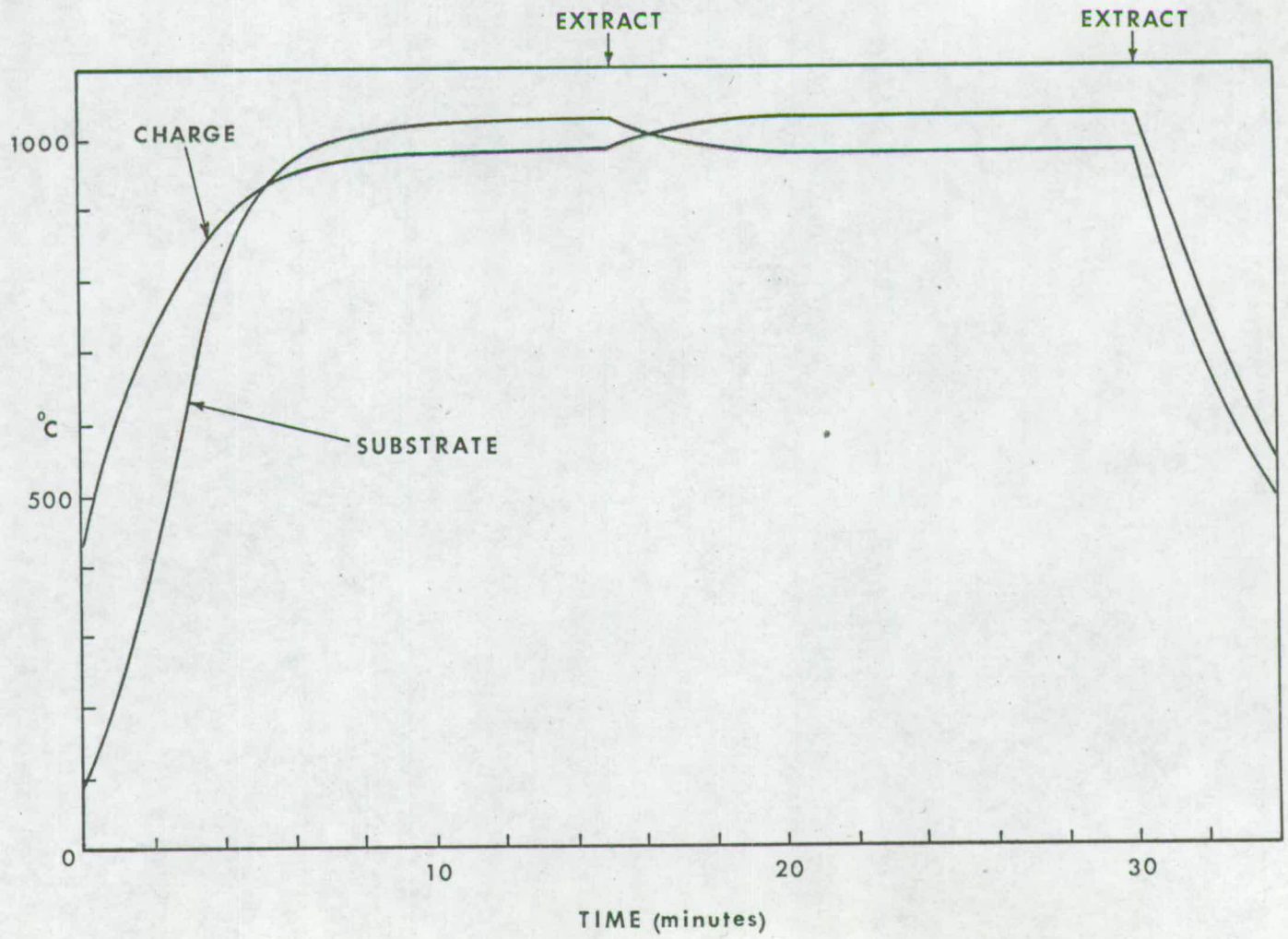
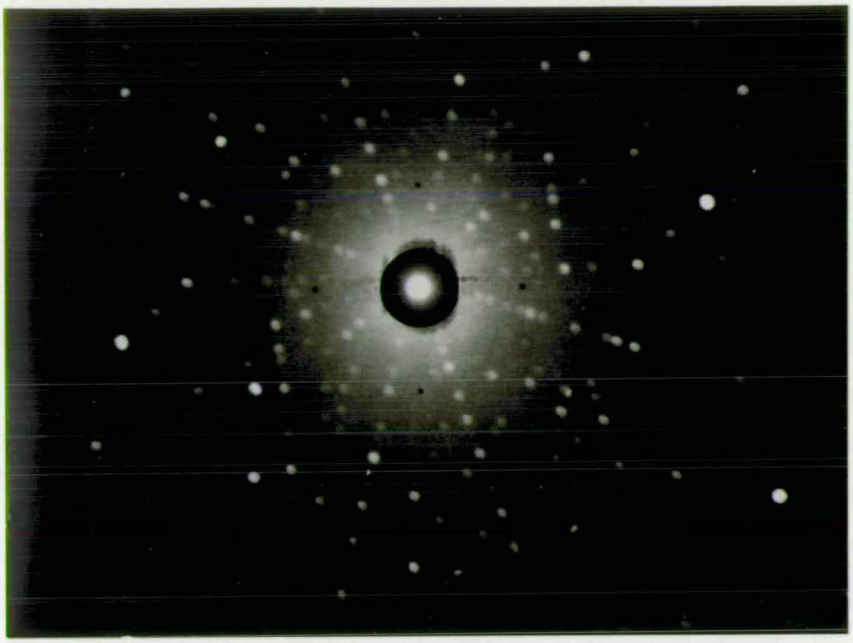
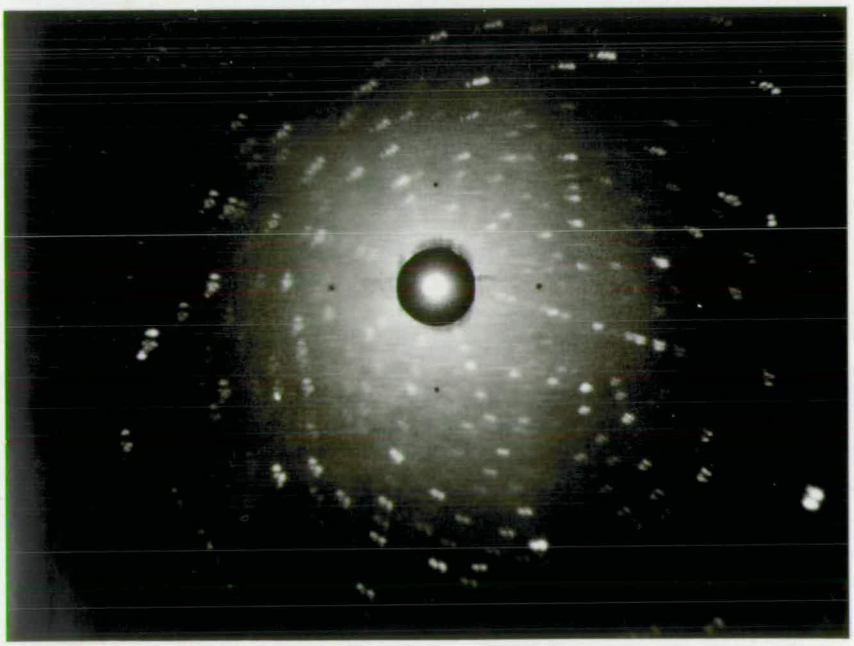

EXTRACT
EXTRACT
1000
CHARGE
°C
SUBSTRATE
500
0
10
20
30
TIME (minutes)

FIG 4.59.



- FIG. 4.5.11. -



- FIG. 4.5.12 -



- FIG. 4.5.13 -

It is evident that the success of the basic microscopic recrystallisation depends on the existence of an equilibrium situation where interchange of species with the vapour phase may occur in conjunction with surface diffusion and reorientation. Bulk recrystallisation has been observed not to depend on the substrate [115].

CHAPTER 5

PREPARATION OF SUBSTRATES.

5.1 CHEMICAL SUBSTRATE ETCHING :

In order to generate sufficient interaction between the host lattice and the mobile condensate to control ultimate characteristics of the deposited layer, it was found essential to chemically etch the substrate surface prior to insertion of the substrate into the reaction chamber.

The sapphire substrates employed were prepared with surfaces mechanically polished to better than 0.03 micron and although this technique yields surfaces with a high degree of flatness, it appears to induce, on an atomic scale, lattice damage sufficient to virtually obscure the host lattice from the condensate, to such an extent that the deposit is unaware of the crystallographic orientation of the substrate. This has been clearly demonstrated experimentally.

Since lattice damage is initiated basically by forcible displacement of atoms from their equilibrium locations with resultant bond strains and bond fractures, a non-mechanical means of material removal from the substrate surface is favoured. This poses immediate difficulties in the case of sapphire and these difficulties may be attributed directly to its lack of chemical reactivity with common reagents. Initial attempts [165] to remove

surface layers by immersion in orthophosphoric acid at temperatures up to 400°C, revealed the inconveniently slow nature of the process, etch rates being of the order of 1 micron/hour. This procedure did, however, display damaged sites by preferential etching and yielded a mass of randomly directed surface scratches.

A more vigorous [166] alternative procedure which used molten vanadium pentoxide was found to be more satisfactory and did not appear to suffer from a disadvantage encountered with orthophosphoric acid [166] of residual incorporation of the etchant in the substrate. Ideally, the molten material should be contained in a platinum crucible but, in the absence of this, a carbon crucible was designed, Fig. 5.1.1, into which the substrate was gently lowered subsequent to the entire assembly being raised to 800°C. Substrates were suspended by 0.5mm diameter platinum wire in the etchant for a period which depended on the history of the etchant and the crystallographic orientation of the sapphire.

On the basis of experimental results in cadmium sulphide depositions, the exact amount of material removed from substrate surfaces did not prove to be critical, provided that sufficient reaction occurred to yield on optical examination a surface free from polishing scratches. This necessitated removal of 30-70 microns of material on average. Sensitivity of etching rate to concentration of alumina in the

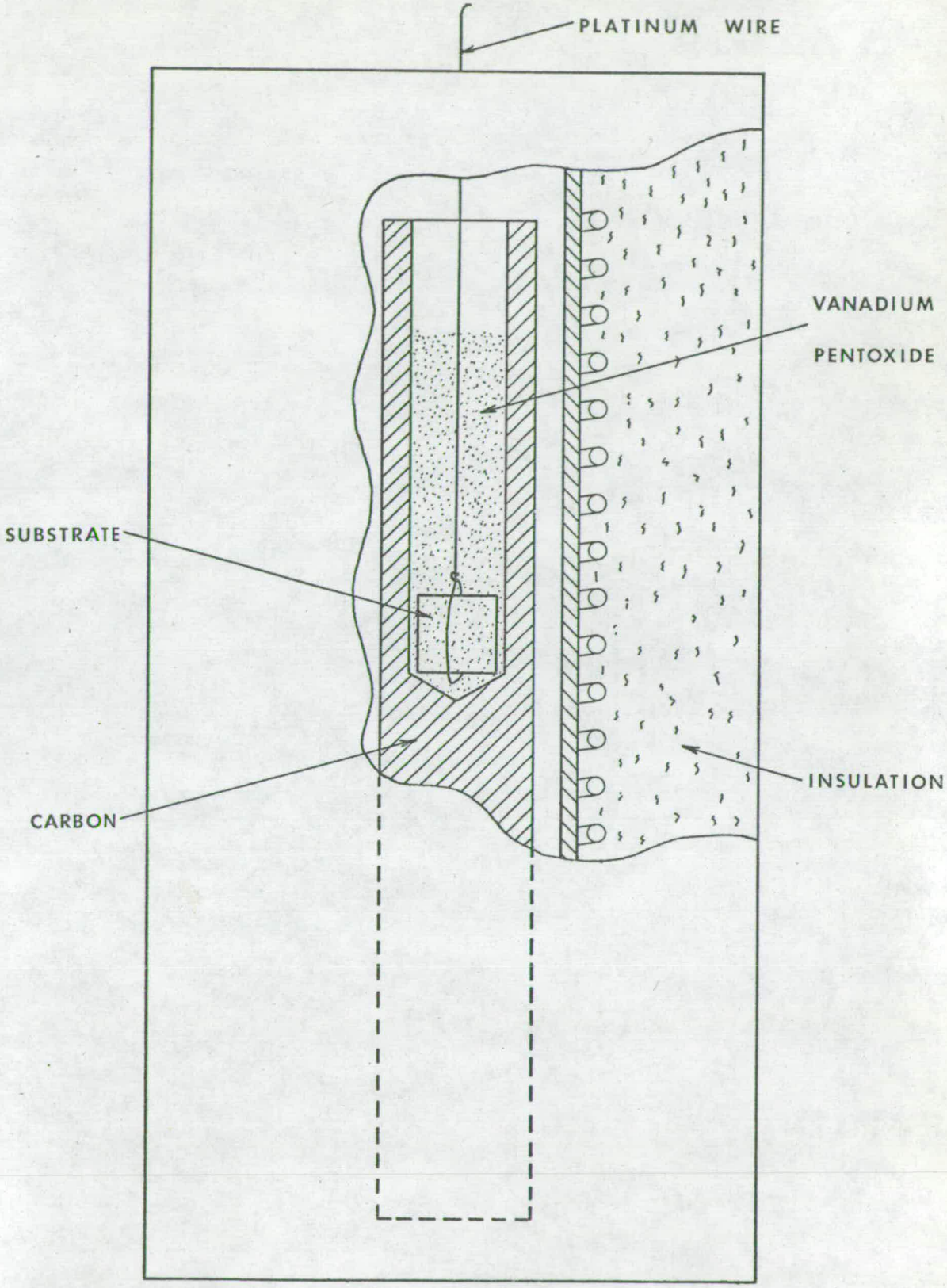

PLATINUM WIRE
VANADIUM
PENTOXIDE
SUBSTRATE
CARBON
INSULATION

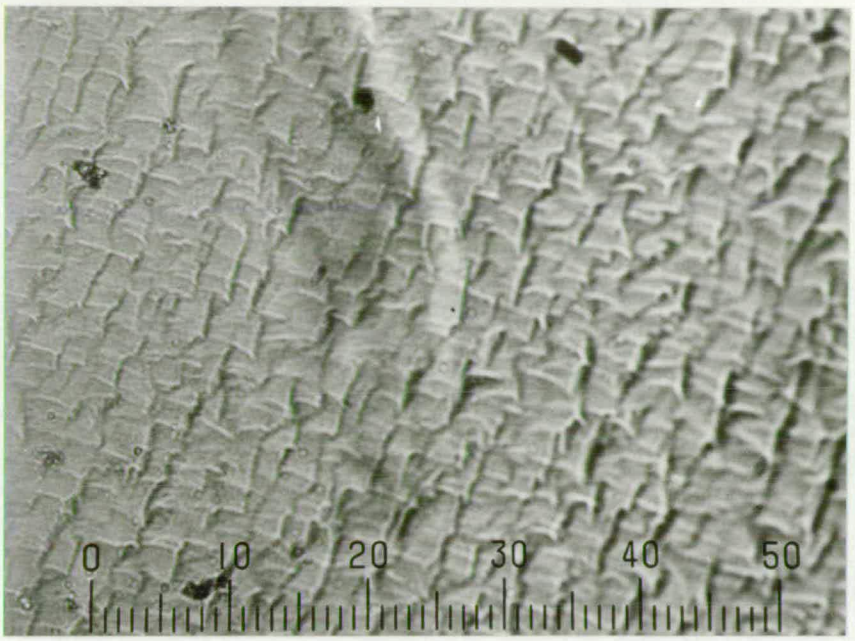
FIG 5.1.1

melt was observed but no serious attempt was made to tabulate this in view of the periodic additions of fresh vanadium pentoxide powder made to the crucible to compensate for the characteristic 3:1 volume reduction of the material on melting.

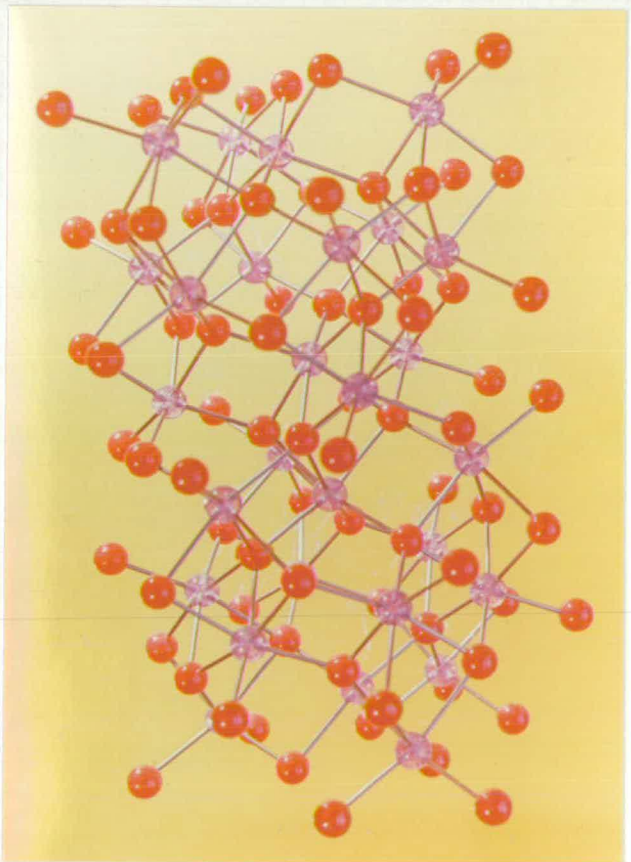
Orientation sensitive etching rates were also observed in $(11\bar{2}0)$, (0001) and $(10\bar{1}2)$ samples, the rate increasing in order of presentation. A reaction period of 20 minutes at 800°C proved satisfactory in all cases and was adopted as standard procedure in view of the stated uncritical etch depth. Removal of excess vanadium pentoxide after etching was effected by immersion in cold concentrated hydrochloric acid for approximately 12 hours followed by ultrasonic cleaning and rinsing in doubly distilled water. Substrates were stored under water until required. Fig. 5.1.2,displays a typical etched surface.

5.2 OPTICAL CRYSTALLOGRAPHIC EXAMINATION :

Since cadmium sulphide and sapphire are both transparent, useful preliminary information of their orientation is available by the technique of optical examination under polarized light. Although cubic crystals are optically isotropic, non cubic crystals are optically anisotropic and divide an entering ray of light into two polarized rays which pursue slightly different paths and travel with different velocities, at least one of which is dependent on the



- FIG. 5.1.2. -
Typical V_2O_5 etched Surface of Sapphire.



- FIG. 5.4.4. -
Lattice Structure of Sapphire.

direction of propagation of the ray. It is this property of birefringence, Fig. 5.2.1, which permits rapid determination of crystal orientation since the crystals of interest are uniaxial with their optic axis co-directional with the crystallographic "c" axis in each case.

5.3 ORIENTATION BY X-RAY EXAMINATION :

The principle of back reflection X-ray analysis, Fig. 5.3.1, is that an impinging X-ray beam is reflected from successive atomic planes near the crystal surface. Reflected rays, since they exhibit phase differences, may interfere and corresponding to the condition for constructive interference which is :

$$n \lambda = 2d \sin \theta \qquad (5.3.1)$$

an emerging beam of X-rays indicating the orientation of one particular set of mutually parallel atomic planes may be detected. To obtain information relating to other atomic planes either θ or λ may be adjusted. Adjustment of θ implies a rotation of the specimen under examination and the use of a monochromatic X-ray beam.

Mechanically more convenient is exposure of a stationary specimen to white radiation, Fig. 5.3.2, yielding Laue back reflection patterns in which each atomic plane chooses the correct wavelength for reflection. In general, each spot is due to one set of mutually parallel planes and one particular

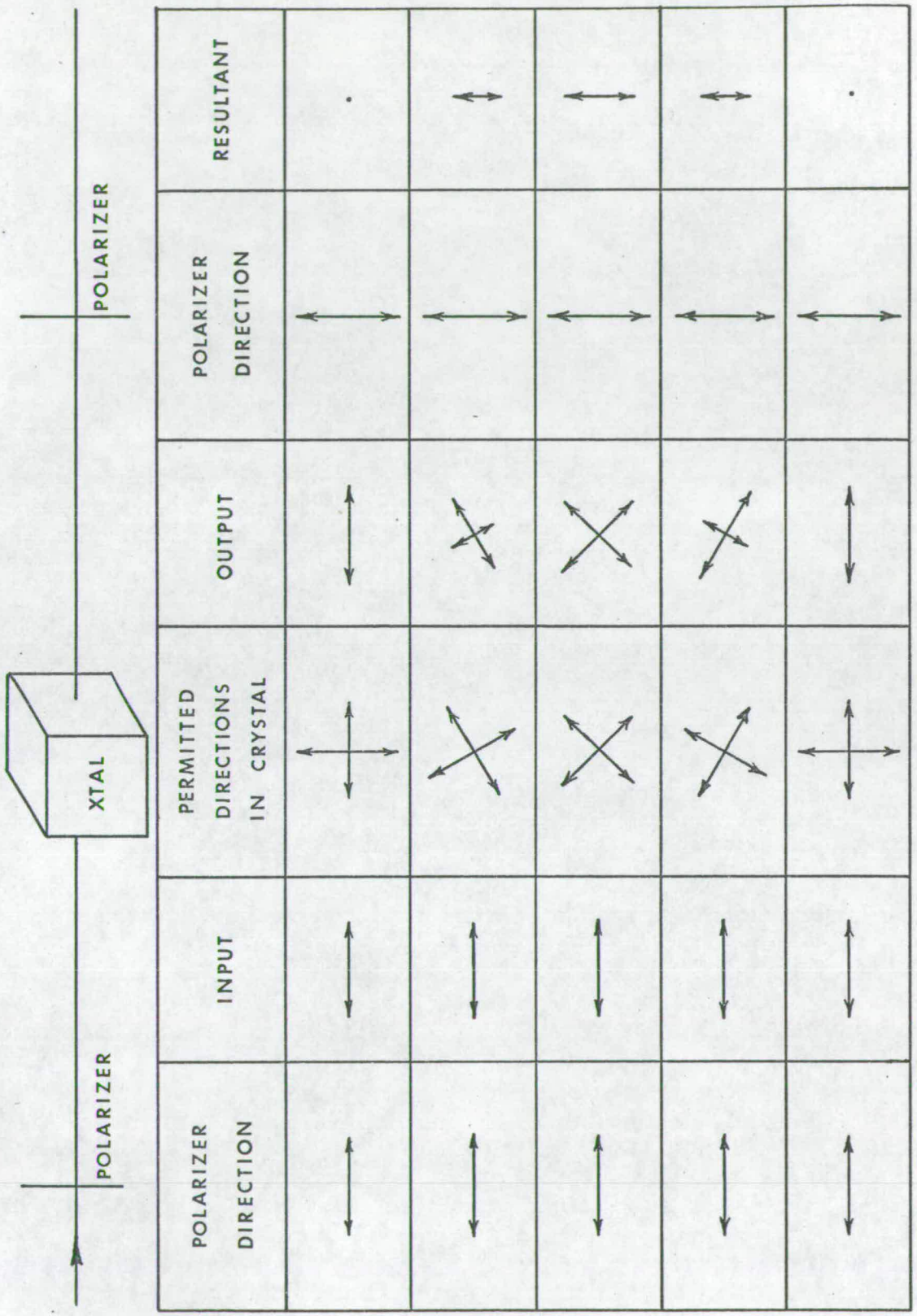

POLARIZER
XTAL
POLARIZER
POLARIZER DIRECTION
INPUT
PERMITTED DIRECTIONS IN CRYSTAL
OUTPUT
POLARIZER DIRECTION
RESULTANT

FIG 5.2.1.

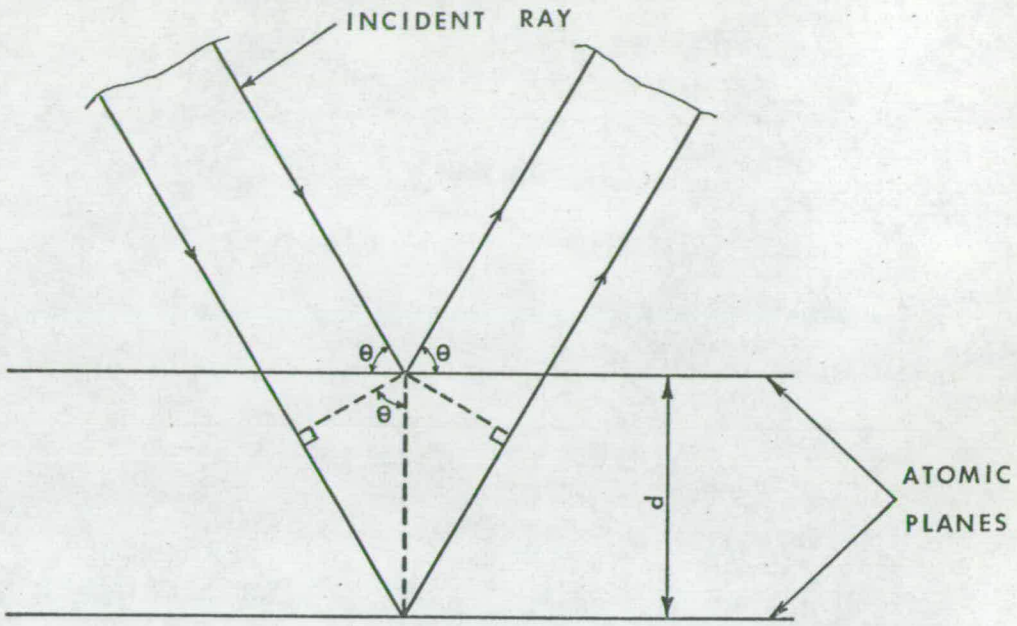


FIG 5.3.1.

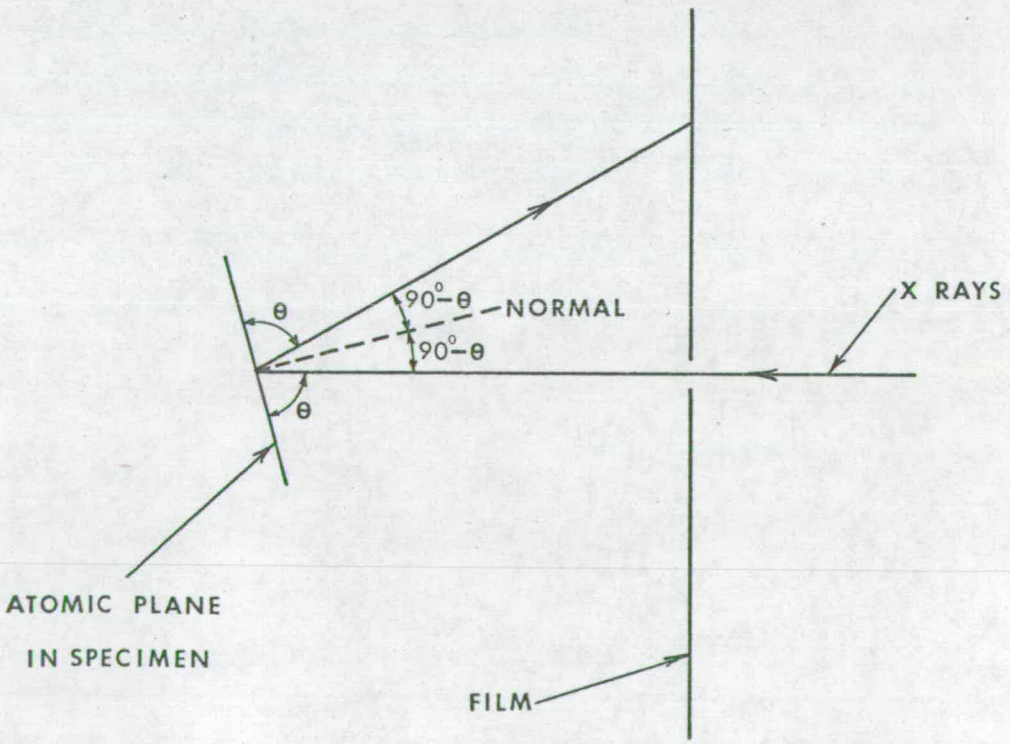


FIG 5.3.2.

wavelength if it corresponds to a high intensity portion of the beam wavelength spectrum, will yield a strong spot regardless of whether it arises from a principal plane or not. Reflections from zones fall on curves which intersect in reflections from principal planes. In the cases of zone axes parallel to the film, the curves become straight lines and the symmetry of the Laue photograph reflects directly the crystal symmetry. In order to assign Miller indices to the principal planes, a knowledge of angles between planes is useful, extraction of this information being facilitated by the Greniger net [167] which is calibrated so that the angles between plane normals or a plane normal and the impinging beam, may be read directly [168]. Since the Laue back reflection photograph encompasses only reflections of planes whose normals lie within approximately 30° of the direct X-ray beam, use of the stereographic projection to extend this range expedites correct labelling of planes. As a check on correct orientation, the point representing any plane on the stereographic projection may be rotated to the centre and the entire projection modified to correspond. The resulting projection may then be compared with the standard projection for that plane.

In view of the difficulties encountered in obtaining sapphire substrates of the required orientation from external suppliers the procedure eventually adopted was to obtain single crystal sapphire boules,

determine by X-ray analysis the location of the preferred axis, mark the boules and return them to the supplier for cutting and polishing. Orientation was performed to within one degree of the preferred orientation by the Laue back reflection technique employing the procedure outlined in this paragraph.

5.4 ANGLES BETWEEN PLANES - SAPPHIRE (α CORUNDUM):

Assuming the usual hkil notation, the angle θ between planes $h_1k_1i_1\ell_1$ and $h_2k_2i_2\ell_2$ is given by :

$$\cos\theta = \frac{h_1h_2 + k_1k_2 + \frac{1}{2}(h_1k_2 + h_2k_1) + \frac{3}{4}\frac{a^2}{c^2}l_1l_2}{\left[\left(h_1^2 + k_1^2 + h_1k_1 + \frac{3}{4}\frac{a^2}{c^2}l_1^2\right)\left(h_2^2 + k_2^2 + h_2k_2 + \frac{3}{4}\frac{a^2}{c^2}l_2^2\right)\right]^{\frac{1}{2}}} \quad (5.4.1.)$$

where a and c are the lattice constants 4.7591 Å and 12.9894 Å, respectively.

For angles relative to the [0001] axis, equation 5.4.1 becomes ,

$$\cos\theta = \frac{0.1007\, l_2}{\left[0.1007\,(h_2^2 + k_2^2 + h_2k_2 + 0.1007\, l_2^2)\right]^{\frac{1}{2}}} \quad (5.4.2.)$$

The angles between planes are tabulated in Figs. 5.4.1 - 5.4.3 and a model of the α corundum lattice is illustrated in Fig. 5.4.4. The structure can be regarded as a distortion of a hexagonal close packing of oxygen atoms with aluminium atoms in the octahedral interstices. The octahedra are however surprisingly irregular and there is a suggestion of metal to metal bonds with interatomic distance 2.65 Å. The structure has been determined by Newham and de Haas [169].

ANGLES BETWEEN PLANES FOR α CORUNDUM

PLANE	PLANE	ANGLE
$10\bar{1}0$	0001	90°
$10\bar{1}1$	0001	72.48°
$10\bar{1}2$	0001	57.60°
$10\bar{1}3$	0001	46.43°
$10\bar{1}4$	0001	38.20°
$10\bar{1}5$	0001	32.20°
$10\bar{1}6$	0001	27.69°
$10\bar{1}7$	0001	24.25°
$10\bar{1}8$	0001	21.50°

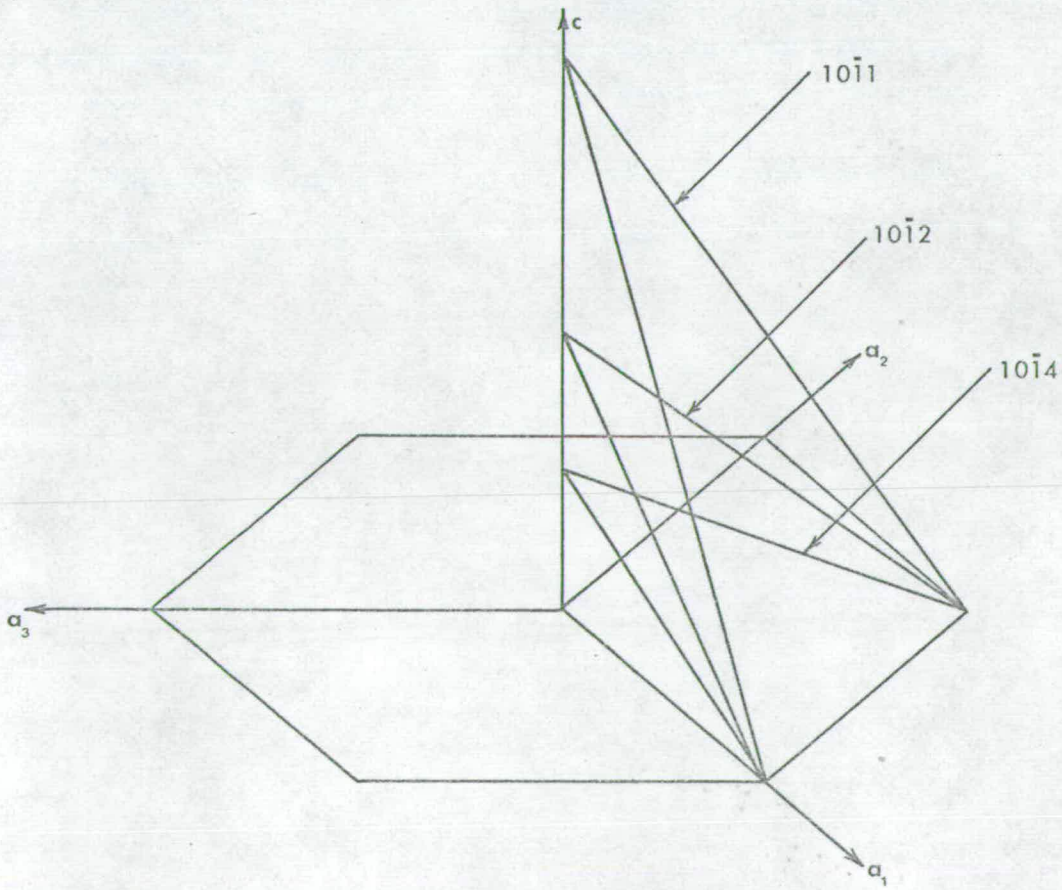


FIG 5.4.1

ANGLES BETWEEN PLANES FOR α CORUNDUM

PLANE	PLANE	ANGLE
$11\bar{2}0$	0001	90^{o}
$11\bar{2}1$	0001	79.62^{o}
$11\bar{2}2$	0001	69.88^{o}
$11\bar{2}3$	0001	61.92^{o}
$11\bar{2}4$	0001	53.76^{o}
$11\bar{2}5$	0001	47.52^{o}
$11\bar{2}6$	0001	42.30^{o}
$11\bar{2}7$	0001	37.95^{o}
$11\bar{2}8$	0001	34.30^{o}

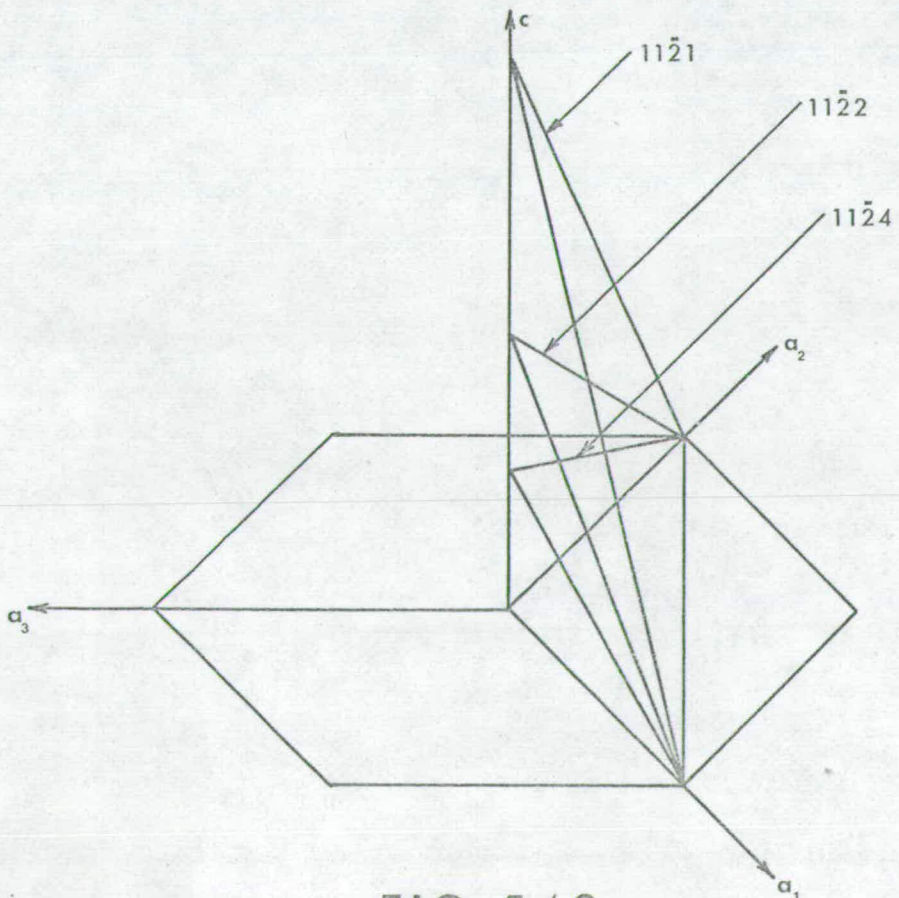


FIG 5.4.2.

ANGLES BETWEEN PLANES FOR α CORUNDUM

PLANE	PLANE	ANGLE
$11\bar{2}1$	$11\bar{2}0$	10.38°
$11\bar{2}2$	$11\bar{2}0$	20.12°
$11\bar{2}3$	$11\bar{2}0$	28.08°
$11\bar{2}4$	$11\bar{2}0$	36.24°
$11\bar{2}5$	$11\bar{2}0$	42.48°
$11\bar{2}6$	$11\bar{2}0$	47.70°
$11\bar{2}7$	$11\bar{2}0$	52.05°
$11\bar{2}8$	$11\bar{2}0$	55.70°
$10\bar{1}0$	$11\bar{2}0$	30.00°
$10\bar{1}1$	$11\bar{2}0$	34.38°
$10\bar{1}2$	$11\bar{2}0$	43.02°
$10\bar{1}3$	$11\bar{2}0$	51.15°
$10\bar{1}4$	$11\bar{2}0$	57.59°
$10\bar{1}5$	$11\bar{2}0$	62.49°
$10\bar{1}6$	$11\bar{2}0$	66.26°
$10\bar{1}7$	$11\bar{2}0$	69.17°
$10\bar{1}8$	$11\bar{2}0$	71.50°

FIG 5.4.3.

5.5 ANGLES BETWEEN PLANES FOR CADMIUM SULPHIDE (WURTZITE):

A model of the wurtzite cadmium sulphide lattice is presented in Fig. 2.1.1. Equation 5.4.1 yields angles between planes tabulated in Figs. 5.5.1 and 5.5.2. In the case of cadmium sulphide a and c have the values 4.135 $\mathring{A}$ and 6.712 $\mathring{A}$ [47] respectively.

5.6 SPECIMEN ORIENTATIONS BY LAUE BACK REFLECTION TECHNIQUE:

Specimen Laue back reflection photographs of the (0001) and $(10\bar{1}2)$ planes of cadmium sulphide are presented in Figs. 4.4.11and 4.4.13. Other specimen orientations are presented in Figs. 5.6.1 - 5.6.3.

All photographs of cadmium sulphide were obtained using molybdenum radiation with X-ray tube operated at 20KV and 20mA. The exposure time was 40 minutes on Polaroid type 57 film. Any attempts to employ a higher tube voltage were frustrated by the onset of fluorescent radiation from the specimen.

Figs. 5.6.4 - 5.6.9,indicate specimen orientations of α corundum. The exposure time was 7 minutes to molybdenum radiation with the X-ray tube operated at 30 Kv and 10mA.

It is convenient, although perhaps occasionally misleading, to adopt a hexagonal notation to describe α corundum which, since its unit cell is in fact rhombohedral, exhibits only threefold symmetry. In consequence the $(2\bar{1}\bar{1}0)$, $(\bar{1}2\bar{1}0)$ and $(\bar{1}\bar{1}20)$ planes, for example, are identical to each other but not the $(11\bar{2}0)$, $(\bar{2}110)$ and $(1\bar{2}10)$ planes as the hexagonal notation might suggest. Stereographic projections for α corundum and the cadmium sulphide wurtzite structure are illustrated in Figs. 5.6.10 and 5.6.11, respectively.

ANGLES BETWEEN PLANES FOR CADMIUM SULPHIDE (WURTZITE).

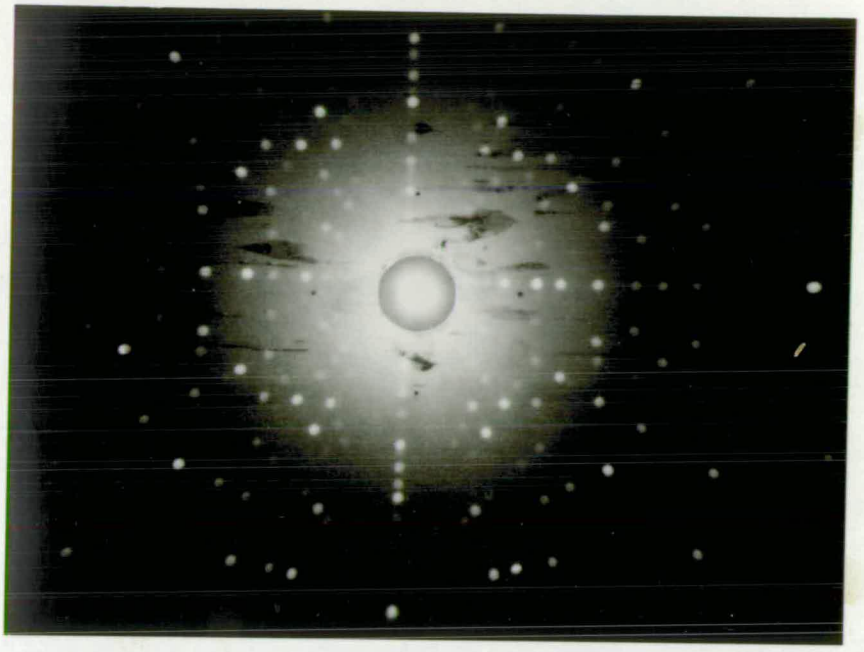
PLANE	PLANE	ANGLE
$10\bar{1}0$	0001	90°
$10\bar{1}1$	0001	61.92°
$10\bar{1}2$	0001	43.13°
$10\bar{1}3$	0001	32.00°
$10\bar{1}4$	0001	25.10°
$10\bar{1}5$	0001	20.52°
$10\bar{1}6$	0001	17.30°
$10\bar{1}7$	0001	14.95°
$10\bar{1}8$	0001	13.10°
$11\bar{2}0$	0001	90°
$11\bar{2}1$	0001	72.87°
$11\bar{2}2$	0001	58.37°
$11\bar{2}3$	0001	47.25°
$11\bar{2}4$	0001	39.05°
$11\bar{2}5$	0001	33.00°
$11\bar{2}6$	0001	28.40°
$11\bar{2}7$	0001	24.87°
$11\bar{2}8$	0001	22.08°

FIG 5.51

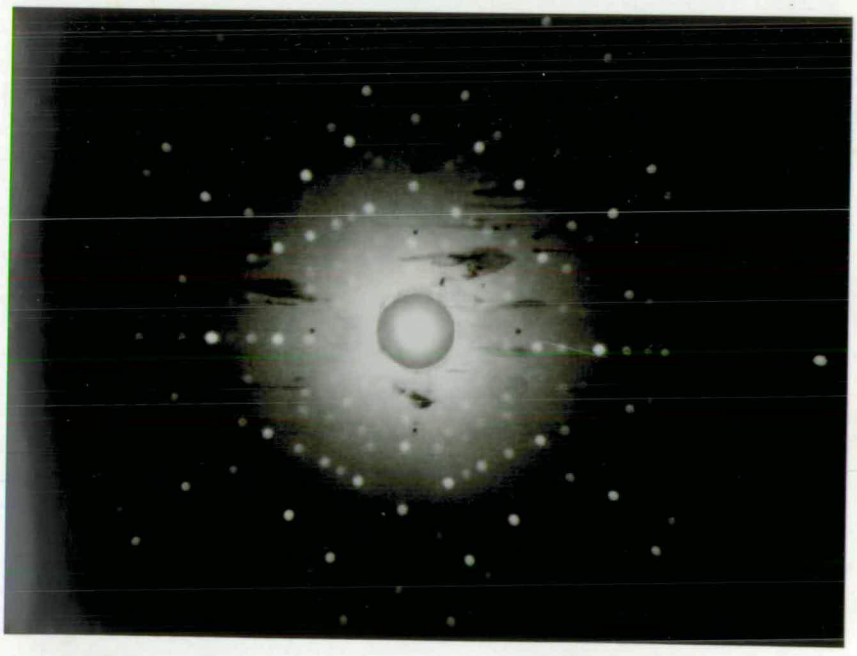
ANGLES BETWEEN PLANES FOR CADMIUM SULPHIDE (WURTZITE)

PLANE	PLANE	ANGLE
$11\bar{2}1$	$11\bar{2}0$	17.13°
$11\bar{2}2$	$11\bar{2}0$	31.63°
$11\bar{2}3$	$11\bar{2}0$	42.75°
$11\bar{2}4$	$11\bar{2}0$	50.95°
$11\bar{2}5$	$11\bar{2}0$	57.00°
$11\bar{2}6$	$11\bar{2}0$	61.60°
$11\bar{2}7$	$11\bar{2}0$	65.13°
$11\bar{2}8$	$11\bar{2}0$	67.92°
$10\bar{1}0$	$11\bar{2}0$	30.00°
$10\bar{1}1$	$11\bar{2}0$	40.19°
$10\bar{1}2$	$11\bar{2}0$	53.69°
$10\bar{1}3$	$11\bar{2}0$	62.69°
$10\bar{1}4$	$11\bar{2}0$	69.29°
$10\bar{1}5$	$11\bar{2}0$	72.30°
$10\bar{1}6$	$11\bar{2}0$	75.04°
$10\bar{1}7$	$11\bar{2}0$	78.50°

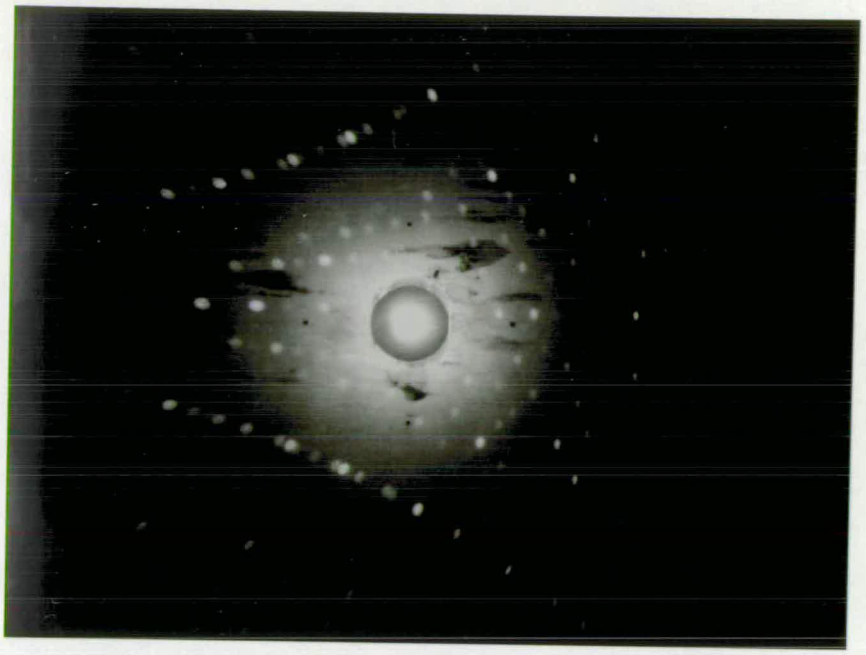
FIG 5.5.2.



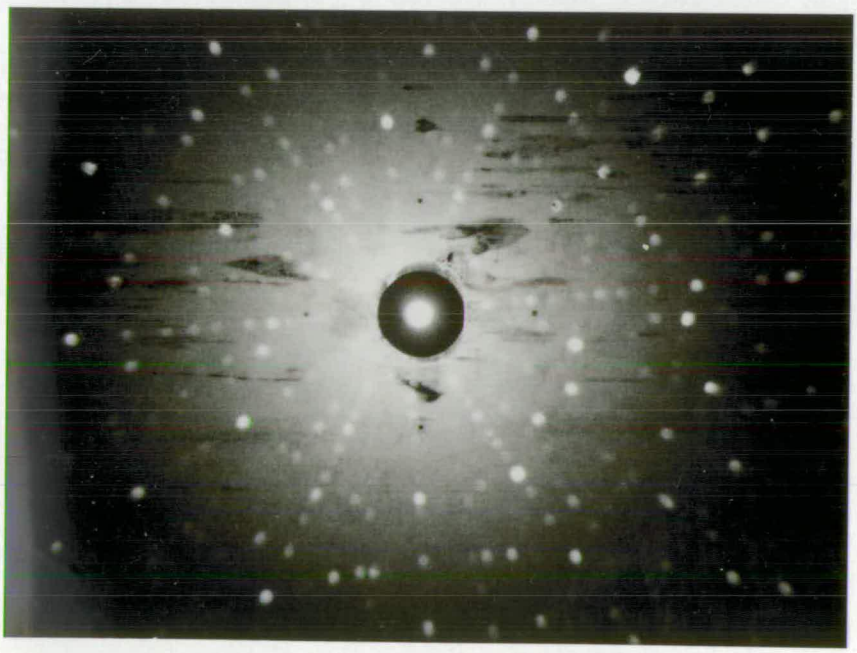
- FIG. 5.6.1. -
Cadmium Sulphide ($10\bar{1}0$) Plane.



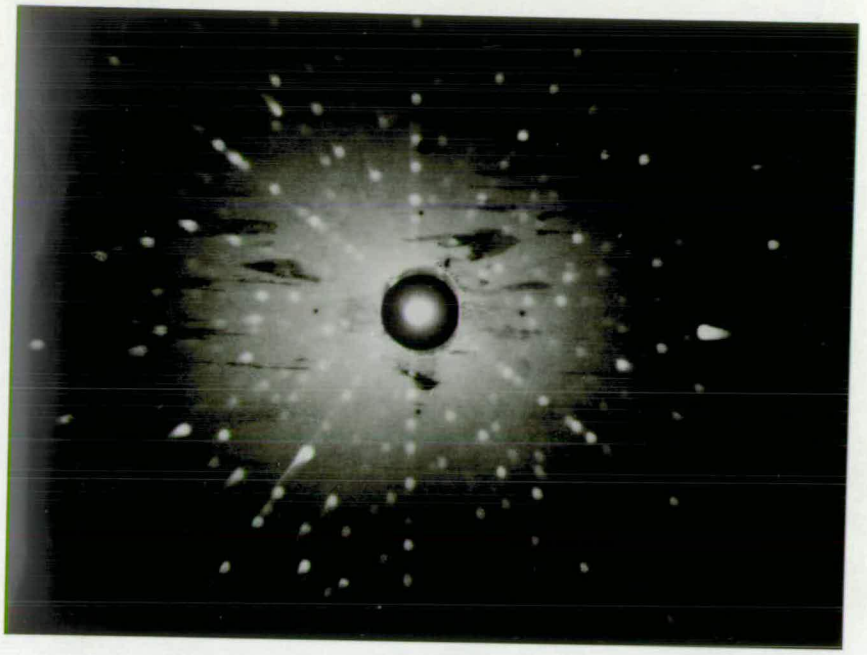
- FIG. 5.6.2. -
Cadmium Sulphide ($11\bar{2}0$) Plane.



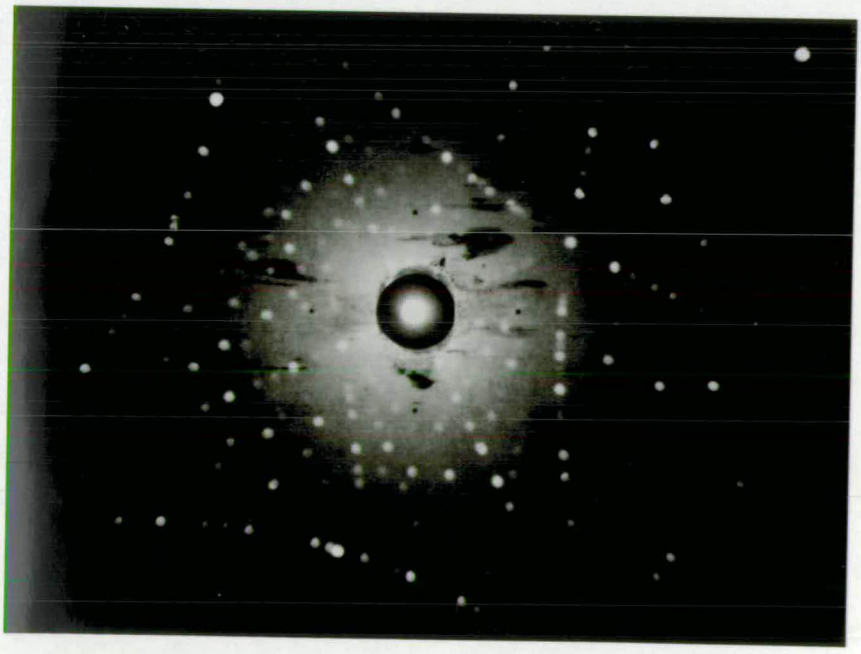
- FIG. 5.6.3. -
Cadmium Sulphide ($11\bar{2}4$) Plane.



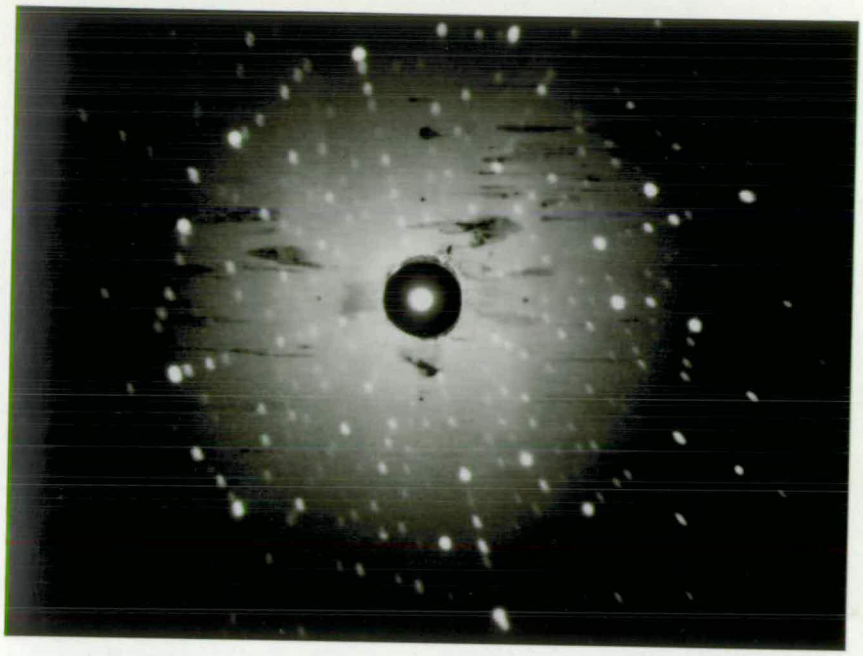
- FIG. 5.6.4. -
Sapphire (0001) Plane.



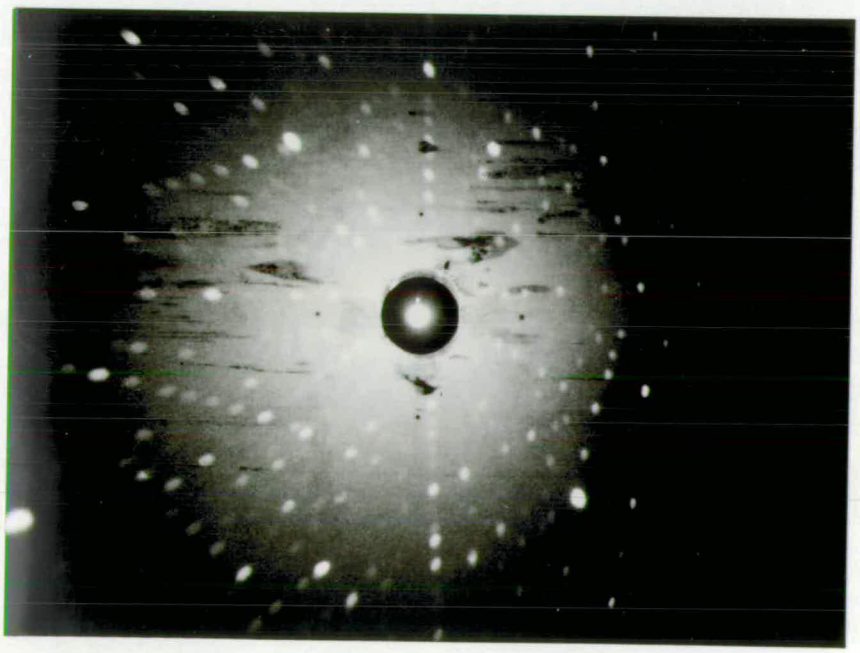
- FIG. 5.6.5. -
Sapphire ($2\bar{1}\bar{1}0$) Plane.



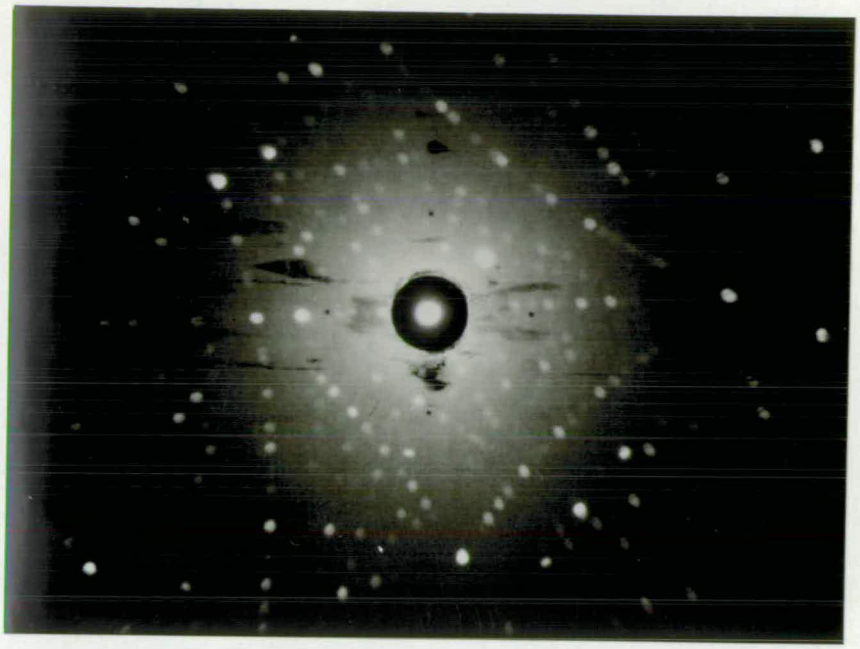
- FIG. 5.6.6. -
Sapphire ($10\bar{1}0$) Plane



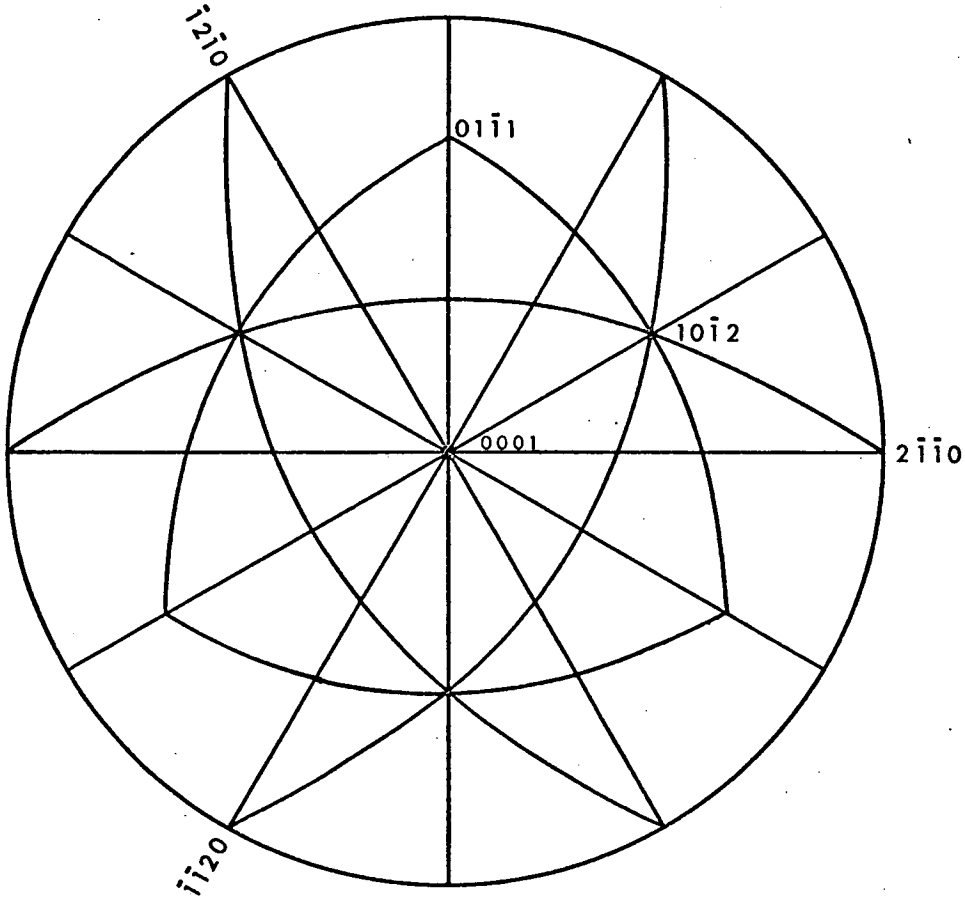
- FIG. 5.6.7. -
Sapphire($10\bar{1}2$)Plane.



- FIG. 5.6.8. -
Sapphire($10\bar{1}4$)Plane.

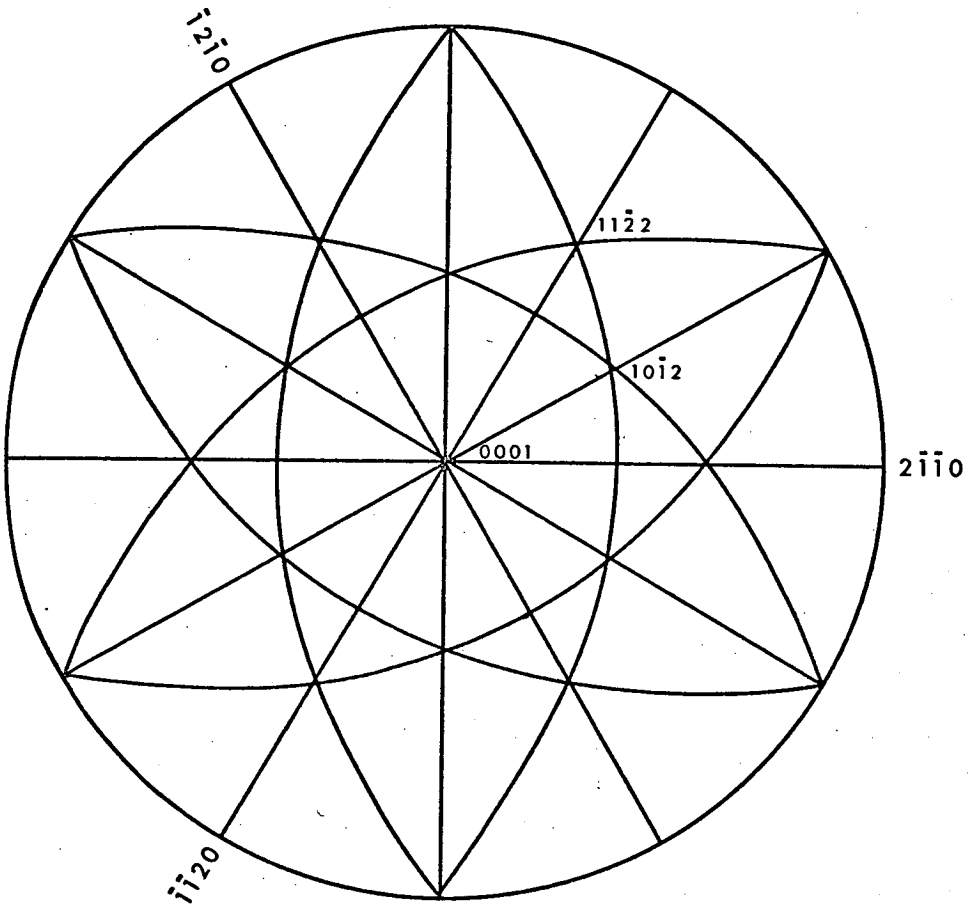


- FIG. 5.6.9. -
Saphhire($11\bar{2}6$)Plane.



STEREOGRAPHIC PROJECTION Al_2O_3

FIG 5.6.10



STEREOGRAPHIC PROJECTION CdS

FIG 5.6.11.

CHAPTER 6.

ELECTRICAL MEASUREMENTS ON CADMIUM SULPHIDE FILMS

6.1 THE METAL-SEMICONDUCTOR CONTACT :

Intimate contact of a metal electrode to a semiconductor involves a redistribution of charge at the junction. This results from the difference in Fermi levels of the two materials. An electrode with higher work function than the semiconductor, Fig.6.1.1, yields generally a rectifying contact, Fig. 6.1.2, since, on initial contact, the electron flow from semiconductor to metal establishes a dynamic equilibrium across the junction by positively charging the semiconductor with respect to the electrode thus inducing an asymmetrical potential barrier. Because of the high resistivity space charge layer formed by immobile ionized donors in the semiconductor externally applied voltages appear across this layer and by influencing the barrier height permit a significant flow of electrons from cadmium sulphide to the electrode. Electrons attempting to gain access to the semiconductor from an electrode must surmount a potential barrier ($\phi_m - x_s$) whereas oppositely directed electrons face a potential barrier ($\phi_m - \phi_s$) which unlike the ($\phi_m - x_s$) barrier, is modified directly by an externally applied voltage.

Conversely, an electrode metal of lower work function than the semiconductor , Fig. 6.1.3 , yields

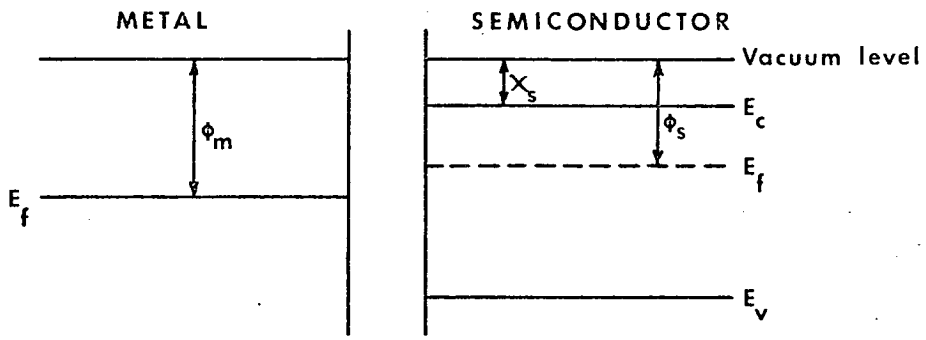


FIG 6.1.1.

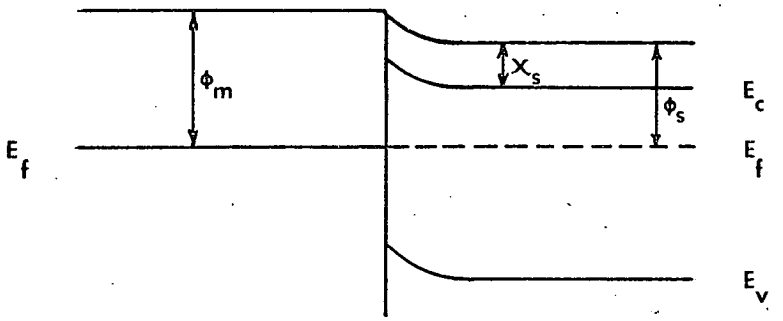


FIG 6.1.2.

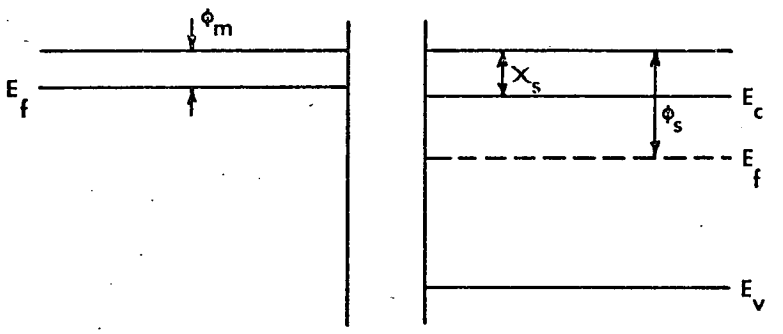


FIG 6.1.3.

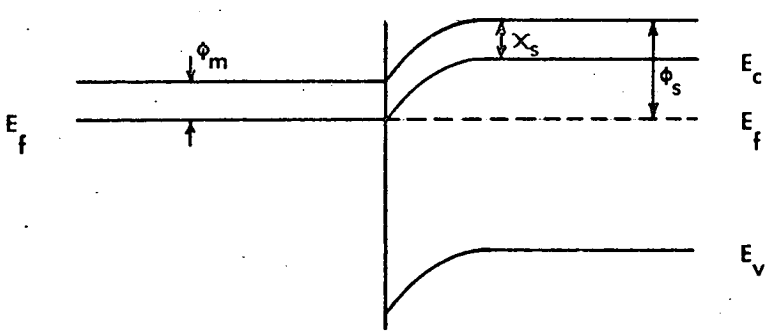


FIG 6.1.4.

generally an ohmic contact, Fig.6.1.4. Dynamic equilibrium is again achieved by charge redistribution at the junction, but in this case no high resistivity space charge region exists in the semiconductor near the junction since electrons supplied by the electrode are free to move in the semi-conductor conduction band. Externally applied voltages do not appear at the junction to influence the barrier height ($\phi_s - X_s$) which depends only on the semiconductor material.

This model is obviously an oversimplification since at any crystalline surface the normal ordered array of atoms and bonds is interrupted and surface discontinuities and adsorbed impurities may superficially modify the energy band structure. Various more elegant models have been proposed to explain observed results [126]. The basic model, however, does indicate the increasing difficulty of making ohmic contacts to higher resistivity material, a feature apparent in practice.

6.2 TECHNIQUES OF OHMIC CONTACT FABRICATION :

According to the simple model, aluminium electrodes favour an ohmic contact to cadmium sulphide. It is, however, difficult to obtain ohmic aluminium - cadmium sulphide contacts by simple evaporation and this is attributed to the formation of an insulating interfacial layer of aluminium oxide which is brought about by oxygen adsorption at the semiconductor surface or by residual gases.

To overcome this difficulty, trivalent metals such as indium or gallium may be diffused into the surface where they act as donor impurities. Excessive initial diffusion or subsequent heating to quite moderate temperatures may result in undesirable modification of the electrical properties of the entire semiconductor. Alternatively, exposure of the crystal to ion bombardment yields surfaces which produce ohmic contacts with most metals[170]. The apparent source of conduction electrons is the highly disordered region near the crystal surface and in the model proposed by Kroger et al [174], ohmic contact of metal to a highly resistive n-type semiconductor depends on a thin layer of lower resistivity separated from the junction by an extremely narrow barrier through which electrons may tunnel readily. Ohmic contacts have also been produced by sequential multilayer evaporation techniques [171] and by passing large currents through non-ohmic contacts to cause barrier breakdown [172,173].

6.3 EXAMINATION OF CONTACTS :

Three techniques of contact fabrication were studied. These were :

a) Evaporation of aluminium electrodes on to untreated cadmium sulphide films with substrates at room temperature.

b) Evaporation of aluminium electrodes on to untreated cadmium sulphide films with the substrate at 300°C to reduce gas adsorption.

c) Evaporation of aluminium electrodes on to ion bombarded cadmium sulphide films with the substrate at room temperature.

To determine the voltage drop across the contact region, samples were probed with tungsten wire etched to a 2 micron diameter point and indium plated, mounted in an x y z manipulator. In all cases the probe was positioned adjacent to the contact and the contact to probe potential difference was measured by an electrometer of input resistance 10^{14} ohm over a range of sample currents passed in both directions.

Due to formation of an insulating interfacial layer of aluminium oxide it was not expected that contacts produced by the first method would exhibit reproducible electrical characteristics. The results are, however, included as a comparison, Fig. 6.3.1. Heating of the substrate to 300°C during the evaporation of aluminium contacts was performed with a view to reducing gas adsorption on the semiconductor.

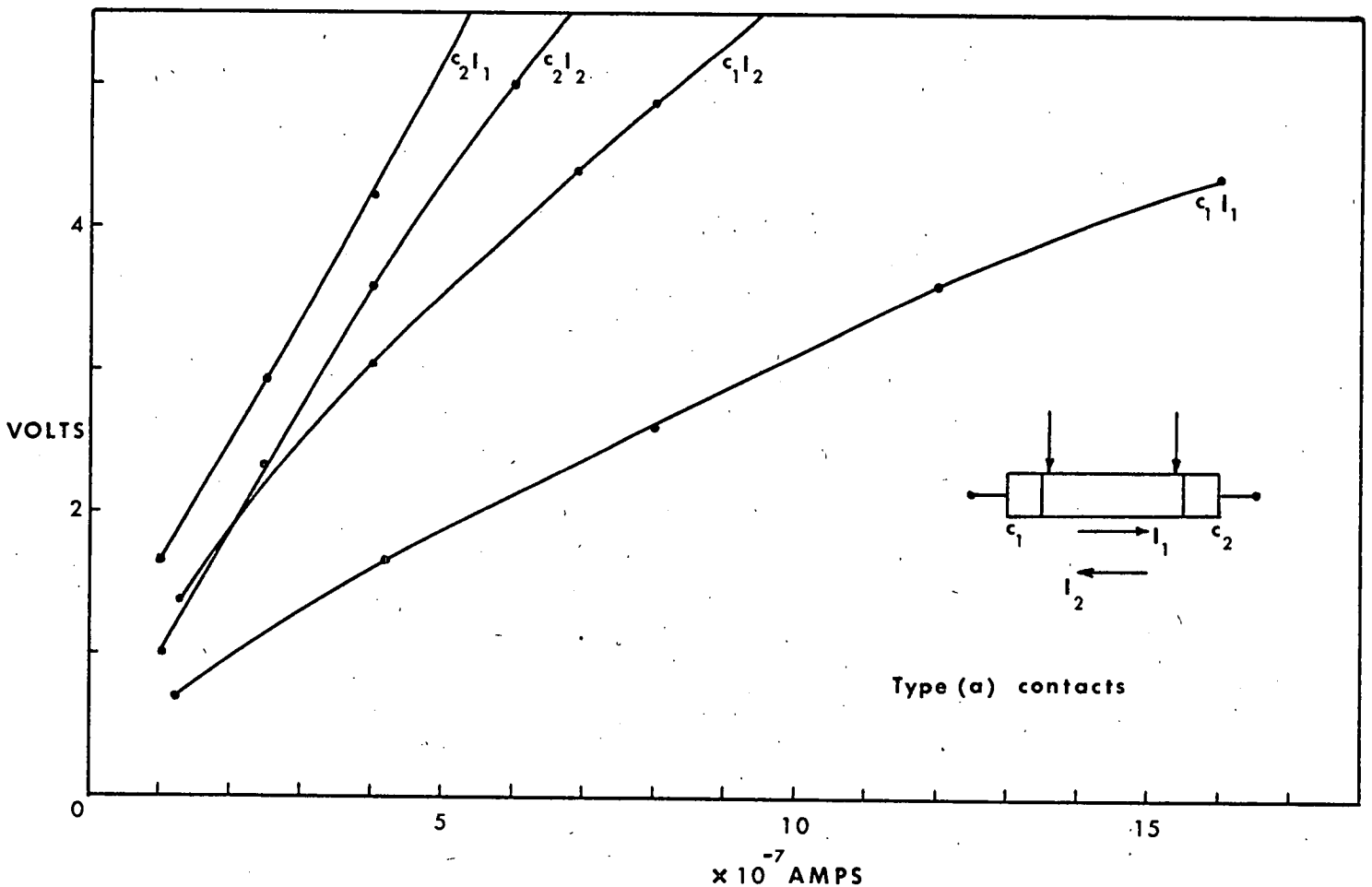

C_2I_1
C_2I_2
C_1I_2
C_1I_1
VOLTS
4
2
0
5
10
15
$\times 10^{-7}$ AMPS
C_1
I_1
C_2
I_2
Type (a) contacts

FIG 6.3.1.

and although this procedure yielded more reproducible results, Fig. 6.3.2, some traces of non-ohmic behaviour persisted.

Ion bombardment of the cadmium sulphide film is considered to increase the surface conductivity by increasing the contribution of surface states. through an increase in their density. It is to be expected that prior to any surface treatment, surface states resulting from surface imperfections, foreign atoms on the surface etc. exist and their presence is reflected in modifications to the simple energy band structure illustrated in Figs. 6.1.1. - 6.1.4. The effect of ion bombardment on the electrical characteristics of aluminium contacts is illustrated in Fig. 6.3.3. which, in contrast to Fig. 6.3.1., indicates reproducible contacts of an ohmic nature. This situation is commensurate with the presence of a region of enhanced conductivity adjacent to the contact.

Method (c) was adopted as a standard procedure. Ion bombarding was performed in an atmosphere of argon at 5×10^{-2} torr and evaporation of aluminium to form the contact was performed at approximately 10^{-5} torr. A liquid nitrogen cold trap was employed at all times.

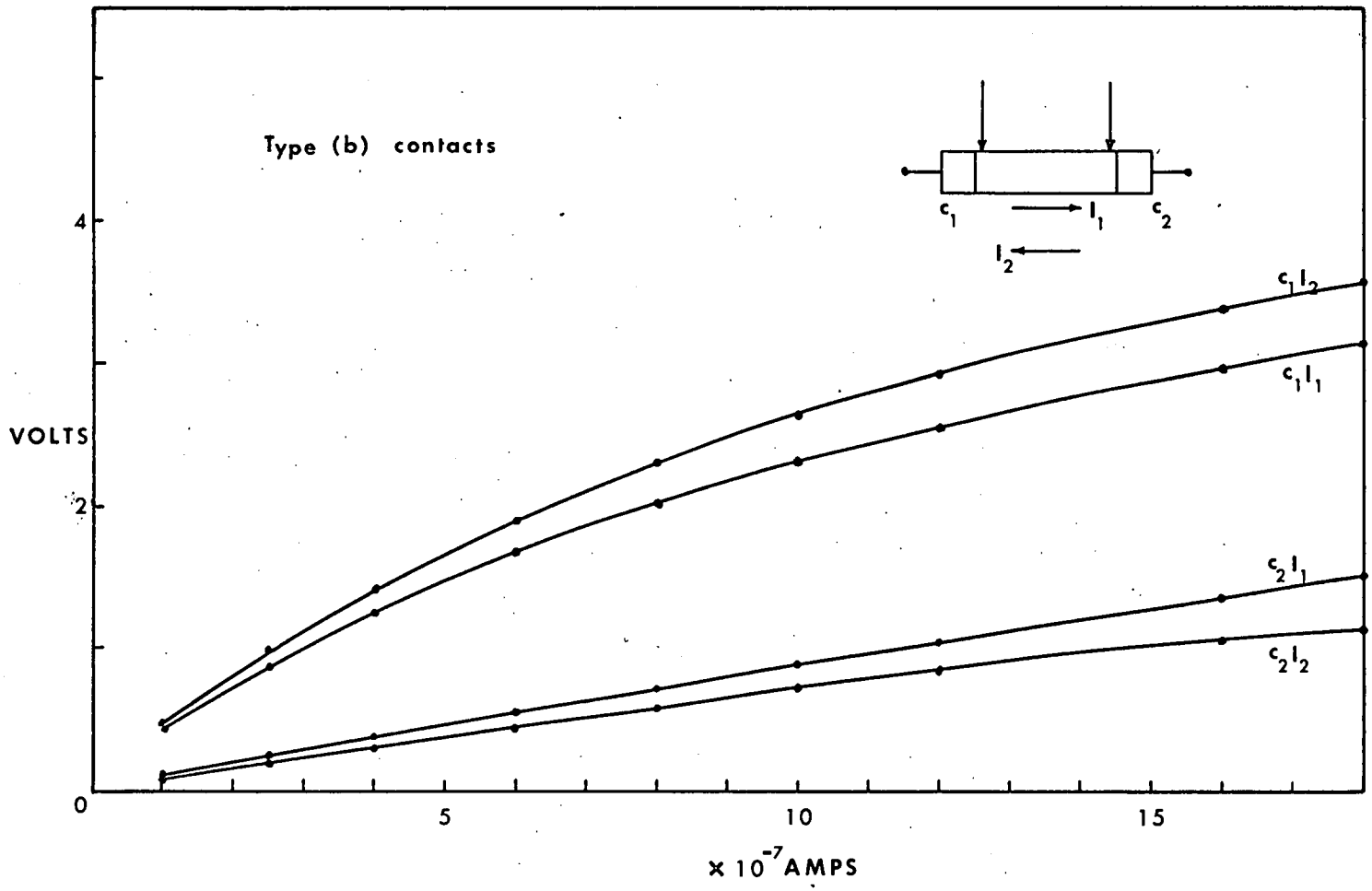

Type (b) contacts
c_1
I_1
c_2
I_2
$c_1 I_2$
$c_1 I_1$
$c_2 I_1$
$c_2 I_2$
VOLTS
0
2
4
5
10
15
$\times 10^{-7}$ AMPS

FIG 6.3.2.

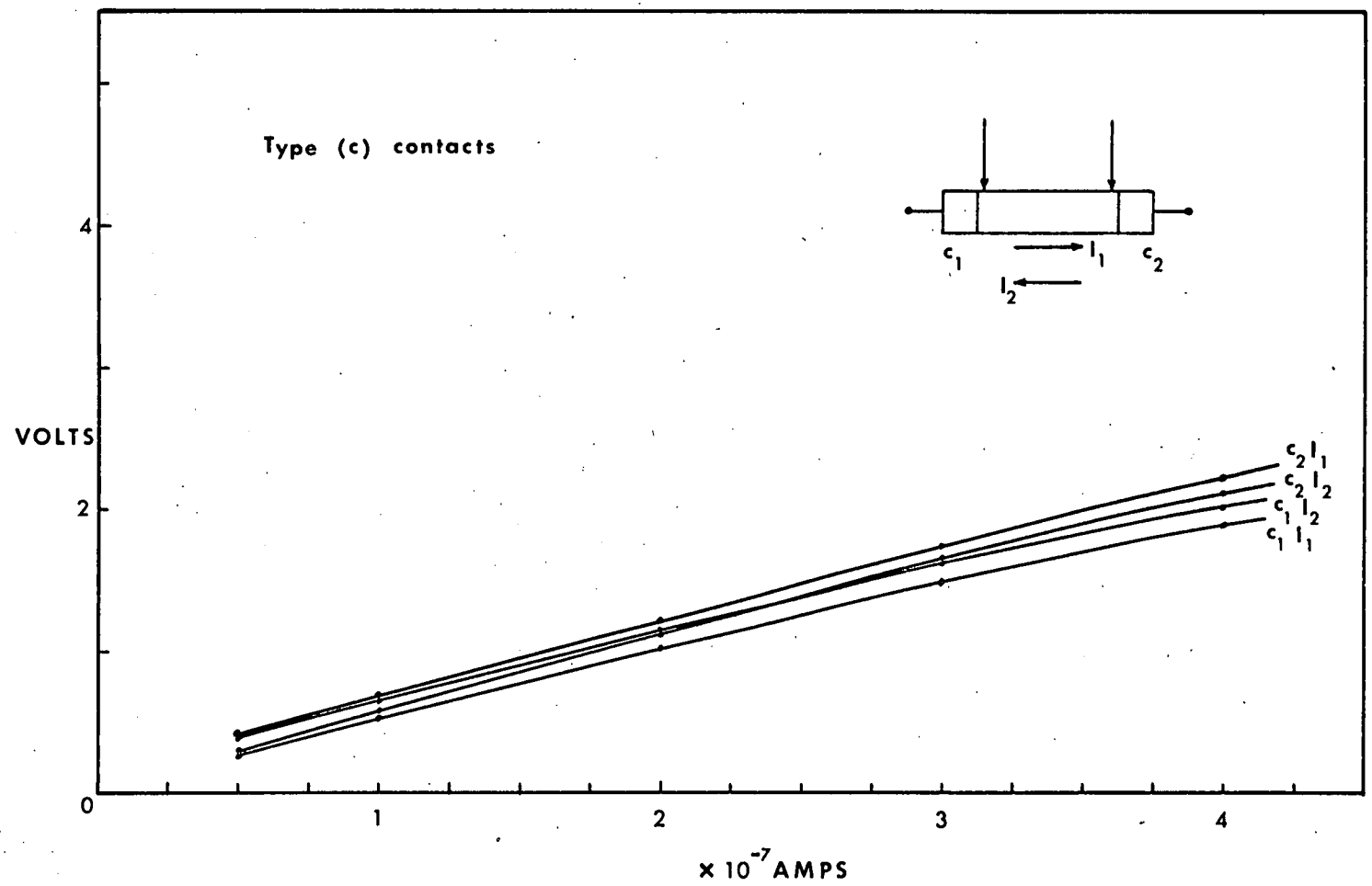

Type (c) contacts
c_1
I_1
c_2
I_2
VOLTS
0
2
4
1
2
3
4
$\times 10^{-7}$ AMPS
$c_2 I_1$
$c_2 I_2$
$c_1 I_2$
$c_1 I_1$

FIG 6.3.3.

6.4 ELECTRICAL CHARACTERISTICS :

Although the electrical resistivity of cadmium sulphide reflects the stoichiometry and impurity content of the material, observations may be modified by grain boundaries in polycrystalline films. Various unpredictable degrees of masking of the intrinsic film properties are possible according to the prevailing degree of polycrystallinity and for this reason resistivity measurements on polycrystalline films must be regarded as approximations.

Resistivity measurements were performed using the circuit indicated in Fig. 6.4.1. using a digital voltmeter of input impedance 10^{10} ohm or an electrometer of input resistance 10^{14} ohm for voltage measurements. The samples were enclosed in a light tight compartment during investigation and the V-I chracteristics, for films deposited at various substrate temperatures, are presented in Figs. 6.4.1. - 6.4.3.

Predictably, the enhanced crystalline order achieved at higher substrate temperatures is complemented by improved stoichiometry and high resistivity, substrate temperatures at 975^{o}C under normal equilibrium conditions yielding films of resistivity 10^{7} ohm metre, which exhibit a light to dark resistivity ratio of approximately 10^{4}:1. At low substrate temperatures, the resistivity

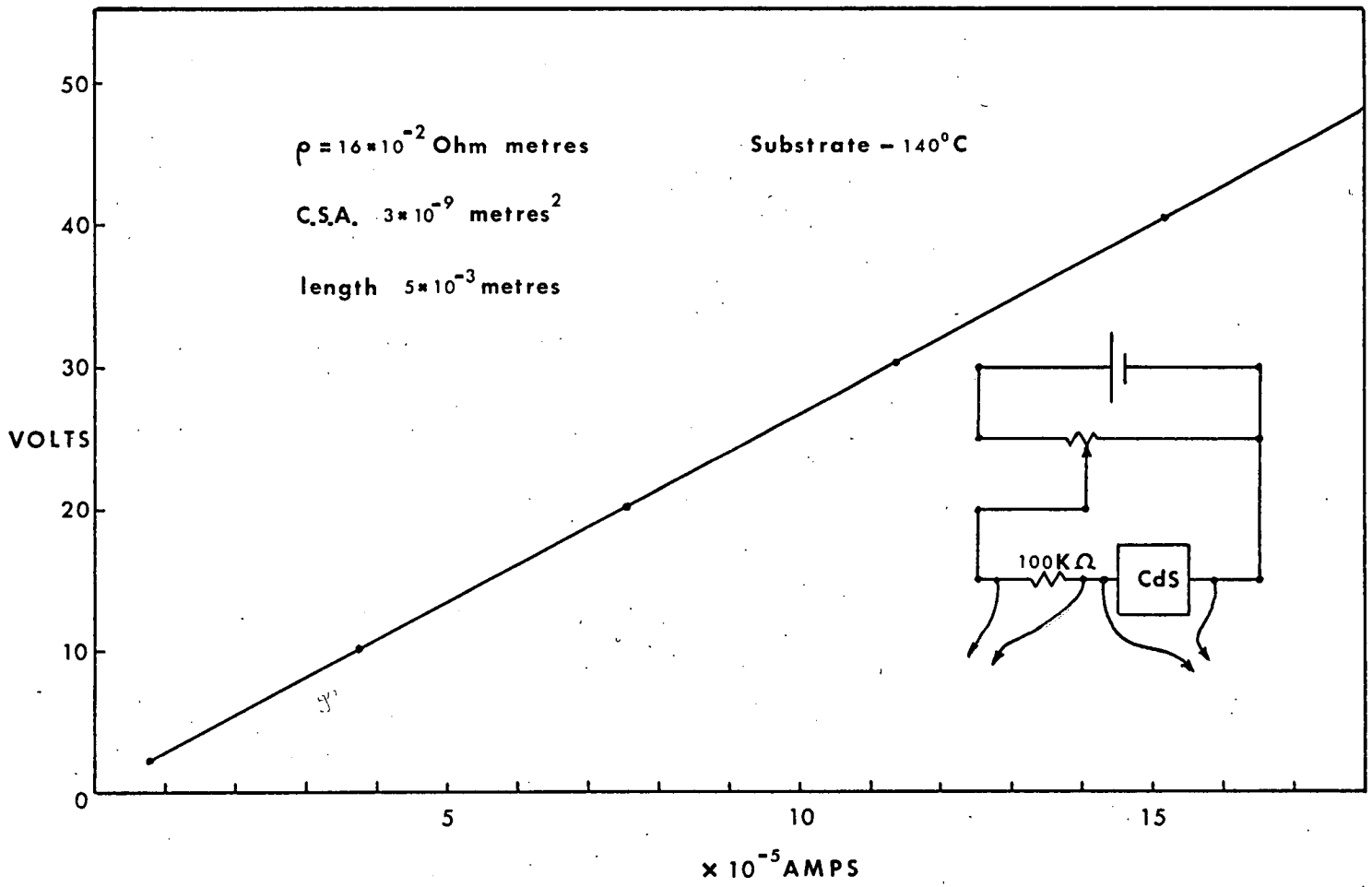

ρ = 16 * 10^-2 Ohm metres
C.S.A. 3 * 10^-9 metres^2
length 5 * 10^-3 metres
Substrate – 140°C
VOLTS
0
10
20
30
40
50
5
10
15
× 10^-5 AMPS
100KΩ
CdS

FIG 6.4.1.

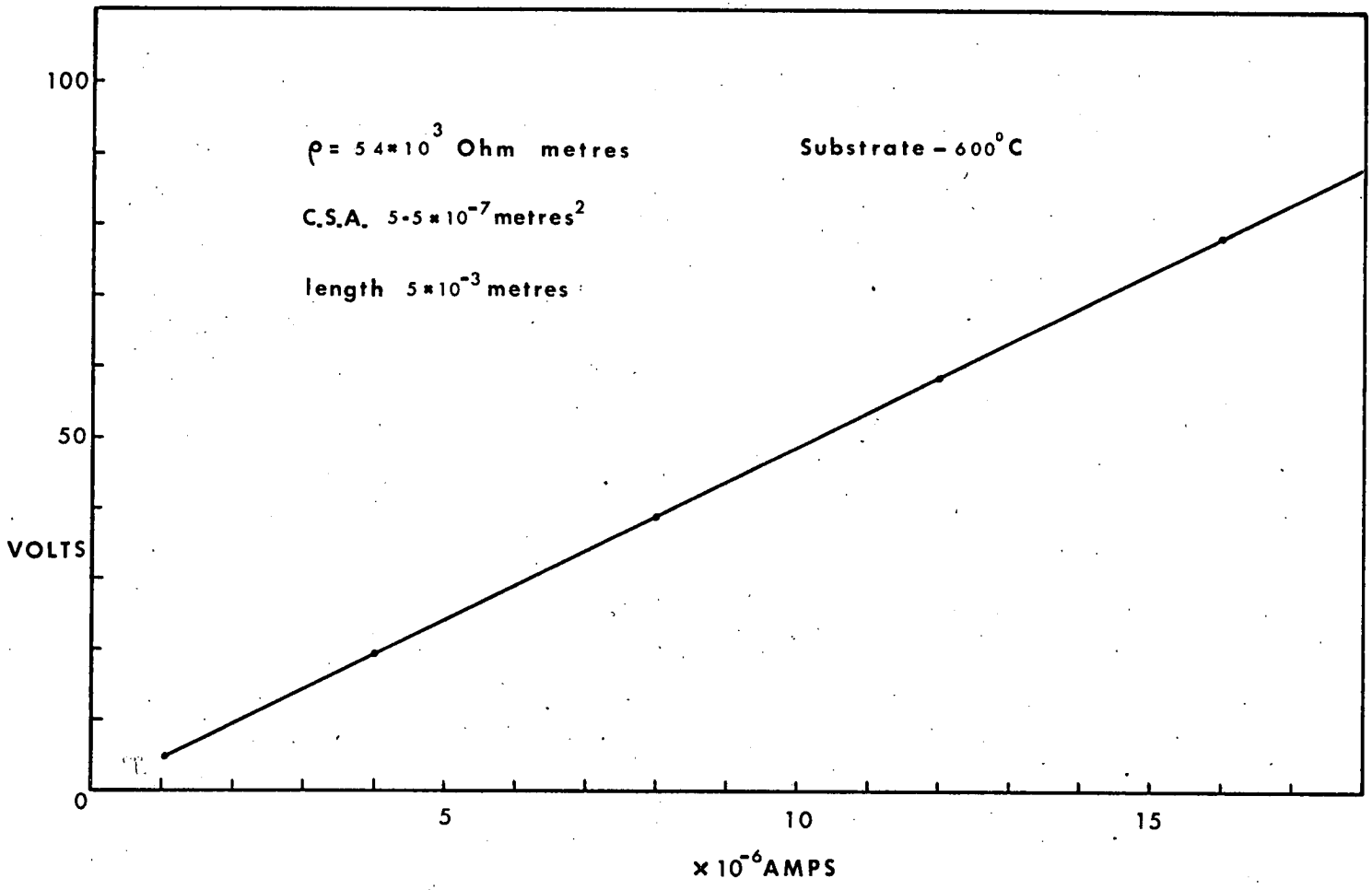

100
50
0
VOLTS
ρ = 5.4 * 10^3 Ohm metres
Substrate – 600°C
C.S.A. 5·5 * 10^-7 metres^2
length 5 * 10^-3 metres
5
10
15
× 10^-6 AMPS

FIG 6.4.2.

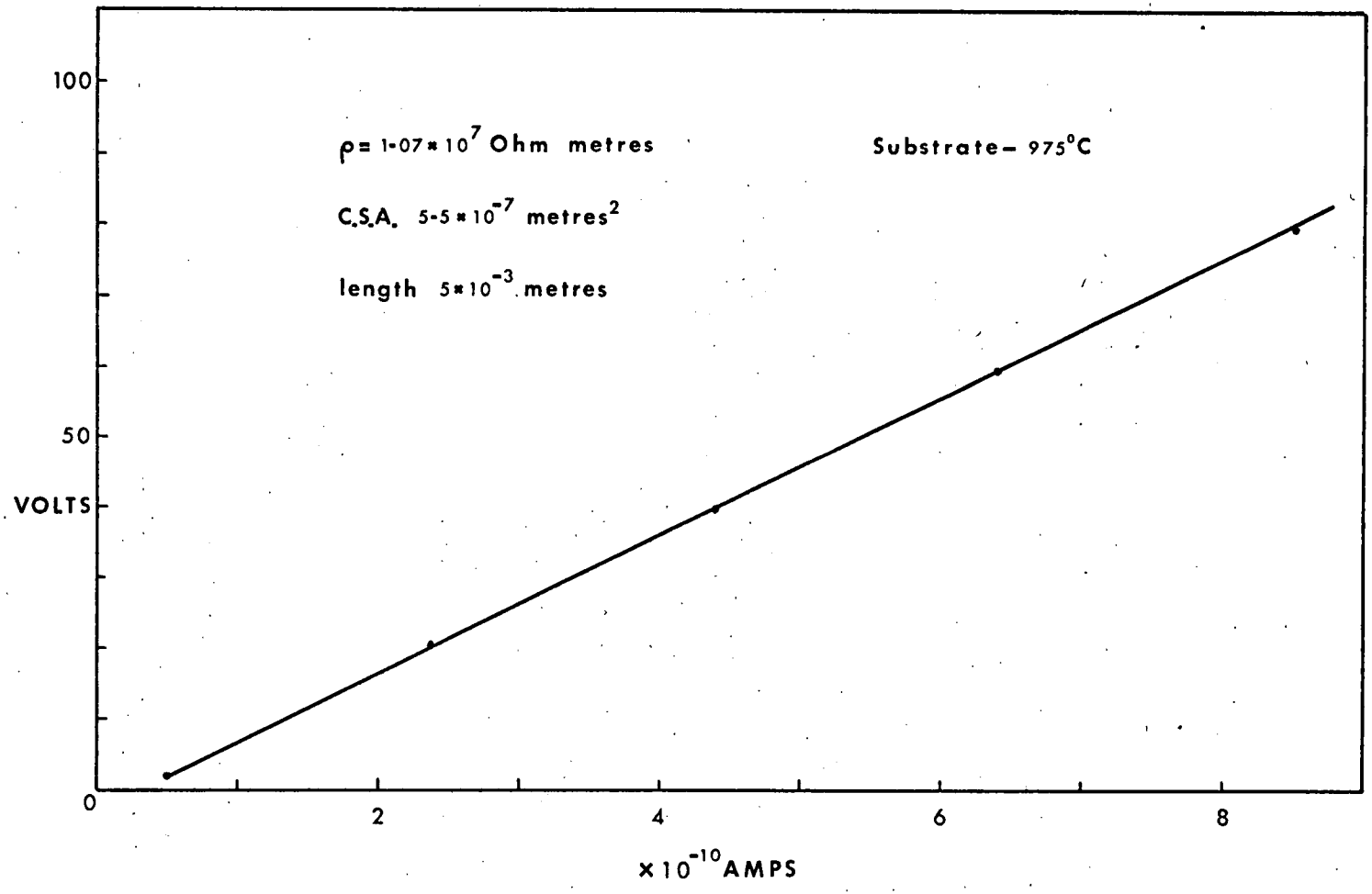

100
50
0
VOLTS
ρ= 1·07×10^7 Ohm metres
Substrate– 975°C
C.S.A. 5·5×10^-7 metres^2
length 5×10^-3 metres
2
4
6
8
×10^-10 AMPS

FIG 6.4.3.

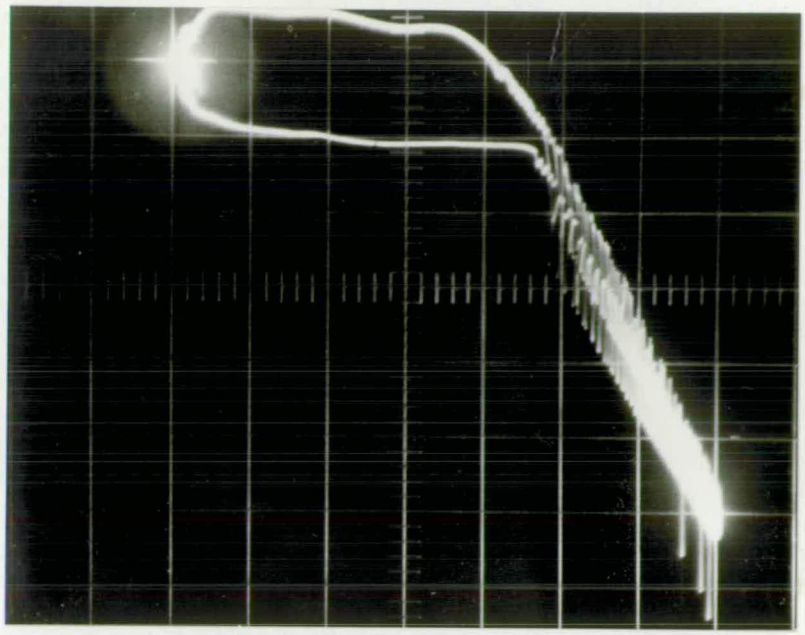
differs little from values observed in conventional systems.

Film resistivity at substrate temperaturesof 975^{o}C was found to vary little from sample to sample provided that the pumping and bakeout procedure specified in paragraph 4.2 was strictly adhered to. Some indication of the sensitivity of the results to deposition conditions was demonstrated by a reduction of the pumping and bakeout time to 1 hour. This yielded films with a dark resistivity an order of magnitude higher than normal, probably due to impurity incorporation in the films.

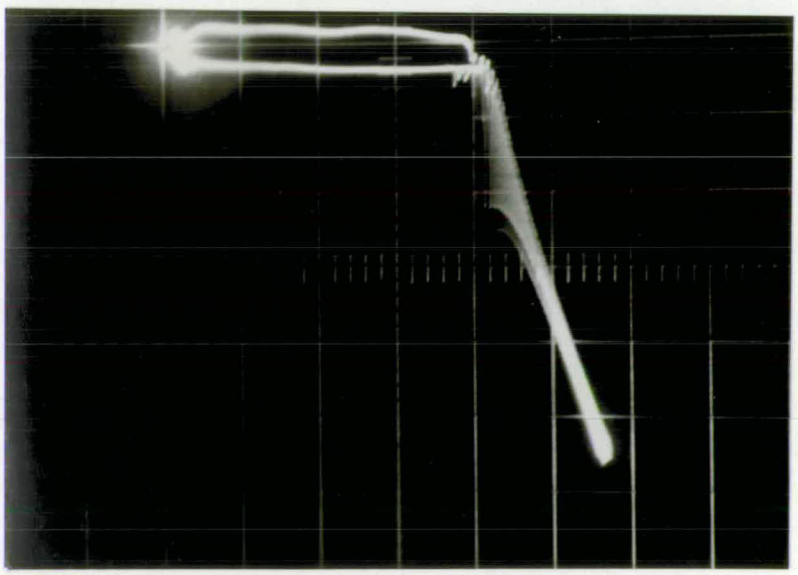
Attempts were made to determine the drift mobility of deposited films by a method in which a pulsed electron beam provides an excess carrier concentration in the specimen near one electrode. Application of a drift field to the specimen reflects the mobile excess species as an increase in drift current which persists until excess charge has either been carried through the specimen or has recombined. The drift mobility may thus be inferred from the applied field and from the duration of the current pulse observed to pass through the sample. The time of flight may be assumed sufficiently short to neglect the effects of recombination provided that the pulse length is observed to be inversely proportional to the applied field. Although drift fields of up to 2 x 10^{5} volt/metre were employed, the above condition could not

be attained and the current pulse length remained almost constant at 10^{-4} second inferring a drift mobility of less than 2.5×10^{-4} metre ^{2}/ volt sec. This suggests that the mobility is trap dominated.

As an alternative method, tests were conducted in an attempt to observe the characteristic knee which occurs in the V-I plot and is attributed to acoustoelectric coupling. In single crystal samples, the V-I plot remained linear at all illuminated levels when drift-fields up to 6×10^5 volt/metre were applied although one polycrystalline sample did exhibit current oscillations, Fig. 6.4.4, at a drift field of 1.8×10^5 volt/metre. The form of the V-I curve, however, is inconsistent with that usually observed in acoustoelectric oscillators since it exhibits a current saturation at approximately 10^4 volt/metre and a reversion to ohmic behaviour at 1.8×10^5 volt/metre in contrast to the expected ohmic followed by saturated behaviour. Probe tests revealed no contact abnormalities and illumination of the specimen was not observed to affect the breakover voltage. After a prolonged period of oscillation the breakover voltage increased, Fig. 6.4.5, and eventually oscillation ceased altogether leaving only the saturated region. The effect proved to irreversible and resulted in an increase of film resistivity from 10^4 to 10^7 ohm metre. Adhesion of the film crystallites to



- FIG. 6.4.4. -
Horizontal Scale 200 volts/div.
Vertical Scale 500 n A/div.



- FIG. 6.4.5. -
Horizontal Scale 500 volts/div.
Vertical Scale 2μ A/div.

the substrate was impaired as was the mutual adhesion and it seems likely that crystallite barrier effects were responsible for the observed current saturation and oscillation. Crystallite dimensions varied from 10^{-4} to 5×10^{-4} metre in cross-section viewed normal to the substrate.

6.5 COMMENT :

Depositions of cadmium sulphide films performed in conventional evaporation equipment yield material which is inferior in quality from every aspect when compared with bulk single crystals. Since the polycrystalline nature of these films is particularly detrimental to their acoustic properties, emphasis has been placed on development and investigation of a technique designed to overcome this disability.

Resistivity of the deposited material has been observed to vary in a manner commensurate with the theory presented in paragraph 2.3. Results obtained in the conventional low substrate temperature region, where the characteristic imbalance in condensation coefficients of the constituents dominates the growth process, appear to deviate little from those available in conventional systems. However, due to the design criteria of a high purity charge operating in a chemically clean environment under strict temperature control, no problems of clouding or peeling were observed

in the films. Reluctance to contaminate the deposition environment with undesired and unknown impurities suppressed any impulse to examine the effects of less pure charge material although there is no obvious reason to assume any departure from the tolerance exhibited by conventional systems to this factor.

In its ability to elevate the substrate temperature to hitherto relatively unexplored levels while maintaining prescribed deposition conditions, the system surpasses conventional single source or co-evaporation systems and has demonstrated a critical dependence of epitaxy on substrate surface condition and crystallographic orientation. The observed occurrence of single crystal epitaxy at substrate temperatures of over 900°C suggests that little hope exists of observing this phenomenon in conventional systems unless some means of increasing the mobility of the condensate on the substrate surface can be found. It would be interesting from this aspect to observe the effects of deposition under glow discharge conditions.

Two distinct crystallographic orientations of the film may be produced by selecting specific substrate planes provided that the deposition conditions are optimised and the substrate surface is chemically etched to reveal its true nature.

This result has illustrated the significance of the role which surface atoms play in the process of epitaxy and the inability of the condensate to respond significantly to the substrate lattice at low substrate temperatures perhaps explains in some measure the lack of emphasis placed on substrate orientation by most workers.

The mobility measurements which were performed employed in all cases a planar electrode structure hence the tendency is to measure a surface rather than a bulk mobility. More sophisticated procedures for mobility measurements would obviously be advantageous. Absence of a knee in the V-I characteristic due to acoustoelectric interaction implies failure to attain an electron drift velocity in excess of the sound wave velocity in the sample, although another contributing factor is that observation of the V-I knee in semi-insulating cadmium sulphide becomes increasingly difficult as the resistivity increases [11]. In this region the effects of trapping are more noticeable and, in addition, acoustic amplification within the specimen, already curtailed by the high resistivity, may be insufficient at low current densities to overcome the lattice attenuation. This restricts the amplitude of the acoustoelectric field in accordance with the theory of acoustoelectric amplification presented in Chaper 1. A threshold current density

of 4×10^5 amp/metre^2 is quoted by Simhony et al [176]. The maximum current density attained in the tests was 6×10^2 amp/metre^2. These factors are also liable to preclude the observation of acousto-electric oscillations in high resistivity samples. Even in bulk single crystal samples, oscillations terminate as the resistivity is increased [11].

In view of the present results it appears that the effects of barriers associated with crystallites are relevant to the form of V-I characteristics observed in cadmium sulphide films. This effect could contribute significantly to the apparent acoustoelectric interaction observed temporarily by Mason [177] in polycrystalline films of crystallite size approximately three orders of magnitude less than in the present case. Significantly increasing the drift field in the search for acoustoelectric interactions in untreated films was not considered profitable in view of the planar electrode structure employed which is liable to encourage flashover at fields significantly lower than the absolute breakdown strength of air.

Comparative observations of film defect density on Verneuil and Czochralsky grown sapphire would be of interest in view of the degree of interfacial interaction attained. The resources available, however, did not permit this. It is possible that

on higher quality substrates, the chemical etching process, rather than at present the substrate perfection, could become the dominant factor. In this case an alternative etching process using atomic hydrogen might be considered. Although a range of substrate orientations has been investigated, the possibilities have by no means been exhausted, the $(10\bar{1}0)$ substrate plane for example. (0001) plane films on $(10\bar{1}2)$ substrates are less favoured than $(10\bar{1}2)$ plane films on $(2\bar{1}\bar{1}0)$ plane substrates, although further increase in substrate temperature and substrate perfection would be expected, in the light of present experience, to overcome this.

The deposition system might be modified to remove the conical joint in the inner capsule from the lowest temperature position in order to counteract occasional seizure of this component due to cadmium sulphide deposition. To complement this modification, the capsule vacuum pumping tube might be reduced in length to improve pumping speed by installation of a fixed outer capsule and moveable furnace. To obtain full advantage from this, the conical joint could be separated during pumpdown and bakeout. The apparatus would then retain its convenience of inner capsule loading under "clean-room" conditions followed by transfer to the outer capsule and deposition apparatus which need not

demand these conditions.

The deposition method is equally applicable, in theory, to other II-VI compounds and preliminary tests with zinc oxide[178], although thermally limited by capsule material failure, have produced films with small crystallites exhibiting some degree of orientation. It is hoped that some interest in extending this method to the production of other compound films may be stimulated by this work.

ACKNOWLEDGEMENTS

I am indebted to Professor W.E.J. Farvis and Dr. M.A. Reid for their support and guidance throughout the course of this work. For valuable assistance I wish to thank P.M. Dryburgh, J.D.M. Fraser, A.J. Hay and J.M. Robertson of this Department, M.M. Faktor and R.W. Lawson of G.P.O. Dollis Hill and C.P.Sandbank of S.T.L. Harlow.

I am also grateful to my parents and to the Science Research Council for financial support.

Finally, mention must be made of the appreciated assistance of Mrs. L. Manson, Mrs. A. Black and B. Wishart in preparing this work.

APPENDIX 1.

SOLID STATE CONTROL UNIT.

Manual Version

The circuit diagram for a solid state manual controller designed to operate the lower furnace element is presented in Fig. A.1. Since the element ratings are 25 V at 55 A, operation via a step-down transformer is mandatory and this requires full wave balanced control to avoid steady state magnetic flux build up in the transformer core. Full wave power control is achieved by a phase angle firing circuit with triac output. The firing circuit is unusual in that it features automatic reset of the firing capacitor voltage after both positive and negative half cycles of the input voltage thus ensuring a balanced output. Conventional circuits employing alternate reset, or no reset, were found to be unsatisfactory in this respect. The component values indicated provide 95 : 1 power regulation at currents of up to 10 A at 250 V.

Automatic Version

Fig. A.2 illustrates a modification to the above controller for automatic temperature control via a platinum-platinum 13% rhodium thermocouple. The circuit operates by comparing the thermocouple signal with a preset stabilised reference signal in an integrated circuit differential amplifier. The voltage differential is amplified and supplied to a

lamp photocell assembly which converts the voltage variation to a resistance variation and this in turn is employed in place of the manual potentiometer to alter the firing angle of the triac control circuit.

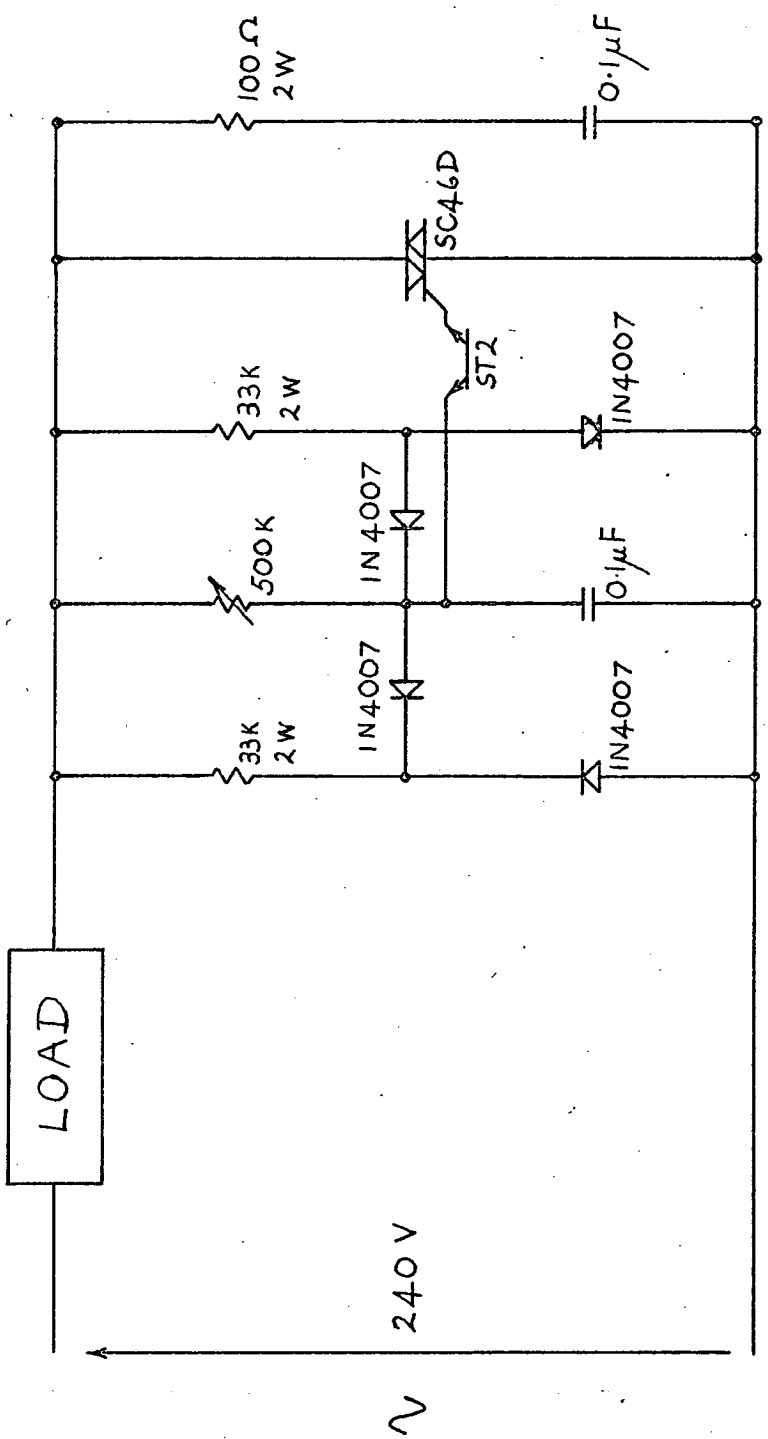

100 Ω
2 W
0·1 μF
SC46D
ST2
33K
2 W
IN4007
IN4007
500K
0·1 μF
IN4007
33K
2 W
IN4007
LOAD
240 V
~

FIG A_1

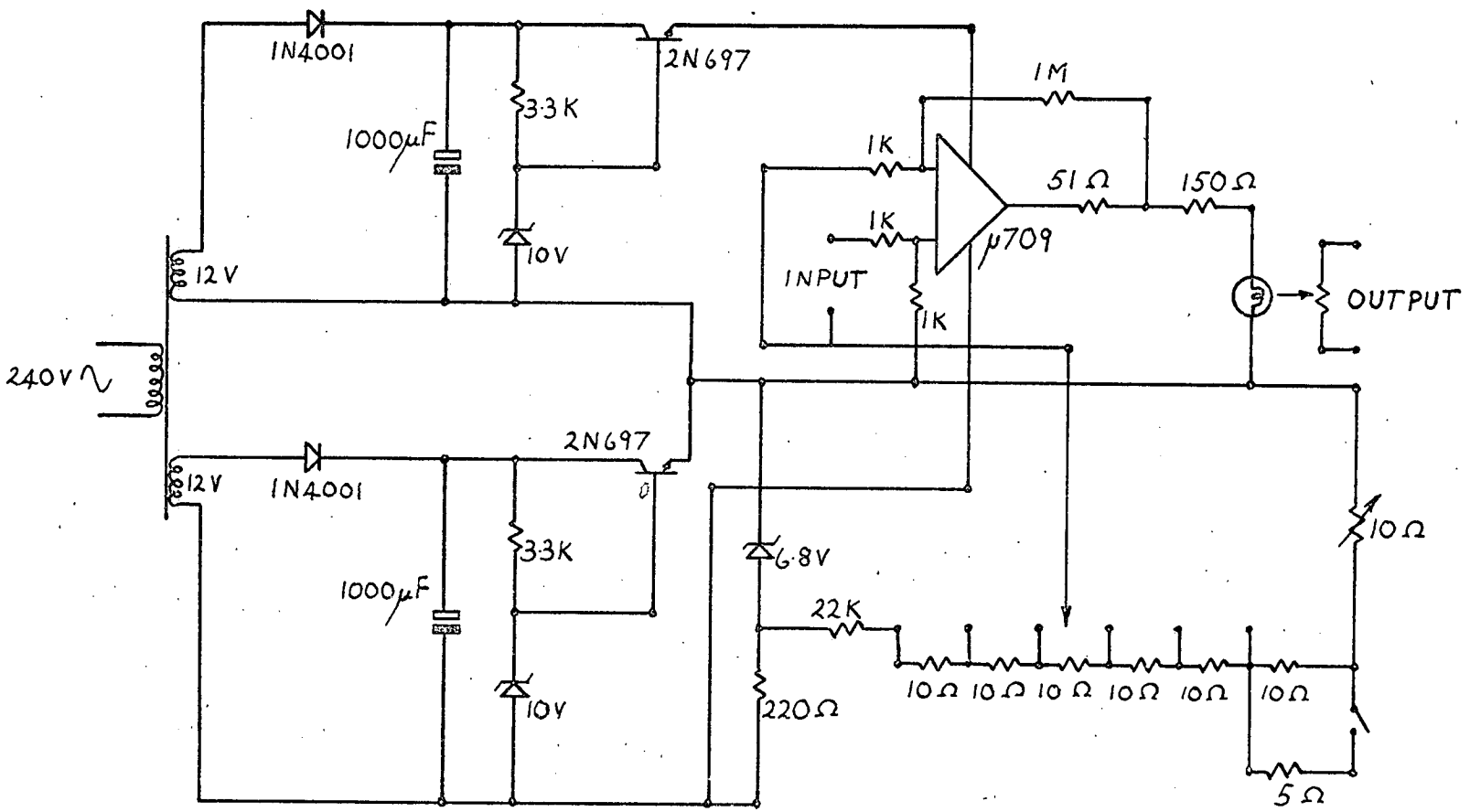

IN4001
2N697
1M
3·3K
1000μF
1K
51Ω
150Ω
1K
10V
μ709
12V
INPUT
1K
OUTPUT
240V
2N697
12V
IN4001
10Ω
3·3K
6·8V
1000μF
22K
10Ω 10Ω 10Ω 10Ω 10Ω 10Ω
10V
220Ω
5Ω

FIG A.2

APPENDIX 2.

HIGH VOLTAGE PULSE GENERATOR.

Testing of cadmium sulphide specimens of low resistivity or large cross sectional area demands a series of short pulses of high voltage, up to 3 KV, rather than a continuous supply. The circuit shown in Fig. A.3 was designed to meet this requirement. It provides pulses of up to 3 KV of length 15 to 150 μs with rise time 5 μs. It operates by generating a wave-train of square pulses using a Schmitt trigger circuit supplied with a 50 Hz sine wave. The square pulses are then differentiated with adjustable time constant to give short pulses of variable duration which provide the input signal for a second Schmitt trigger producing square output pulses of variable duration. These pulses after amplification are supplied via a high voltage trigger circuit to a cathode follower output stage.

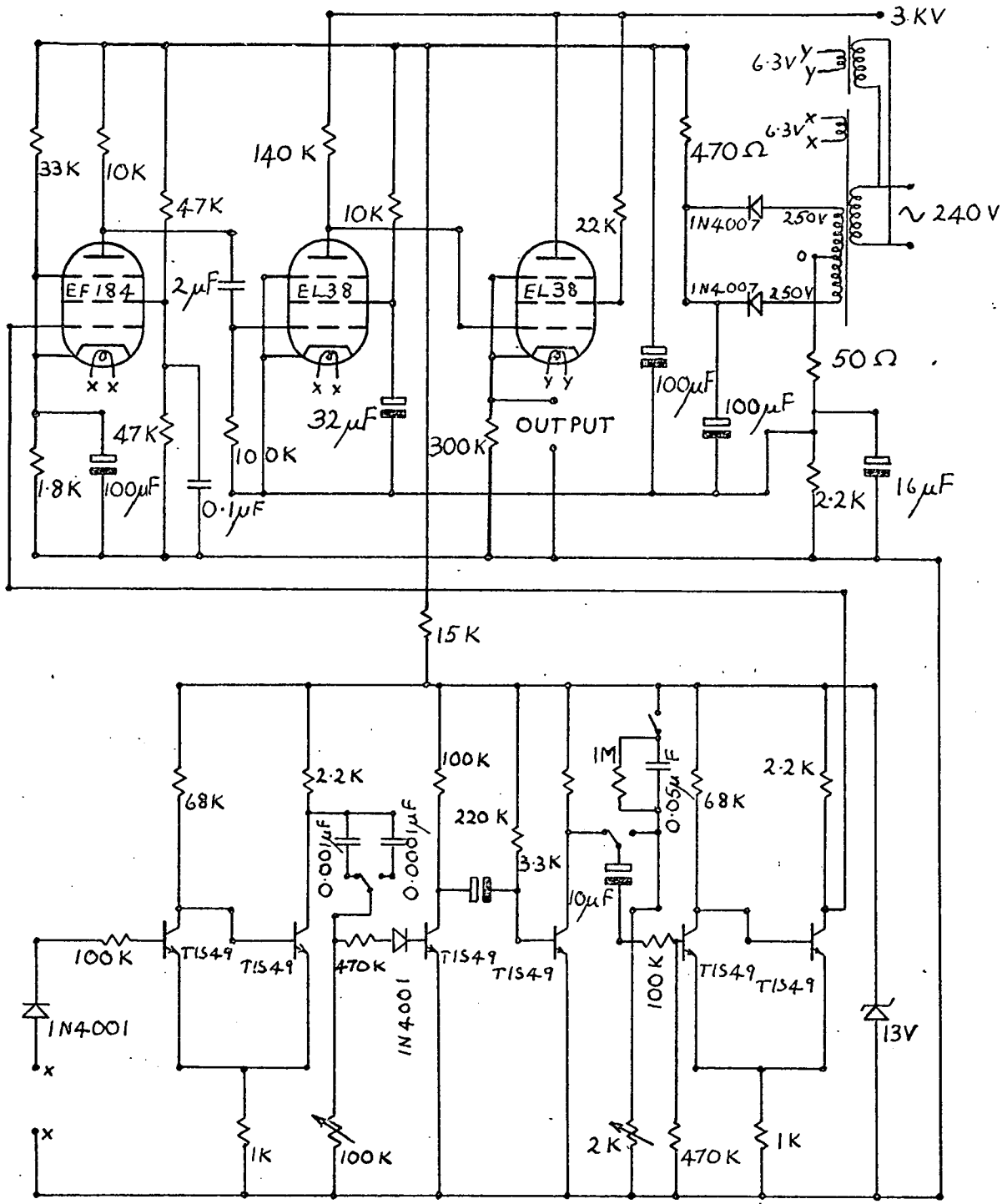

3 KV
6·3V
6·3V
470Ω
~ 240 V
IN4007 250V
IN4007 250V
33K
10K
47K
140 K
10K
22K
EF184
EL38
EL38
2μF
32μF
OUTPUT
100μF
100μF
50Ω
47K
1·8K
100μF
0·1μF
100K
300K
2·2K
16μF
15K
68K
2·2K
100K
220 K
3·3K
1M
0·05μF
68K
2·2K
0·001μF
0·001μF
10μF
100K
T1549
T1549
470K
T1549
T1549
100K
T1549
T1549
IN4001
IN4001
13V
1K
100K
2K
470K
1K

FIG A_3

REFERENCES :-

1. MASON, I.M. Ph.D. Thesis, University of Edinburgh, 1968.

2. KALISKI, S. Proc. Vibration Problems, Warsaw, 4, 7 1966, 277.

3. WEINREICH, G. Physical Review, 104, 2, 1956, 321 -

4. KALISKI, S. Proc. Conf. Acoustics of Solid Media, Warsaw, 1964.

5. KALISKI, S. Proc. Vibration Problems, Warsaw, 4, 6, 1965, 323.

6. WHITE, D.L. Jnl. Applied Physics, 33, 8, 1962, 2547.

7. SOLYMAR, L. & ASH, E.A. Int. Jnl. of Electronics, 20, 2, 1966, 127.

8. HUTSON, A.R. McFEE, J.H. WHITE, D.L. Physical Review Letters, 7, 1961, 237.

9. SMITH, R.W., Physical Review Letters, 9, 1962, 87.

10. KROGER, H., PROHOFSKY, E.W., CARLETON, H.R. Physical Review Letters, 12, 20, 1964, 555.

11. FROOM, J., et al. S.T.L. Report on Research Project RP7 - 21, 1965.

12. RIDLEY, B.K., PRATT, R.G., Physics Letters, 4, 1963, 300.

13. ZHDANOVA, N.G., KAGAN, M.S., KALASHNIKOV, S.G. Soviet Physics, Solid State, 8, 1966, 788.

14. GUNN, J.B., Proc. Symposium on Plasma Effects in Solids. Paris, 1964.

15. GUNN, J.B. Solid State Communications, 1, 1963, 89.

16. HAYDL, W.H., QUATE, C.F. Applied Physics Letters, 7, 1965, 45.

17. YAMASHITA, I. et al. Japanese Journal of Applied Physics, 4, 1965, 470.

18. UCHIDA, I. Japanese Journal of Applied Physics, 8, 1969, 119.

19. HAYDL, W.H., QUATE, C.F. Journal of Applied Physics, 38, 11, 1967, 4295.

20. MANY, A., GELBART, U. Applied Physics Letters, 19, 6, 1971, 192.

21. HAYDL, W.H., Physical Review Letters, 10,1967, 36.

22. HAYDL, W.H., QUATE,C.F. Physics Letters, 20,5,1966,463.

23. McFEE, J.H., TIEN, P.K. Journal of Applied Physics,38.
HODGES, H.L. 1967, 1721.

24. BUTLER, M.B.N., SANDBANK, C.P. I.E.E.E. Trans. Electron Devices, ED. 14, 1967, 663.

25. COLLINS, J.H., HAGON, P.J., Electronics, 42,25, 1969, 102.

26. REEDER, T.M., WINSLOW, D.K. I.E.E.E. Trans Microwave Theory and Techniques, MTT 17,1969 927.

27. OLSON, F.A. The Microwave Journal, 13, 3, 1970, 67.

28. NYE, J.F. Physical Properties of Crystals, Clarendon Press, Oxford, 1967.

29. MASON, W.P. Physical Acoustics and the Properties of Solids, Van Nostrand,1958.

30. BASS, R. Journal of the Acoustical Society of America, 30, 1958, 602.

31. RAYLEIGH, Lord S.W.J., Proc. London Mathematical Society, 17, 1885, 4.

32. ADLER, R. et al. I.E.E.E. Trans. Sonics and Ultrasonics, SU 15, 1968, 157.

33, WHITE, D.L. Sonics and Ultrasonics Symposium Vancouver B.C. 1967, Paper N.1.

34. VAN DER HEUVEL, A.P. Hybrid Microelectronics Symposium, Chicago, 1968.

35. TIERSTEN, H.F. Journal of Applied Physics, 40, 1969, 770.

36. ASH, E.A. et al. I.E.E.E. Trans. Microwave Theory and Techniques, M.T.T. 17. 11, 1969,882.

37. WHITE, R.M., VOLTMER, F.W. Applied Physics Letters, 8, 1966, 882.

38, COLLINS, J.H. et al. Applied Physics Letters, 13, 1968, 312.

39. BROERS, A.N. et al. G. M.T.T. Symposium, Dallas, Texas. 1969.

40. TURNER, C.W., MASON, I.M., Electronics Letters, CHAMBERS,J. 7, 23, 1971, 696

41. BUTLER, M.B.N. et al. S.T.L. Report on Research Project, RP7 - 21. 1967.

42. ZIMAN, J.M. Electrons and Phonons, Clarendon Press, Oxford, 1960.

43. KAYE and LABY, Physical and Chemical Constants, Longmans Green & Co., 1956.

44. HOLLAND, M.G. Physical Review, 134, 1964, A471.

45. PHILLIPS, L.S. Electronic Components, 12, 1971, 39.

46. WILSON, R.B. Jnl. Scientific Instruments, 44, 1967, 159.

47. Handbook of Chemistry & Physics. The Chemical Rubber Co.

48. MEDCALF, W.E., FAHRIG, R.H., Jnl. Electro-Chemical Society, 105,1958, 719.

49. BELYAEV, L.N. et al. Soviet Physics Cryst. 6, 1962, 516.

50. WARDZUMSKI, W., Proc. Royal Society, London, 260, 1961, 370.

51. HEINZ, D.M. Jnl. Chemical Phys. 24, 1956, 391.

52. LORENZ, M.R., Jnl. Applied Physics, 33, 2, 1962,3304.

53. YAMADA, S. Jnl. Phys. Society., Japan, 15, 1940.

54. GOLDFINGER, P. JEUNHOMME, M. Trans. Faraday Society, 59, 1963, 2851.

55. SPANDAU, H., KLANBERG, F., Z. Anorg. Allgem. Chem. 295, 1958, 309.

56. HSIAO, C.M., SCHLECHTEN, A.W. Jnl. Metals, 4, 1952, 65.

57. BULAKH, B.M. Jnl. Crystal Growth, 5, 1969, 243.

58. CAVENEY, R.J. Jnl. Crystal Growth, 7, 1970, 102.

59. SAMUELSON, H. Jnl. Applied Physics, 32, 1961, 309.

60. REYNOLDS, D.C., GREEN, L.C. Jnl. Applied Physics, 29, 1958, 559.

61. DE MARIA, G. et al. Trans Faraday Society, 68, 1968, 2146.

62. PASHINKIN, A.S., SALAMANTIN, B.A., Society Inorgan. Mater., 5, 1969, 256.

63. MARQUART, J.R., BERKOWITZ, J. Jnl. Chemical Physics, 89, 1963, 288.

64. SOMORJAI, G.A., JEPSEN, D.W. Jnl. Chemical Physics, 41, 5, 1964, 1394.

65. HILDISCH, L. Jnl. Crystal Growth, 3, 4, 1968, 131.

66. HARSY, M. et al. Jnl. Crystal Growth, 9, 1971, 209.

67. SOMORJAI, G.A., JEPSEN, D.W. Jnl. Chemical Physics, 41, 5, 1964, 1389.

68. SOMORJAI, G.A., Trans. Am. Society Metals, 57, 1964, 26.

69. Proc. Int. Conf. on the Physics and Chemistry of Solid Surfaces, June 1964, Brown University, Rhode Island.

70. HEMMAT, N., WEINSTEIN, M. Jnl. Electrochemical Society Solid State Science, 114, 8, 1967, 851.

71. FAKTOR, M.M. et al. Journal of the Chemical Society, 1970, A2657.

72. CLARK, L., and WOODS, J., British Jnl. Applied Physics, 17, 1966, 319.

73. JEUNHOMME, M., Ph.D. Thesis, University-Libre de Bruxelles, 1962.

74. REISMAN, A., BBRKENBLIT, M., WITZEN, M., Jnl. Phys. Chem. 66, 1962, 2210.

75. NELSON, R.C. Jnl. Optical Society, America, 45, 1955, 774.

76. VECHT, A. Physics of Thin Films. Vol.3. Academic Press, 1966.

77. THUN, R.E., Physics of Thin Films, Vol.1. Academic Press, 1963.

78. GÜNTHER, K.G. The use of Thin Films in Physical Investigations, Academic Press, 1966.

79. AITCHINSON, R.E., Nature, 167, 1951, 812.

80. GILLIES. J., VAN CAKENBERGHE, J. Nature, 182, 1958, 862.

81. VEITH, W. Comptes Rendus. Acad. Sci. Paris, 230, 1950, 947.

82. GANS, F. Bull. Sci. A.I.M. 11, 1953, 897.

83. KUWABARA, G., Jnl. Phys. Society, Japan, 9, 1954, 97.

84. LAWRANCE, R., British Jnl. Applied Physics Correspondence, 10, 1959, 298.

85. TERASAKI, Y. et al. Review of the Electrical Communication Lab. 14, 7-8, 1966, 425.

86. SHALLCROSS, F.V. Trans. Metallurgical Society of A.I.M.E. 236, 1966, 309.

87. DRESNER, J. and SHALLCROSS, F.V. Jnl. Applied Physics, 34, 8, 1963, 2390.

88. AGGARWAL, P.S. GOSWAMI, A. Indian Jnl. Pure Applied Physics, 1, 1963, 366.

89. ZHDAN, A.G., et al. Radio Engineering and Electronic Physics, 11, 21966, 1399.

90. WENDLAND, P., Jnl. Optical Society, America, 52, 1962, 581.

91. VECHT, A., APLING, A. Physica Status Solidi, 3, 1963, 1238.

92. MILLER, R.J., BACHMAN, C.H. Jnl. Applied Physics, 29, 1958, 1277.

93. PIZZARELLO, F.A., Jnl. Applied Physics, 35, 9, 1964, 2730.

94. DE KLERK, J., KELLEY, E.F., Review of Scientific Instruments, 36, 4, 1965, 506.

95. FOSTER, N.F. Jnl. Applied Physics, 38, 1, 1967, 149.

96. VAN DIJK, H. et al. Crystal Growth, Pergamon, 1967.

97. SEILER, H., and REIMERS, P. Mater.Res.Bulletin, 4, 1969, 119.

98. HEYRAUD, J.C., and CAPELLA, L. Jnl. Crystal Growth, 2, 1968, 405.

99. CURTISS, B.J., BRUNNER, H. Jnl. Crystal Growth, 6, 1970, 269.

100. CAVENEY, R.J. Jnl. Crystal Growth, 2, 1968, 85.

101. CAPELLA, L. Comptes Rendus Acad.Sci., Paris, 261, 1965, 4053.

102. JACOBS, J.E., and HART,C.W. Proc.Nat.Electronics Conf. 11, 1955, 1 -

103. LAKSHMANAN, T.K., MITCHELL, J.M., Trans. of the 10th. Nat. Vacuum Symp. 1963 Macmillan, N.Y. 1963.

104. LICHTENSTEIGER, M. Applied Physics Letters, 15, 12, 1969, 418.

105. HECHT, G., HERBERGER, J., WEISSMANTEL,I, Thin Solid Films, 2, 1968, 293.

106. MOLLWO, E. Reichsber Physik, 1, 1944, 1

107. SHIVONEN, Y.T., et al. Jnl. Electrochemical Society, 114, 1967, 96.

108. THOMSEN, S.M. and BUBE, R.H., Review of Scientific Instruments, 26, 1955, 664.

109. CHAMBERLIN, R.R., SKARMAN, J.S. Jnl. Electrochemical Society, 113, 1966, 86.

110. REID, M.A., I.E.R.E. Conf.Proc. No.7. 1966. Applications of Thin Films in Electronic Engineering, Paper 33.

111. DRESNER, J., and SHALLCROSS, F.V. Solid State Electronics, 5, 1962, 205.

112. BERGER, H. Physica Status Solidi, 3, 1963, 1238.

113. ZULEEG, R., SENKOVITS, E.J. Electrochemical Society Meeting, Pittsburg, April, 1963.

114. APONICK, A.A. Report No. ESL-R-229, M.I.T. Project DSR. 99 48

115. ADDISS, R.R., Trans. 10. Nat. Vacuum Symp.1963, Macmillan, N.Y. 1963.

116. SEMILETOV, S.A., Krystallografiya, 1, 1956, 306.

117. ESCOFFERY, C.A., Jnl. Applied Physics, 35, 1964, 2273.

118. WEINSTEIN, G.A., et al, Applied Physics Letters, 6, 1965, 73.

119. DISTLER, G.I. Jnl.Crystal Growth, 3, 4, 1968, 175.

120. SHALIMOVA, K.V. et al. Soviet Physics Cryst. 8, 1964, 618.

121. HOLLOWAY, H., WILKES, E. Jnl. Applied Physics Communications, 39, 5, 1968, 5807.

122. NEWMAN, R.C. Phil. Mag. 2, 1957, 750.

123. HIRTH, J.P. POUND, G.M. Progress if Materials Science, 11, 41, Macmillan, New York.

124. RHODIN, T.N., WALTON, D. Metal Surfaces. American Society For Metals, Metals Park, Ohio.

125. CHAKRAVERTY, B.K. POUND, G.M. Acta. Met. 12, 1964, 851.

126. REID, M.A. Ph.D. Thesis, Edinburgh University, 1968.

127. FRANK, F.C., VAN DER MERWE, J.H. Proc. Royal Society, A200, 1949, 125.

128. RHODIN, T.N. Discussions Faraday Society, N-5, 1949, 215.

129. BASSET, G.A. Structure and Properties of Thin Films, Wiley, New York, 1959.

130. PASHLEY, D.W., Advances in Physics, 14, 1965, 327.

131. CHOPRA, K.L. Jnl. Applied Physics Communications, 40, 2, 1969, 906.

132. BERGER, H., Physica Status Solidi, 1, 1961,739.

133. ESBITT, A.S., Physica Status Solidi, 12, 1965, 35.

134. SAKI, Y., OKIMURA, H. Jnl.Applied Physics, Japan, 3, 1964, 144.

135. BERGER, H. et al. Physica Status Solidi, 7, 1964, 679.

136. BOER, K.W., ESBITT, A.S., KAUFMAN, W.M., Jnl. Applied Physics, 37, 7, 1966, 2664.

137. BRUNNSCHWEILER, A. Nature, 209, 1966, 492.

138. HUDOCK, P. Trans.Metallurgical Society of A.I.M.E., 239, 1967, 338.

139. IGARASHI, O. Japanese Journal of Applied Physics, 8, 6, 1969, 642.

140. LORENZ, R. Chem. Ber. 24, 1891, 1509.

141. FRERICHS, R. Naturwiss, 33, 1946, 387.

142. FRERICHS, R. Physical Review, 72, 1947, 594.

143. HERFORTH, L. KRUMBIEGEL, J. Naturwiss, 40, 1953, 270.

144. KROGER, F.A., et al. Z. Phys. Chem. Leipzig, 203, 1954, 1

145. SCHOSSBERGER, F. Journal of the Electro-Chemical Society, 102, 1955, 22.

146. BUBE, R.H., THOMSEN, S.M. J. Chem. Phys. 23, 1955, 15.

147. BISHOP, M.E., LIEBSON, S.H., Journal of Applied Physics, 24, 5, 1953, 660.

148. CZYZAK, S.J. et al. Journal of Applied Physics, 23, 1952, 932.

149. GREENE, L.C., et al. J. Chem. Phys. 29, 6, 1958, 1375.

150. FOCHS, P.D. Journal of Applied Physics, 31, 10, 1960, 1733.

151. PIPER, W.W., POLICH. S.J., Journal of Applied Physics, 32, 7, 1961, 1278.

152. SINHARAY, N. Postgraduate Diploma in Electronics and Radio. University of Edinburgh. Report EDR-61. 1960.

153. KENNEDY, C.J. Postgraduate Diploma in Electronics and Radio, University of Edinburgh, Report EDR-73, 1964.

154. CLARK,L., WOODS,J. Journal of Crystal Growth, 3, 4, 1968, 127.

155. FOCHS, P.D., GEORGE W. AUGUSTUS P.D. Journal of Crystal Growth, 3, 4, 1968, 122.

156. HOLT, D.B., WILCOX, D.M. Journal of Crystal Growth, 9, 1971, 193.

157. KUBASCHEWSKI, R., EVANS, E.Ll. Metallurgical Thermochemistry, Pergamon Press Limited, 1958.

158. ISAKOVA, R.A., NESTEROV, V.N., Russian Journal of Inorganic Chemistry, 11, 5, 1966, 522.

159. JACKSON, P.A. Journal of Crystal Growth, 3, 4, 1968, 395.

160. SCHULSON E.M., et al. Proc. 2nd. S.E.M. Symposium, I.I.T. Research Institute, Chicago, 1969.

161. WRAY, L., PRUTTON, M. Private Communication.

162. BROWELL, T.P., HETHERINGTON, G., Vitreous Silica for the Scientific Glassblower, Journal of the British Society of Scientific Glassblowers, 3, 1 1966 2.

163. Research Triangle Institute - Integrated Silicon Device Technology, Technical Report, ASD-TDR-63-316, 10 ,1965,60.

164. TOYAMA, M., Japanese Journal of Applied Physics, 5 12, 1966, 1204.

165. HAY, A.J. B.Sc. Honours Degree in Electrical Engineering Students' Reports on Prescribed Special Projects. Project No. HSP.111. Edinburgh University, 1971.

166. FAKTOR, M.M. et al. Journal of the Electrochemical Society, Electrochemical Science, 114, 4, 1967 356

167. GRENIGER, A.B. Zeitschrift Für Kristallographie 91, 1935, 424

168. WOOD, E.A. Crystal Orientation Manual. Columbia University Press, 1963.

169. NEWHAM, HASS. Zeits Für Kryst, 117, 1962, 235.

170. BUTLER, W.M., MUSCHEID, W. Annals of Physics, 14, 1954, 215, 15, 1954, 82.

171. BOËR, K.W., HALL, R.B., Journal of Applied Physics, 37, 13, 1966. 4739.

172. SIHVONEN, Y.T., BOYD, D.R. Journal of Applied Physics, 29, 1958, 1143.

173. ITAKURA, M., TOYODA, H. Japanese Journal of Applied Physics, 3, 1964, 197.

174. KROGER, F.A., DIEMER, G. KLASENS, H.A., Physical Review, 103, 7, 1956, 279.

175. FROOM, J. S.T.L. Report on Research Project RP7 - 21, 1966.

176. SIMHONY, M., WILLIAM, R. Journal of Applied Physics, 40, 2 1969 691.

177. MASON, I.M. Electronics Letters, 5 51, 1969, 519.

178. REID, P.M., B.Sc. Honours Degree in Electrical Engineering Students' Projects on Prescribed Special Projects, Project No. HSP. 116. Edinburgh University,1971.